# THE ROLE OF NITRIC OXIDE IN THE BLOOD STORAGE LESION

BY

CHEN LIU

A Dissertation Submitted to the Graduate Faculty of

WAKE FOREST UNIVERSITY GRADUATE SCHOOL OF ARTS AND SCIENCES

in Partial Fulfillment of the Requirements

for the Degree of

DOCTOR OF PHILOSOPHY

Physics

December 2013

Winston-Salem, North Carolina

Approved By:

Daniel B. Kim-Shapiro, Ph.D., Advisor

George J. Christ, Ph.D., Chair

Martin Guthold, Ph.D.

Freddie R. Salsbury Jr., Ph.D.

Richard T. Williams, Ph.D.

ACKNOWLEDGEMENTS

I would like to express my deepest appreciation to my advisor, Dr. Daniel Kim-Shapiro, for his patient guidance and enthusiastic encouragement. I cannot find words to express my gratitude to his kindness, support, and friendship throughout my graduate study. My grateful thanks are also extended to Dr. Mark Gladwin, Dr. George Christ, and Dr. Chang Chen for their useful critiques of this research work. I would also like to thank Dr. Ivan Azarov, Dr. Swati Basu, Dr. Weixin Zhao, Dr. Christine Helms, Dr. Tennille Presley, Dr. Landon Bellavia, Andrea Belanger, and Andreas Perlegas for their assistance with projects in this study. I thank Xiaohua Liu and Jack Janes for being excellent teammates with me in recent projects. In addition, I would like to thank the NIH and the Center for Molecular Signaling and Communication at Wake Forest University for the support.

I would like to thank my parents and sister for their support and love. Without them, I would not have reached the point where I am today. I am grateful to the Cain family for their love and being a second family to me. Many thanks to my dear friends Yong Lin, Jana Gold, Jeff Nimmer, and all others who have supported me during my time at Wake. Finally, I would like to offer my special thanks to my beloved girlfriend, Luxiao Dong, for her love, support, and all the joy she brought to me. I am so grateful to have had her with me over the past two years and am excited for the journey ahead of us.

TABLE OF CONTENTS

LIST OF FIGURES

LIST OF TABLES

# LIST OF ABBREVIATIONS

| | |
|---|---|
| NO | Nitric oxide |
| RBC | Red Blood Cell |
| Hb | Hemoglobin |
| MP | Microparticle |
| MetHb | Methemoglobin (ferric heme) |
| HbNO | Iron-nitrosyl hemoglobin (where NO is bound to the ferrous heme) |
| OxyHb | Oxygenated hemoglobin |
| DeoxyHb | Deoxygenated hemoglobin |
| CFZ | Cell-free zone |
| PBS | Phosphate buffered saline |
| Hct | Hematocrit (percentage by volume of membrane-encapsulated Hb) |
| EPR | Electron paramagnetic resonance |

ABSTRACT

Liu, Chen

THE ROLE OF NITRIC OXIDE IN THE BLOOD STORAGE LESION

Dissertation under the direction of
Daniel B. Kim-Shapiro, Ph.D., Professor of Physics

The blood storage lesion refers to changes in red blood cells (RBCs) during storage. It includes a number of chemical and morphological changes in RBCs, which result in reduced integrity of the erythrocyte membrane with formation of microparticles, and increased cell-free hemoglobin in plasma. The geometry of the red blood cell tends to become more spherical, the mean cell hemoglobin concentration (MCHC) in RBCs decreases, RBC volume varies, and the structure of RBC membrane changes significantly. The adverse effects associated with the blood storage lesion are under investigation. We hypothesize that increased nitric oxide (NO) scavenging due to red cell breakdown contributes to the blood storage lesion. In this study, we examined the rate of cell-free hemoglobin and microparticles reacting with NO and found that microparticles scavenge NO only 3 times slower than cell-free hemoglobin but still about 1000 times faster than RBCs. Thus, release of cell-free hemoglobin and microparticles during storage and post transfusion reduces NO bioavailability. We further explored factors that would determine the extent to which red cell microparticles contribute to NO scavenging, such as the ability of these microparticles to concentrate in the cell free zone. We found that microparticles, like cell-free hemoglobin, enter the cell-free zone and as little as 5 μM

hemoglobin encapsulated in microparticles has the potential to reduce NO bioavailability and impair endothelial-dependent vasodilation. Additionally, we examined the rate of NO scavenging by fresh and old stored RBCs and found that old stored RBCs scavenge NO about 2 times faster than fresh stored RBCs. In order to understand the mechanisms of increased NO scavenging by older stored RBCs, we simulated NO scavenging by RBCs using 3D single RBC models. Our work shows that the rate of NO scavenging by RBCs increases as RBC MCHC or volume decreases. RBC membrane permeability needs to increase 5 to 70 fold to compensate the effect of geometry and explain our experimental findings. In summary, we have elucidated the extent and mechanisms of reduced NO bioavailability due to red cell breakdown thereby establishing how it contributes to pathological consequences of the storage lesion.

# CHAPTER I

## INTRODUCTION

Blood transfusion is one of the most common medical therapies, with about 14 million units of red blood cells (RBCs) having been transfused in the United States in 2011 and approximately 40% of all critically ill patients receiving at least one unit of packed RBCs in the intensive care unit [1-4]. RBCs preserved in ADOSL can be stored up to 42 days and the average age of red blood cells at transfusion is approximately 18days [4]. In recent years, a growing body of literature has demonstrated an association between an increased incidence of adverse clinical outcomes of blood transfusion and the storage of RBCs [5-10]. The adverse effect of blood transfusion is also suggested to be related to the number of units transfused [11, 12]. These effects include increased risk of infection, renal failure, respiratory failure, and multiple organ failure and death, particularly in physiologically compromised patient populations [5-10].

Nitric oxide (NO) functions as the endothelial derived relaxing factor, decreases platelet activation and vascular cell adhesion, influences oxidative and nitrosative stress, functions in host defense, and influences a large number of cellular functions through protein modification [13-17]. Given that cell-free hemoglobin (Hb) scavenges NO at a very high rate of 3 to 8 $\times 10^7$ $M^{-1}s^{-1}$ and that there is so much Hb in the blood (10 mM in heme), the ability of NO to function as an important signaling molecule without being scavenged by Hb was seen as a paradox [18-21]. However, it has been explained by the fact that when Hb is encapsulated inside of a RBC, it scavenges NO up to one-thousand times slower than when the Hb is not encapsulated (as cell-free Hb) [22-25]. A similar

effect is observed for the uptake of oxygen [26-28]. The reasons for the reduction of the rate of NO scavenging by red cell-encapsulated vs. cell-free Hb have been extensively investigated and the difference in the scavenging rates has been attributed to three mechanisms. One mechanism that accounts for the reduced rate of NO scavenging by red cell-encapsulated Hb is the formation of a cell-free zone [23, 24]. During blood flow, red blood cells are pushed inward away from the endothelium forming a cell-free zone next to the endothelium. In addition, an unstirred layer forms around the red blood cells because NO reacts so fast with Hb, any NO that is close to a red blood cell after mixing is rapidly scavenged [22, 28-31]. The rate of NO scavenging by a red cell is thus limited by the time for external diffusion to the red blood cell. Another mechanism that has been proposed to account for slower NO scavenging by red blood cells compared to cell-free Hb is that the red cell membrane has a finite permeability to NO, so that there is a physical barrier to NO diffusion across the membrane [32, 33].

However, a number of chemical and morphological changes in RBCs occur during blood storage including a reduction in levels of 2, 3-diphosphoglycerate, ATP, and pH values, as well as an increase of potassium and lactate [34]. These changes result in a reduced deformability, increased osmotic fragility, spheroechinocyte formation, reduced integrity of the erythrocyte membrane with formation of microparticles (MPs), and increased cell-free hemoglobin (Hb) in plasma [35-41]. The geometry of the red blood cell tends to be more spherical during storage which has smaller surface area to volume ratio, the mean cell hemoglobin concentration (MCHC) in RBCs decreases, and the structure of RBC membrane changes significantly during storage [42, 43]. Changes in RBCs during storage are referred as the blood storage lesion. Precise mechanisms that

explain how the blood storage lesion is associated with adverse effect of blood transfusion remain unclear.

Microparticles are small phospholipid vesicles released from a variety of cells, such as platelets, erythrocyte, leukocyte, or endothelial cells [44]. Microparticles contain a subset of protein derived from their parent cells and have long been considered as cell fragments without any biological function. However, research shows that microparticles are involved in many biological activities, such as haemostasis, thrombosis, inflammation, transfer of surface proteins, or even angiogenesis [44-47]. Microparticles in body fluids constitute a heterogeneous population, differing in cellular origin, numbers, size, antigenic composition, and functional properties. The clinical significance of microparticles has been studied for years. In this study, we focused on microparticles derived from red blood cells and formed during blood storage and post transfusion.

In the laboratory of Daniel B. Kim-Shapiro, we hypothesize that NO scavenging due to red cell breakdown contributes to the blood storage lesion. Thus, the work described in the dissertation was aimed to elucidate the extent to which older stored blood scavenges more NO than fresher stored blood by studying the extent of hemolysis, microparticle formation, and intrinsic changes of older stored red blood cells to NO scavenging.

In this dissertation, the second chapter, “Nitric Oxide Scavenging By Red Blood Cell Microparticles and Cell-Free Hemoglobin as a Mechanism for the Red Cell Storage Lesion”, and the third chapter, “Mechanisms of Slower Nitric Oxide Uptake by Red Blood Cells and Other Hemoglobin-Containing Vesicles”, describe how we explored the rate of cell-free hemoglobin and microparticles reacting with NO using time-resolved

stopped-flow spectroscopy, laser photolysis technique, and electron paramagnetic resonance spectroscopy and conclude that both cell-free hemoglobin and microparticles scavenge NO about 1000 times faster than RBCs. In the fourth chapter, "Nitric Oxide Scavenging by Red Cell Microparticles", we explored factors that would determine the extent to which red cell microparticles contribute to NO scavenging, such as the ability of these microparticles to concentrate in the cell free zone using computational simulation and single vessel myography. Our work shows that microparticles, like cell-free hemoglobin, enter the cell-free zone and in this case as little as five μM hemoglobin in red cell microparticles has the potential to reduce NO bioavailability and impair endothelial-dependent vasodilation. In chapter five, "Mechanism of Faster NO Scavenging by Older Stored Red Blood Cells", we examined the rate of NO scavenging by both fresh and old stored RBCs using time-resolved stopped-flow absorption spectroscopy and electron paramagnetic resonance spectroscopy. We found that old stored RBCs scavenge NO about 2 times faster than fresh stored RBCs. In this chapter, computational simulations were also conducted to explore the effects of morphological changes, RBC volume, MCHC, and permeability to NO on the rate of NO scavenging using 3D single RBC models. We used results of these simulations to account for the observed increase in NO scavenging by RBCs as a function of storage age and found that the spherical geometry which represents the geometry for old stored RBCs scavenges NO slower than the biconcave geometry which stands for fresh stored RBCs. In addition, we found that the rate of NO scavenging by RBCs increases as RBC MCHC and volume decrease. RBC membrane permeability to NO needs to increase 1000 to 3000 folds in order to explain our experimental finding that older stored RBCs scavenges NO faster.

REFERENCES


1. Vincent, J.L., et al., *Anemia and blood transfusion in critically ill patients.* JAMA, 2002. **288**(12): p. 1499-507.
2. Napolitano, L.M., et al., *Clinical practice guideline: red blood cell transfusion in adult trauma and critical care.* Crit Care Med, 2009. **37**(12): p. 3124-57.
3. Corwin, H.L., et al., *The CRIT Study: Anemia and blood transfusion in the critically ill--current clinical practice in the United States.* Crit Care Med, 2004. **32**(1): p. 39-52.
4. *The 2011 National Blood Collection and Utilization Survey Report*, 2013, United States Department of Health and Human Services.
5. Koch, C.G., et al., *Duration of red-cell storage and complications after cardiac surgery.* New England Journal of Medicine, 2008. **358**(12): p. 1229-1239.
6. de Watering, L.V., et al., *Effects of storage time of red blood cell transfusions on the prognosis of coronary artery bypass graft patients.* Transfusion, 2006. **46**(10): p. 1712-1718.
7. Vandromme, M.J., et al., *Transfusion and pneumonia in the trauma intensive care unit: an examination of the temporal relationship.* J Trauma, 2009. **67**(1): p. 97-101.
8. Weinberg, J.A., et al., *Transfusions in the less severely injured: does age of transfused blood affect outcomes?* J Trauma, 2008. **65**(4): p. 794-8.
9. Leal-Noval, S.R., et al., *Transfusion of blood components and postoperative infection in patients undergoing cardiac surgery.* Chest, 2001. **119**(5): p. 1461-8.
10. Zallen, G., et al., *Age of transfused blood is an independent risk factor for postinjury multiple organ failure.* Am J Surg, 1999. **178**(6): p. 570-2.

11. Edgren, G., et al., *Duration of red blood cell storage and survival of transfused patients (CME).* Transfusion, 2010. **50**(6): p. 1185-95.

12. Triulzi, D.J. and M.H. Yazer, *Clinical studies of the effect of blood storage on patient outcomes.* Transfus Apher Sci, 2010. **43**(1): p. 95-106.

13. Furchgott, R.F. and J.V. Zawadzki, *The Obligatory Role of Endothelial-Cells in the Relaxation of Arterial Smooth-Muscle by Acetylcholine.* Nature, 1980. **288**(5789): p. 373-376.

14. Ignarro, L.J., et al., *Endothelium-Derived Relaxing Factor from Pulmonary-Artery and Vein Possesses Pharmacological and Chemical-Properties Identical to Those of Nitric-Oxide Radical.* Circulation Research, 1987. **61**(6): p. 866-879.

15. Katsuki, S., et al., *Stimulation of Guanylate Cyclase by Sodium Nitroprusside, Nitroglycerin and Nitric-Oxide in Various Tissue Preparations and Comparison to Effects of Sodium Azide and Hydroxylamine.* Journal of Cyclic Nucleotide Research, 1977. **3**(1): p. 23-35.

16. Palmer, R.M.J., A.G. Ferrige, and S. Moncada, *Nitric-Oxide Release Accounts for the Biological-Activity of Endothelium-Derived Relaxing Factor.* Nature, 1987. **327**(6122): p. 524-526.

17. Ignarro, L.J., *Nitric Oxide Biology and Pathobiology*2000, San Diego: Academic press.

18. Lancaster, J.R., *Simulation of the Diffusion and Reaction of Endogenously Produced Nitric-Oxide.* Proceedings of the National Academy of Sciences of the United States of America, 1994. **91**(17): p. 8137-8141.

19. Doyle, M.P. and J.W. Hoekstra, *Oxidation of Nitrogen-Oxides by Bound Dioxygen in Hemoproteins.* Journal of Inorganic Biochemistry, 1981. **14**(4): p. 351-358.

20. Eich, R.F., et al., *Mechanism of NO-induced oxidation of myoglobin and hemoglobin.* Biochemistry, 1996. **35**(22): p. 6976-6983.

21. Herold, S., M. Exner, and T. Nauser, *Kinetic and mechanistic studies of the NO center dot-mediated oxidation of oxymyoglobin and oxyhemoglobin.* Biochemistry, 2001. **40**(11): p. 3385-3395.

22. Liu, X.P., et al., *Diffusion-limited reaction of free nitric oxide with erythrocytes.* Journal of Biological Chemistry, 1998. **273**(30): p. 18709-18713.

23. Butler, A.R., I.L. Megson, and P.G. Wright, *Diffusion of nitric oxide and scavenging by blood in the vasculature.* Biochimica Et Biophysica Acta-General Subjects, 1998. **1425**(1): p. 168-176.

24. Liao, J.C., et al., *Intravascular flow decreases erythrocyte consumption of nitric oxide.* Proceedings of the National Academy of Sciences of the United States of America, 1999. **96**(15): p. 8757-8761.

25. Vaughn, M.W., L. Kuo, and J.C. Liao, *Effective diffusion distance of nitric oxide in the microcirculation.* Am. J. Physiol.-Heart Circ. Physiol., 1998. **43**(5): p. H1705-H1714.

26. Huxley, V.H. and H. Kutchai, *The Effect of the Red-Cell Membrane and a Diffusion Boundary-Layer on the Rate of Oxygen-Uptake by Human-Erythrocytes.* J. Physiol. (London), 1981. **316**(JUL): p. 75-83.

27. Coin, J.T. and J.S. Olson, *Rate of Oxygen-Uptake by Human Red Blood-Cells.* Journal of Biological Chemistry, 1979. **254**(4): p. 1178-1190.

28. Vandegriff, K.D. and J.S. Olson, *Morphological and Physiological Factors Affecting Oxygen-Uptake and Release by Red-Blood-Cells.* Journal of Biological Chemistry, 1984. **259**(20): p. 2619-2627.

29. Azarov, I., et al., *Nitric oxide scavenging by red blood cells as a function of hematocrit and oxygenation.* J. Biol. Chem., 2005. **280**(47): p. 39024-38032.

30. Vandegriff, K.D. and J.S. Olson, *A Quantitative Description in 3 Dimensions of Oxygen-Uptake by Human Red-Blood-Cells.* Biophysical Journal, 1984. **45**(4): p. 825-835.

31. Liu, X.P., et al., *Nitric oxide uptake by erythrocytes is primarily limited by extracellular diffusion not membrane resistance.* Journal of Biological Chemistry, 2002. **277**(29): p. 26194-26199.

32. Vaughn, M.W., et al., *Erythrocytes possess an intrinsic barrier to nitric oxide consumption.* Journal of Biological Chemistry, 2000. **275**(4): p. 2342-2348.

33. Vaughn, M.W., et al., *Erythrocyte consumption of nitric oxide: Competition experiment and model analysis.* Nitric Oxide-Biology and Chemistry, 2001. **5**(1): p. 18-31.

34. van de Watering, L., *Red cell storage and prognosis.* Vox Sang, 2011. **100**(1): p. 36-45.

35. Dumaswala, U.J., et al., *Improved red blood cell preservation correlates with decreased loss of bands 3, 4.1, acetylcholinestrase, and lipids in microvesicles.* Blood, 1996. **87**(4): p. 1612-1616.

36. Tinmouth, A. and I. Chin-Yee, *The clinical consequences of the red cell storage lesion.* Transfus Med Rev, 2001. **15**(2): p. 91-107.

37. Tinmouth, A., et al., *Clinical consequences of red cell storage in the critically ill.* Transfusion, 2006. **46**(11): p. 2014-2027.

38. Greenwalt, T.J., D.J. Bryan, and U.J. Dumaswala, *Erythrocyte-Membrane Vesiculation and Changes in Membrane-Composition During Storage in Citrate-Phosphate-Dextrose-Adenine-1.* Vox Sanguinis, 1984. **47**(4): p. 261-270.

39. Latham, J.T., J.R. Bove, and F.L. Weirich, *Chemical and Hematologic Changes in Stored Cpda-1 Blood.* Transfusion, 1982. **22**(2): p. 158-159.

40. Aubuchon, J.P., T.N. Estep, and R.J. Davey, *The Effect of the Plasticizer Di-2-Ethylhexyl Phthalate on the Survival of Stored Rbcs.* Blood, 1988. **71**(2): p. 448-452.

41. Salzer, U., et al., *Vesicles generated during storage of red cells are rich in the lipid raft marker stomatin.* Transfusion, 2008. **48**(3): p. 451-462.

42. Almizraq, R., et al., *Storage of red blood cells affects membrane composition, microvesiculation, and in vitro quality.* Transfusion, 2013. **53**(10): p. 2258-2267.

43. Liu, X., et al., *Diffusion-limited reaction of free nitric oxide with erythrocytes.* Journal of Biological Chemistry, 1998. **273**(30): p. 18709-13.

44. Diamant, M., et al., *Cellular microparticles: new players in the field of vascular disease?* European Journal of Clinical Investigation, 2004. **34**(6): p. 392-401.

45. Freyssinet, J.M., et al., *Procoagulant microparticles - Disrupting the vascular homeostasis equation?* Arteriosclerosis Thrombosis and Vascular Biology, 2006. **26**(12): p. 2594-2604.

46. Ratajczak, M.Z., et al., *Platelet-derived microparticles stimulate proliferation, survival, adhesion, and chemotaxis of hematopoietic cells.* Experimental Hematology, 2002. **30**(5): p. 450-459.

47. Brill, A., et al., *Platelet-derived microparticles induce angiogenesis and stimulate post-ischemic revascularization.* Cardiovascular Research, 2005. **67**(1): p. 30-38.

CHAPTER II

# NITRIC OXIDE SCAVENGING BY RED BLOOD CELL MICROPARTICLES AND CELL-FREE HEMOGLOBIN AS A MECHANISM FOR THE RED CELL STORAGE LESION

C. Donadee, N. J. H. Raat, T. Kanias, J. Tejero, J. S. Lee, E. E. Kelley, X. Zhao, C. Liu, H. Reynolds, I. Azarov, S. Frizzell, E. M. Meyer, A. D. Donnenberg, L. Qu, D. Triulzi, D. B. Kim-Shapiro, M. T. Gladwin

The following manuscript was published in Circulation, volume 124, pages 465-476, 2011, and is reprinted with permission. Stylistic variations are due to the requirements of the journal. I. Azarov, C. Liu, and H. Reynolds performed experiments using stopped-flow and laser photolysis techniques. I. Azarov and C. Liu analyzed kinetic absorbance data.

# Nitric Oxide Scavenging By Red Blood Cell Microparticles and Cell-Free Hemoglobin as a Mechanism for the Red Cell Storage Lesion

Chenell Donadee, MD[1,2]; Nicolaas J.H. Raat, PhD[1,2,3]; Tamir Kanias, PhD[1]; Jesús Tejero PhD[1], Janet S. Lee, MD[1,2]; Eric E. Kelley, PhD[1,4]; Xuejun Zhao, PhD[1,2]; Chen Liu, BS[5]; Hannah Reynolds[5]; Ivan Azarov, PhD[5]; Sheila Frizzell, BA[1]; E Michael Meyer, BS[6]; Albert D. Donnenberg, PhD[6,7]; Lirong Qu, MD, PhD[8,9]; Darrel Triulzi, MD[8,9]; Daniel B. Kim-Shapiro, PhD[5*]; Mark T. Gladwin, MD[1,2*]

From: [1]Vascular Medicine Institute, University of Pittsburgh, Pittsburgh, PA, 15213;
[2]Department of Medicine, Division of Pulmonary, Allergy and Critical Care Medicine, University of Pittsburgh School of Medicine, Pittsburgh, PA, 15213;
[3]Department of Experimental Anesthesiology, Erasmus Medical Center, Rotterdam, Netherlands;
[4]Department of Anesthesiology, University of Pittsburgh School of Medicine, Pittsburgh, PA 15213;
[5]Department of Physics, Wake Forest University, Winston-Salem, NC 27109;
[6]University of Pittsburgh Cancer Institute, Pittsburgh, PA 15203;
[7]Department of Medicine, Division of Hematology/Oncology, University of Pittsburgh School of Medicine, Pittsburgh, PA 15213;
[8]Department of Pathology, University of Pittsburgh School of Medicine, Pittsburgh PA 15213;
[9]Institute for Transfusion Medicine, Pittsburgh PA 15213.

*Shared senior authors.
Address correspondence to: Dr. Mark T. Gladwin, Pulmonary, Allergy and Critical Care Medicine, University of Pittsburgh, Phone: 412-692-2210; Fax: 412-692-2260; E-mail: gladwinmt@upmc.edu; or Dr. Daniel B. Kim-Shapiro, Department of Physics, Wake Forest University, Phone: 336-758-4993; Fax: 336-758-6142; E-mail: shapiro@wfu.edu.

## Abstract

***Background****:* Intravascular red cell hemolysis impairs NO-redox homeostasis, producing endothelial dysfunction, platelet activation and vasculopathy. Red blood cell storage under standard conditions results in reduced integrity of the erythrocyte membrane, with formation of exocytic microvesicles or microparticles and hemolysis, which we hypothesized could impair vascular function and contribute to the putative storage lesion of banked blood.

***Methods and Results:*** We now find that storage of human red blood cells under standard blood banking conditions results in the accumulation of cell free and microparticle-encapsulated hemoglobin which, despite 39 days of storage, remains in the reduced ferrous oxyhemoglobin redox state and stoichiometrically reacts with and scavenges the vasodilator nitric oxide (NO). Using stopped-flow spectroscopy and laser triggered NO release from a caged NO compound we found that both free hemoglobin and microparticles react with NO about 1000 times faster than with intact erythrocytes. In complementary in vivo studies we show that hemoglobin, even at concentrations below 10 μM (in heme), produces potent vasoconstriction when infused into the rat circulation, while controlled infusions of methemoglobin and cyanomethemoglobin, which do not consume NO, have substantially reduced vasoconstrictor effects. Infusion of the plasma from stored human red cell units into the rat circulation produces significant vasoconstriction related to the magnitude of storage related hemolysis.

***Conclusions:*** The results of these studies suggest new mechanisms for endothelial injury and impaired vascular function associated with the most fundamental of storage lesions, hemolysis.

**Key words:** Hemoglobin, microparticles, nitric oxide, blood transfusion, storage lesion, reactive oxygen species

**Short Clinical Summary:**

Transfusion of blood represents one of the most common medical therapies with over 14.5 million packed red blood cell units, or 48.9 units per thousand persons, administered in the United States per year.[1] It is remarkable that approximately 40% of all critically ill patients receive at least one unit of packed red blood cells in the intensive

care unit, with a mean of 5 units per patient.[2-4] In recent years a growing body of literature has demonstrated an increased incidence of adverse clinical outcomes associated with the transfusion of a large number of units or, potentially, with increased storage time of the units. We now find that storage of human red blood cells under standard blood banking conditions results in progressive red blood cell hemolysis, with the accumulation of cell free and microparticle-encapsulated hemoglobin. This cell-free hemoglobin and red cell microparticles released during blood storage react with and destroy an important blood vessel dilating molecule called nitric oxide about 1000 times faster than intact red cells. This scavenging of nitric oxide increases with the age of blood in storage and produces vasoconstriction in animal models in proportion to the levels of cell-free hemoglobin and red cell microparticles that accumulate. These studies suggest that red blood cell hemolysis during storage and after transfusion could contribute to the observed adverse cardiovascular effects of transfusion.

**Background**

Transfusion of blood represents one of the most common medical therapies with over 14.5 million packed red blood cell units, or 48.9 units per thousand persons, administered in the United States per year.[1] It is remarkable that approximately 40% of all critically ill adult patients receive at least one unit of packed red blood cells in the intensive care unit, with a mean of 5 units per patient.[2-4] The five-unit mark is notable when one considers that this represents 50% of the human blood volume. Since the 1960's multiple red cell transfusion, or hypertransfusion, has been recognized as a risk factor for acute lung injury. It was first noted during the Vietnam War that "the lungs are a vulnerable target organ to a variety of pathogenetic stimuli," including blood.[5-7] In

recent years a growing body of literature has demonstrated an increased incidence of adverse clinical outcomes associated with the transfusion of a large number of units or, potentially, with increased storage time of the units. These events include increased risk of infection, renal failure, respiratory failure, multiple organ failure and death, particularly in physiologically compromised patient populations.[8-13] This is an active area of investigation with competing studies suggesting a risk and others suggesting that storage duration risk is confounded by the number of units transfused and associated severity of illness.[14,15]

The Food and Drug Administration and American Association of Blood Banks currently permit blood preserved in ADSOL solution to be stored for 42 days. Stored red blood cells undergo a number of morphologic and biochemical changes with increased storage time.[16,17] Morphologic changes include reduced deformability, increased osmotic fragility, and spheroechinocyte formation, associated with progressive reduction in the intracellular levels of ATP and DPG and dropping pH values. In addition, prolonged red cell storage favors oxidant stress conditions leading to lipid peroxidation, oxidation of membrane and cytoskeletal proteins and reduced integrity of the erythrocyte membrane.[16-19] These and other changes in red blood cell functionality and integrity during storage are commonly referred to as the "storage lesion."

There is increasing hemolysis during packed red blood cell storage which increases cell free plasma hemoglobin over time.[20-22] Fragmentation and formation of 50-100 nm microparticles, which contain a substantial amount of hemoglobin, also occurs as red blood cells age.[21,23,24] According to current FDA guidelines, at the end of the storage period, only 75% of erythrocytes are required to be recoverable 24 hours after transfusion,

suggesting that further hemolysis and microparticle formation occurs in vivo after transfusion, although much of this is likely extravascular red cell clearance. These findings are concerning as it is known that free hemoglobin reacts with the vasodilator nitric oxide (NO) in a 1:1 stoichiometric reaction that occurs at high rate of 6-8x$10^7$ mol/L/s.[25] This consumption of NO by cell free plasma hemoglobin has been shown to cause changes in vascular function in subjects with sickle cell anemia who had plasma heme concentrations as low as 6 μM.[26] Approximately half of the observed "hemolysis" in stored blood is also encapsulated in microparticles, and, in theory, based on their small molecular size, microparticles may also exhibit accelerated NO scavenging rates compared with intact erythrocytes.[27] The effect of microparticles on NO scavenging could be especially important, particularly in the microvasculature where their clearance may not be reflected by systemic clearance rates. Indeed, in a rat model, approximately 90% of red cell microparticles are cleared systemically by 30 minutes after injection and distribute predominantly into the liver but also throughout multiple organs such as the bone, kidneys, skin, and lungs.[28] Hemolysis also decreases NO bioavailability by releasing red cell arginase-1, an enzyme that converts arginine to ornithine, thereby reducing arginine, a substrate for nitric oxide synthase.[29,30]

We therefore initiated in vitro chemistry and biophysical studies of stored blood cell free hemoglobin and microparticles and in vivo physiological studies with infusions of the plasma collected from fresh and aged stored human red cell units, to explore whether the formation of microparticles and accumulation of cell free hemoglobin during in-storage red blood cell hemolysis will increase the rate of NO catabolism and impair endothelial function. The results of these studies suggest new mechanisms for endothelial

injury and impaired vascular function associated with the most fundamental of storage lesions, hemolysis.

## Methods

### Packed Red Blood Cells

Nine randomly selected packed red blood cell units were obtained from the Central Blood Bank, Pittsburgh, PA. These units were non-leukoreduced and preserved in ADSOL solution, which is standard at the University of Pittsburgh Medical Center. Additional units that were leukoreduced were also studied for comparison. The units were stored in a temperature controlled refrigerator at 1-6°C and sampled weekly over 6 weeks starting at an age of 4 days old. At the end of storage samples were cultured to exclude bacterial contamination. Samples collected at weekly intervals were centrifuged at room temperature at 2700 x g for 20 min. The supernatant was stored at -80°C and later thawed for analysis of the free hemoglobin, NO consumption, electron paramagnetic resonance (EPR), hemoglobin spectral deconvolution, and arginase-1 assays as well as for in vivo infusion studies in a rat model as described below.

### Cell-Free Plasma Hemoglobin Levels and Spectral Deconvolution of Species

Cell free plasma hemoglobin was measured by conversion to cyanomethemoglobin using Drabkin's reagent and then measuring absorbance spectrophotometrically at 540nm. (Beckman Coulter DU 800 UV/Visible Spectrophotometer, Brea, CA).[31,32] Hemoglobin concentration and spectra were also measured on an Agilent 8453 UV-Visible Spectrophotometer (Agilent Technologies, Santa Clara, CA) using 1 cm path length cuvettes. The concentrations of oxyhemoglobin and methemoglobin in the plasma samples were analyzed by

deconvoluting the spectrum into components from standard UV-visible spectra of human hemoglobin composed of oxyhemoglobin, methemoglobin and deoxyhemoglobin in PBS buffer using a least-square method as previously described with some adjustments to correct for the background signal from plasma.[33] Additional experimental detail are summarized in the on-line supplement.

**Nitric Oxide Consumption**

The ability of the cell free hemoglobin in the supernatant to scavenge NO was measured with a previously published and validated NO consumption assay using an NO chemiluminescence analyzer (Sievers, Boulder CO).[34] Additional experimental details are summarized in the on-line supplement.

**Arginase-1 Assay**

Plasma levels of arginase-1 were measured via ELISA (Human Arginase 1 ELISA-Test-kit, Hycult biotechnology BV, Netherlands) according to the manufacturer's instructions and our previous publications.[35]

**Electron Paramagnetic Resonance Spin Trap Detection of Reactive Oxygen Species and Free Iron**

The spin probe 1-hydroxy-3carboxy-2,2,5,5-tetramethylpyrrolidine (CPH; Alexis Biochemiclas), was added to each stored red blood cell supernatant sample to achieve a final concentration of 200 μM. Samples were placed in 50 μL glass capillaries and analyzed on a Bruker eScan Spectrometer at 37°C and 21% $O_2$. Spectra were signal averaged (5 scans over 10 minutes). The instrument settings were as follows: field sweep 50G; microwave frequency 9.78 GHz; microwave power 20 mW; modulation amplitude 2G; conversion time 327 ms; time constant 655 ms; and receiver gain $1x10^5$. To evaluate

whether the signal was derived from non-transferrin bound iron versus reactive oxygen species a variety of reagents were added as indicated in the results, including allopurinol, *L*-nitroargine methyl ester (*L*-NAME) and diphenyleneiodonium chloride (DPI), and catalase (Sigma, St. Louis, MO), CuZn superoxide dismutase (OXIS International Inc. Portland, OR), and deferoxamine mesylate (Sigma, St. Louis, MO).

**Detection and Quantification of Red Blood Cell Microparticles**

Quantification of microparticles was performed at 14-day intervals for each unit of packed red blood cells. Two μL of PE-Cy 5 conjugated glycophorin A (BD Pharmingen, San Jose, CA) was added to 5 μL packed red blood cells. After incubation for 30 minutes in the dark at room temperature, 2 μL FITC conjugated Annexin V was added followed by 500 μL Annexin V binding buffer, per kit instructions (Annexin V-FITC Kit, Beckman Coulter, Bera, CA). After 30 minutes of incubation in the dark at room temperature the analysis was performed using a CyAn ADP cytometer (Beckman Coulter, Miami FL). An effort was made to acquire a total of 100,000 events per sample at rates not exceeding 10,000 events/second. The cytometer was calibrated to predetermined photomultiplier target channels prior to each use, using 8-peak Rainbow Calibration Particles (Spherotech, Libertyville, IL, Cat. No. RCP-30-5A). Offline spectral compensation and analyses were performed using the VenturiOne analysis package (Applied Cytometry, Dinnington, Sheffield, UK). Flow cytometric histograms of forward light scatter and fluorescence intensity are displayed on a 4-decade logarithmic scale. Microparticles were quantified as a percent of GPA positive events. The fraction of hemoglobin contained in microparticles compared with the total hemoglobin in the

plasma of stored blood was measured by differential centrifugation at 750 x g for 10 minutes at 4 C for the first spin and 37,000 x g for 10 minutes for the second spin.

**Stopped-Flow Analysis**

Hemoglobin was purified and NO-saturated buffers prepared as described previously.[33] For these experiments a unit of outdated packed red blood cells with ACD anticoagulant was purchased from Interstate Blood Bank, Inc. (Memphis, TN). The microparticles were isolated as previously described.[36] The absence of red blood cells in the microparticle preparation was confirmed by microscopy. The physical stability of microparticles over time was confirmed by measuring the free hemoglobin concentration in a microparticle preparation that had been left at 4 °C for 7 days. Free hemoglobin in a one day old preparation was not detectable by absorbance (intensity in the Soret range).

Stopped-flow experiments of the reaction between NO and free hemoglobin as well as with red cell-encapsulated hemoglobin and microparticle-encapsulated hemoglobin were performed as described previously [37] and in described in detail in the supplementary methods section. Briefly, one syringe of the stopped-flow apparatus was loaded with NO saturated buffer, another with oxygenated cell free hemoglobin, red cell-encapsulated hemoglobin or microparticle-encapsulated hemoglobin, and a third syringe was loaded with deoxygenated PBS for dilution purposes. The hemoglobin concentration after mixing was 0.05 mM in heme and the NO was 1-8 times in molar excess to heme. An upper bound for the dead time of the Stopped Flow instrument was estimated using a procedure similar to that described by Tonomura et. al.[38] as 16.4±7.4 mseconds by observing the reduction of 2,6-dichlorophenolindophenol (DCIP) by L-ascorbic acid.

Photolysis experiments to measure the very fast dioxygenation rate of NO by microparticles compared with cell free hemoglobin were performed under aerobic conditions similarly to those described previously [39] and in described in detail in the supplementary methods section for time-resolved absorption measurements. A solution of microparticle-encapsulated hemoglobin or cell free hemoglobin was mixed 1:1 with a solution of the caged NO donor compound, potassium pentachloronitrosyl-ruthenate (II). A quantum yield of NO in each experiment was calculated from each observed reaction rate between cell free hemoglobin and NO and a $5\times10^7$ $M^{-1}s^{-1}$ bimolecular rate constant for NO scavenging by free oxyhemoglobin [40], a lower bound which we have previously established. Each obtained value for the yield of NO was used to calculate a corresponding bimolecular rate constant for every observed reaction rate between microparticle-encapsulated hemoglobin and NO. The absence of lysis of microparticles during a photolysis experiment was confirmed by measuring the absorbance of the supernatant after photolysis, which showed no detectable amount of cell free hemoglobin. The age of blood used for preparation of vesicles for photolysis experiments was 28 or 33 days old.

**Rat Vasoactivity Model**

This study was reviewed and approved by the ethical committee for animal subjects of the University of Pittsburgh, PA, USA. Wistar male rats (Charles River, Wilmington, MA) with a body weight of 325 ± 4 g (mean ± SEM) were utilized in this study.

Rats were anesthetized with an intraperitoneal injection of a mixture of 90 mg/kg ketamine (Ketaject, Phoenix, St. Joseph, MD), 0.5 mg/kg medetomidine (DexDomitor;

Pfizer,#6295), and 0.005 mg/kg atropine sulfate (Med-Pharmex, Pomona, CA). Details of experimental set-up are summarized in the on-line supplement. A fluid-filled catheter was inserted into the right carotid artery catheter and connected to a pressure transducer (model MLT844, AD instruments, Colorado Springs, CO) that was connected to a data acquisition system (Powerlab 8/30, AD Instruments) for continuous monitoring of mean arterial blood pressure (MAP) and heart rate. MAP was calculated with the use of the formula: (systolic blood pressure - diastolic blood pressure)/3 + diastolic blood pressure. In addition, the jugular vein was cannulated to infuse maintenance anesthesia (ketamine, 58 mg/kg/hr in Ringer's solution). The femoral artery was cannulated for blood withdrawal and arterial blood-gas sampling. The femoral vein was cannulated for the infusion of the packed red blood cell supernatant.

After surgery, the rat was allowed to stabilize for 30 minutes after which 0.2 mL of blood was drawn for blood gas analysis. As replacement for the drawn blood 0.2 mL of 6% Hextend in Ringer's lactate (Hospira, Lake Forest, IL) was infused and the rat was allowed to stabilize for 10 minutes. Subsequently a volume of 4.95 mL/kg of supernatant from either 4 or 39 days stored packed red blood cells was infused for approximately 40 min at a rate of 7.5 ml/kg/hr. Responses in blood pressure and heart rate were recorded continuously up to an hour after the end of the infusion. Experiments were performed on 5 individual days. Each day, the effect on blood pressure of infusion of packed red blood cell supernatant from the same red cell donor obtained at day 4 and day 39, from the same bag and frozen at -80 °C, was determined in two separate rat experiments. Additional experiments with infusion of microparticles are summarized in the supplemental on-line methods.

**Statistical Methods**

Analysis was performed using Microsoft Office Excel 2007 (Redland, OR), Graphpad Prism, version 5 (Graphpad Software, LaJolla, CA), Systat Version 12 ( Systat Software Inc, Chicago, IL) and OriginPro 8 (OriginLab Corp.,Northampton, MA) software. Time course experiments of banked blood were analyzed by repeated measures analysis of variance (RM-ANOVA) with post-test Bonferroni corrections for multiple comparisons at each time point.

**Results**

**Accumulation of Plasma Ferrous Oxyhemoglobin ($Fe^{+2}$-$O_2$) during Red Blood Cell Storage**

It is known that progressive low level hemolysis occurs during standard red blood cell storage in ADSOL preservation solution, a result that we confirm in our 9 packed red blood cell units (Figure 1A and 1B). The cell free plasma hemoglobin concentration (measured in heme) in supernatants from 9 packed red blood cell units increased over time from a baseline 4 day mean of 11.6 ± 2.5 μM (range of 4.6 to 27.7 μM) to a 39 day mean value of 81.0 ± 18.4 μM (range of 31.0 to 173.3 μM). While our primary analysis was performed in non-leukoreduced blood, which is the standard at our center, we also performed the experiments in leukoreduced blood. There were no significant differences in the levels of plasma hemoglobin at 39 days of storage (non-leukoreduced 81.0 ± 18.4 μM ±vs. leukoreduced 88.10 ± 47.84 μM). Because low levels of plasma hemoglobin in the ferrous redox state (oxyhemoglobin or deoxyhemoglobin, but NOT methemoglobin) have the capacity to react with and inactivate NO via the classic dioxygenation reaction

(Eq. 1) we quantified both the extent of hemolysis and the redox state of the cell free plasma hemoglobin in supernatant over 39 days in blood from nine normal blood donors:

(1) $Fe^{+2}$-$O_2$ (oxyhemoglobin) + NO (nitric oxide) → $Fe^{+3}$ (methemoglobin) + $NO_3^-$ (nitrate)

Although it might be expected that cell-free plasma hemoglobin would be oxidized to ferric methemoglobin over 39 days of storage, which could not catabolize NO, we have previously found that normal human plasma actively reduces ferric heme to ferrous heme.[34] To explore the redox status of the cell free plasma hemoglobin during red cell storage we measured the concentration and percentages of methemoglobin, oxyhemoglobin and deoxyhemoglobin by UV-visible spectroscopy and least-squares spectral deconvolution. To some surprise, we found that at least 92% of the cell free plasma hemoglobin remained in the ferrous oxyhemoglobin ($Fe^{+2}$-$O_2$) form (Figure 1C and 1D). The deconvolution model had a larger fitting error at 4 days of storage due to the lower overall hemoglobin levels, and hence lower absorbance signals.

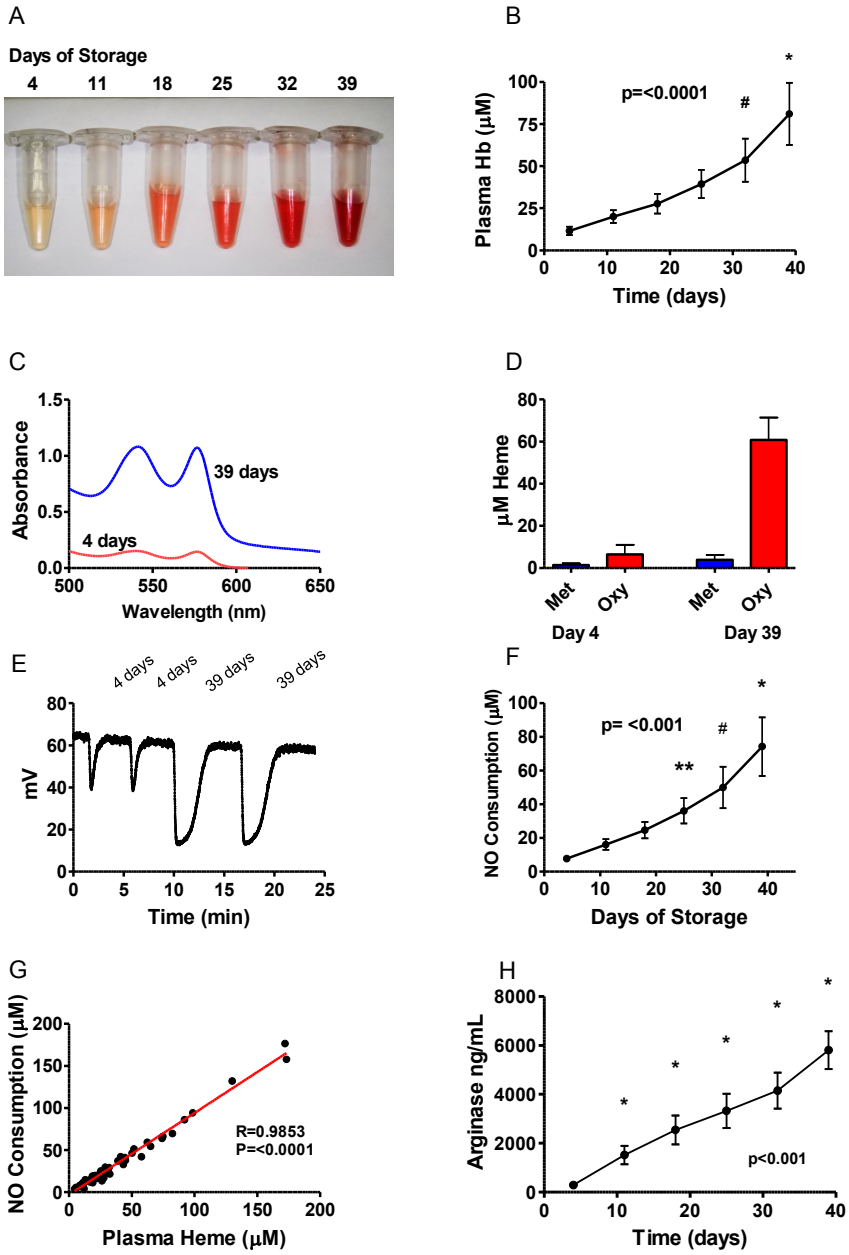


**Figure 1. Cell Free hemoglobin and NO scavenging in stored blood.** (A) Photograph of stored red blood cell supernatant over time. (B) Average cell free plasma heme concentration (μM) over time. (C) Absorbance spectra of representative packed red blood cell supernatants at 4 and 39 days of storage. (D) Concentration (μM) of methemoglobin and oxyhemoglobin by spectral deconvolution of packed red blood cell supernatant. (E) Raw data for NO consumption assay. (F) NO Consumption over Time. An * represents statistically significant from 4, 11, 18, and 25 days of storage, # represents statistically significant from 4 and 11 days of storage, and ** represents statistically significant from 4 days of storage. Overall P value for RM-ANOVA. (G) Nitric oxide consumption is directly proportional to the plasma heme concentration. (H) Arginase-1 levels increasing over time.

**Cell Free Plasma Hemoglobin and Microparticles Released During Red Blood Cell Storage Stoichiometrically Consumes Nitric Oxide via the Dioxygenation Reaction**

Ferrous oxyhemoglobin is known to react with NO via the dioxygenation reaction to form methemoglobin and nitrate (Eq. 1).[41] Consistent with its redox status measured by spectral deconvolution we hypothesized that one heme would react with and consume one NO via this reaction. To measure NO catabolism we injected supernatant from packed red blood cell units taken at one week intervals from 4 to 39 days into an anaerobic solution of NO, generated from the NO donor DETANOate.[34] As shown in Figure 1E we found that the concentration of NO consumed increased dramatically with red cell storage time. Suggesting a 1:1 reaction stoichiometry, the concentration of NO consumed rose to a similar extent as the concentration of cell free plasma hemoglobin (concentration measured and reported in terms of heme; Figure 1F). Indeed, the $R^2$ value for measured stored red cell supernatant heme vs. NO consumption was 0.99; ($P<0.0001$; Figure 1G) indicating a reaction of 1 mole of heme with one mole of NO consistent with Eq. 1. This is interesting as it indicates that hemoglobin remains in the reduced form capable of NO scavenging even after 39 days of storage.

In addition to NO dioxygenation reactions that could modulate NO bioavailability, human red cells also contain arginase-1, which metabolizes arginine to ornithine and thus reduces arginine bioavailability for de novo NO synthesis. We found that the stored red cell supernatant contains increasing concentrations of erythrocyte arginase-1 ranging from an average of 280 ± 69 ng/mL at 4 days of storage to 4633 ± 631 ng/mL at 39 days of storage (Figure 1H). We also found that the amount of cell free plasma hemoglobin and arginase-1 correlated significantly for each individual unit of packed red blood cells

with $R^2$ values for nine units ranged from 0.81-0.99 (all P values <0.015; Table I). While cell-free hemoglobin to arginase-1 correlation was high for individual units, when data from all units was combined the $R^2$ value dropped to 0.51 indicating that the hemoglobin to arginase-1 ratio varied considerably among donors.

**TABLE I. $R^2$ and P values for arginase-1 vs. cell-free plasma hemoglobin for each unit of packed red blood cells.**

| PRBC Unit | $R^2$ | p |
|---|---|---|
| A | 0.93 | 0.002 |
| B | 0.97 | <0.001 |
| C | 0.87 | 0.006 |
| D | 0.99 | <0.001 |
| E | 0.91 | 0.003 |
| F | 0.93 | 0.002 |
| G | 0.97 | <0.001 |
| H | 0.91 | 0.003 |
| I | 0.81 | 0.015 |

**Red Blood Cell Microparticles Inactivate Nitric Oxide at Rates Approaching Cell-Free Hemoglobin**

It has been known that stored red cells undergo membrane oxidation, damage and exocytosis to form microparticles. We measured these microparticles using flow cytometry of whole blood without centrifugation as shown in Figure 2A, for a

representative unit of packed red blood cells at days 4, 18 and 32. A small proportion of microparticles are evident at 4 days, but they increase dramatically over time. The percent microparticles in the packed red blood cell units increased with storage duration (median values were 0.24%, 0.37%, and 1.99% of total events at days 4, 18 and 32, respectively; Figure 2B). The microparticle doubling time was 9.0 days (95% CI: 7.7-10.7 days; $P < 0.001$) as determined by linear regression analysis.

While increases in microparticles have been appreciated for decades, to our knowledge the ability of these microparticles to react with NO faster than red cells has never been evaluated. Because the dioxygenation reaction of NO with hemoglobin (Eq. 1) is limited by compartmentalization within a red blood cell, which is substantially determined by red cell size, we hypothesized that hemoglobin in small microparticles should react with NO much faster than hemoglobin contained in red blood cells. To measure the reaction rates we first performed time-resolved absorptions measurements using a stopped flow apparatus for red cells and microparticles reacting with NO. Time-resolved absorbance spectra of the reaction of 0.05 mM red cell-encapsulated hemoglobin with 0.1 mM NO using the stopped-flow apparatus is described by an observed rate constant of 2.8 $s^{-1}$ (Figure 2C). Consistent with previous measurements [37,42], this gives a bimolecular rate constant on the order of 1000 times slower than for the NO dioxygenation by oxygenated cell free hemoglobin and illustrates the dramatic slowing of NO dioxygenation by intact red blood cells. Figure 2D displays analogous absorbance data, but for a reaction between 0.05 mM oxyhemoglobin encapsulated in microparticles and 0.05 mM NO. This NO concentration provides the slowest possible reaction rate while allowing complete conversion of microparticle-encapsulated hemoglobin into the

ferric form. The only species visible in this case, methemoglobin is the final product of the reaction. This is because the reaction is much faster than the reaction between red cell hemoglobin and NO and it is completely over within the dead time of the stopped flow apparatus. Assuming that it takes at least two lifetimes of the reaction until no kinetics may be observed, the lifetime of the dioxygenation of NO by microparticle–encapsulated hemoglobin must be less than or equal to half of the dead time of the stopped flow instrument. Considering the smallest NO concentration of 0.05 mM used in the reaction, this gives a lower boundary on the dioxygenation bimolecular rate constant for microparticles of at least $2.4 \times 10^{6}$ $M^{-1}s^{-1}$. These studies indicated that the reaction of microparticles with NO is too fast to be observed by stopped-flow, similarly to the reaction of NO and cell-free hemoglobin.

To more accurately measure the kinetics of the reaction of NO with microparticles we employed a laser photolysis method and compared the results to those obtained using cell-free hemoglobin. A mixture of red cell microparticles or hemoglobin and a solution of the NO donor potassium pentachloronitrosyl-ruthenate(II) ("caged NO") was passed through a quartz flow cell and the caged NO was released by laser photolysis as described in the methods section. Figure 2E shows the time-resolved absorbance data collected from the reaction between 0.02 mM cell-free oxyhemoglobin and a solution of 4 mM caged NO. The NO yield for this reaction was calculated to be 155 μM by using the observed rate of $7.75 \times 10^{-3}$ $\mu s^{-1}$ and the known bimolecular rate (see methods) of $5 \times 10^{7}$ $M^{-1}s^{-1}$. Figure 2F shows the absorbance spectra collected from a reaction of 0.02 mM microparticle-encapsulated hemoglobin and the same 4 mM caged NO solution as that used in the experiment of Figure 2E. The observed rate constant for this data set was

$2.74 \times 10^{-3}\ \mu s^{-1}$ giving a bimolecular rate constant of $1.77 \times 10^{7}\ M^{-1}s^{-1}$ when calculated using the NO yield from Figure 2E. The average value for the bimolecular rate constant of the dioxygenation reaction between microparticles and NO, for all experiments was $1.81 \pm 0.40 \times 10^{7}\ M^{-1}s^{-1}$ (n = 301, 3 separate experiments). Thus the dioxygenation reaction between microparticle-encapsulated hemoglobin and NO is only 2.5 to 3 times slower than that for free hemoglobin reacting with NO and approximately 1000 times faster than the reaction with red cell encapsulated-hemoglobin, as measured by photolysis experiments and by stopped flow (Figure 2G). The inset of graph of panel (2G) shows the three bimolecular rate constants on a logarithmic scale, which more clearly highlights the similarity of the cell free hemoglobin and microparticle NO reaction rates and their large difference from red cell-encapsulated hemoglobin. Hence, it is likely that in vivo microparticles will have an effect on NO bioavailability very similar to that of cell free plasma hemoglobin. This could be particularly important as microparticles are continuously elaborated after transfusion and are not known to be cleared by haptoglobin.

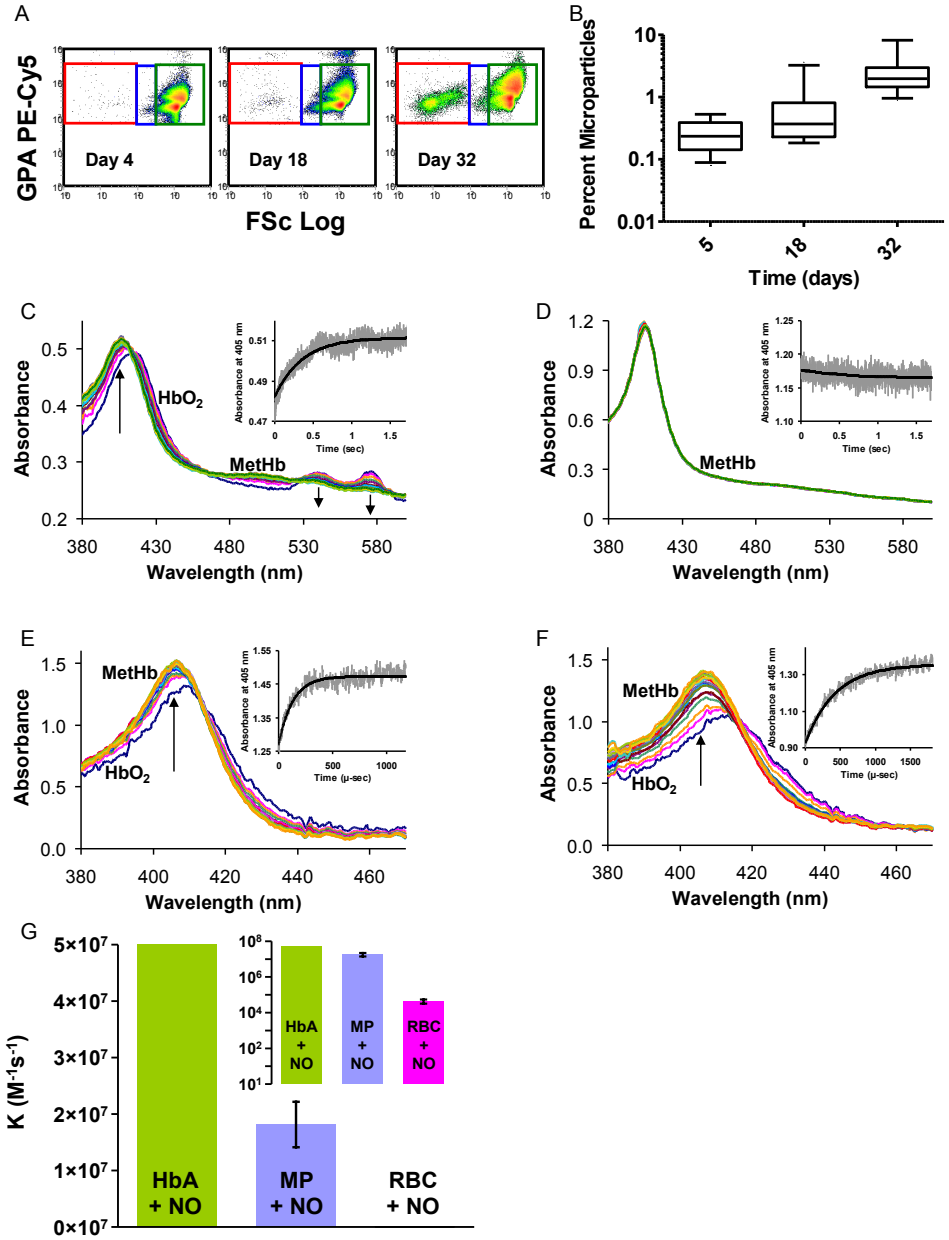


**Figure 2. Microparticle formation and NO scavenging in stored blood.** (A) The flow cytometry histograms show forward light scatter (FSc Log) versus fluorescence intensity of labeled glycophorin A PE-Cy5. Intact red blood cells have relatively high forward light scatter (green box). As they transition (blue box) to microparticles (MP) (red box) forward light scatter and GPA fluorescence intensity decrease. A small proportion of MPs are evident after short storage (4 days), but they increase significantly over time (B). Microparticle median values were 0.24, 0.37, and 1.99% at days 4, 18 and 32 of storage, respectively. (C) A reaction between 0.05 mM red cell-encapsulated oxyhemoglobin and 0.1 mM NO measured by stopped-flow. The arrows point in the direction of changing absorbance at the methemoglobin peak of 405 nm and at the oxyhemoglobin peaks of 541

and 577 nm. The inset shows absorbance at 405 nm. (D) A reaction between 0.05 mM microparticle-encapsulated oxyhemoglobin and 0.05 mM NO as measured by stopped-flow is too fast to be observed. (E) A reaction of 0.02 mM cell-free oxyhemoglobin with NO in a photolysis experiment. The inset shows absorbance at 405 nm. (F) A reaction of 0.02 mM microparticle-encapsulated oxyhemoglobin with NO in a photolysis experiment. The caged NO solution used is the same as that in the experiment of panel E. (G) The measured bimolecular rate constants for the dioxygention of NO by microparticle- and red blood cell-encapsulated oxyhemoglobin compared with the rate for cell-free oxyhemoglobin. The inset displays these data on a logarithmic scale.

**Evaluation of Reactive Oxygen Species and Free Iron Formation During Red Blood Cell Storage**

We explored oxygen free radical generation in the stored red cell supernatant using EPR spin trapping. The hydroxylamine spin probe CPH reacts with ROS as well as free iron to form the CP• radical which demonstrates a characteristic, 3 line EPR spectrum (Figure 3A). Incubation of the packed red blood cell supernatant with CPH for 10 min at 37°C produced a substantive CP• radical that increased significantly after 18 days of storage (Figure 3B). The generation of the CP• radical was inhibited in a dose dependent manner by the Fe chelator, deferoxamine suggesting free iron as the seminal reactant producing the CP• signal ($Fe^{3+}$ + CPH → $Fe^{2+}$ + CP•) rather than ROS (Figure 3C). To exclude contributions of ROS to the observed CP• formation and thus further support the interpretation that our signal was indeed dependent upon reaction of the spin probe and free iron, we exposed the packed red blood cell supernatants to the antioxidant enzymes catalase and superoxide dismutase, as well as a battery of inhibitors of enzymatic sources of ROS, (Figure 3D). Exposure of the 39-day samples to super oxide dismutase and/or catalase did not alter CP• radical production suggesting neither superoxide ($O_2^{\bullet -}$) nor hydrogen peroxide derived hydroxyl radical were responsible for the observed signal. Furthermore, inhibition of NADPH oxidases, xanthine oxidase,

aldehyde oxidase and nitric oxide synthases with the global FAD inhibitor, diphenyleneiodonium and/or specific inhibition of these enzymes (allopurinol for xanthine oxidase, raloxifene for aldehyde oxidase, *L*-NAME for both NO from nitric oxide synthase as well as $O_2^{\bullet-}$ produced from uncoupled nitric oxide synthases) did not alter the CP• intensity, confirming free iron as the seminal reactant responsible for our storage time-dependent CP• radical formation from the packed red blood cell supernatants. These experiments suggest that effects of stored red cell supernatant on NO levels are not driven by ROS-mediated NO catabolism.

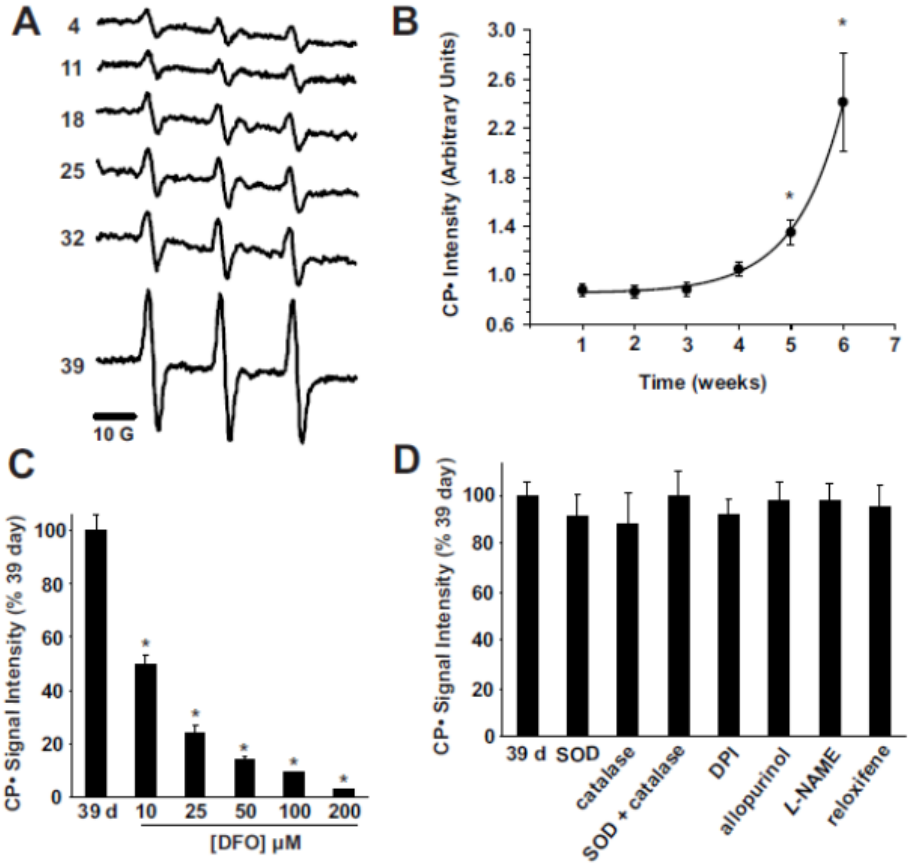


**Figure 3. Storage of packed red blood cells induces time-dependent, iron-mediated radical formation.** (A) Representative EPR spectra of CPH exposed to packed red blood cell supernatants for 10 min at 37°C. Spectra represent a signal average of 5 scans from t=9 to t=10 min. (B) The mean CP• signal intensity is displayed versus time (weeks) of storage (n=3). (C) Supernatants from 39 day old packed red blood cells were exposed to

50 μM CPH in the presence of increasing concentrations (10-200 μM) of deferoxamine (DFO). (D) Supernatants from 39 day old packed red blood cells were exposed to 50 μM CPH in the presence of SOD (100 U/mL), catalase (100 U/mL), SOD + catalase, diphenyleneiodonium (DPI) (100 μM), allopurinol (100μM), L-NAME (100 μM) and reloxifene (100 μM). Data represent mean ± SEM of at least three independent determinations, * indicates $P < 0.05$.

**Supernatant From Stored Red Blood Cells Produces Potent In Vivo Vasoconstriction in a Rat Model that Correlates With the Extent of In-Storage Hemolysis**

We have identified molecular mediators in stored red cell supernatant that have the potential to substantially impair NO signaling following red blood cell transfusion. In order to directly test whether these factors modulate vascular reactivity we infused the stored red cell supernatant from the stored red blood cell units into the rat systemic circulation and compared this with the supernatant from the same human blood donor that was obtained earlier at 4 days of storage. Infusions of stored red cell supernatant for each human donor unit were performed in two rats in the same day to control for potential time effects in the model. The mean cell free plasma hemoglobin concentration of the five packed red blood cell units used in this assay was 26 ± 7 μM (range 13-45 μM) at 4 days of storage and 125 ± 25 μM (range 87 -185 μM) at 39 days of storage. We infused 4.95 mL/kg of stored red cell supernatant into the rats in order to model the amount infused with a 3-unit red blood cell transfusion into humans. We found that the 4-day old stored red cell supernatant increased MAP to a mean of 6 ± 2 % above baseline (n=5) over the approximate 40 minute period of infusion. All five infusions of 39 day old stored red cell supernatant showed a greater increase in MAP compared to infusion of the corresponding supernatant that was obtained at 4 days of storage. The mean increase in

normalized MAP after infusion of supernatant obtained at 39 days of storage was significantly higher (p=0.003) with an increase of 17 ± 4 % (n=5) in MAP above baseline (Figure 4A and B). There was a significant correlation ($R^2$=0.65) between the amount of hemoglobin present in the supernatant and the percentage increase in blood pressure above baseline (Figure 4C).

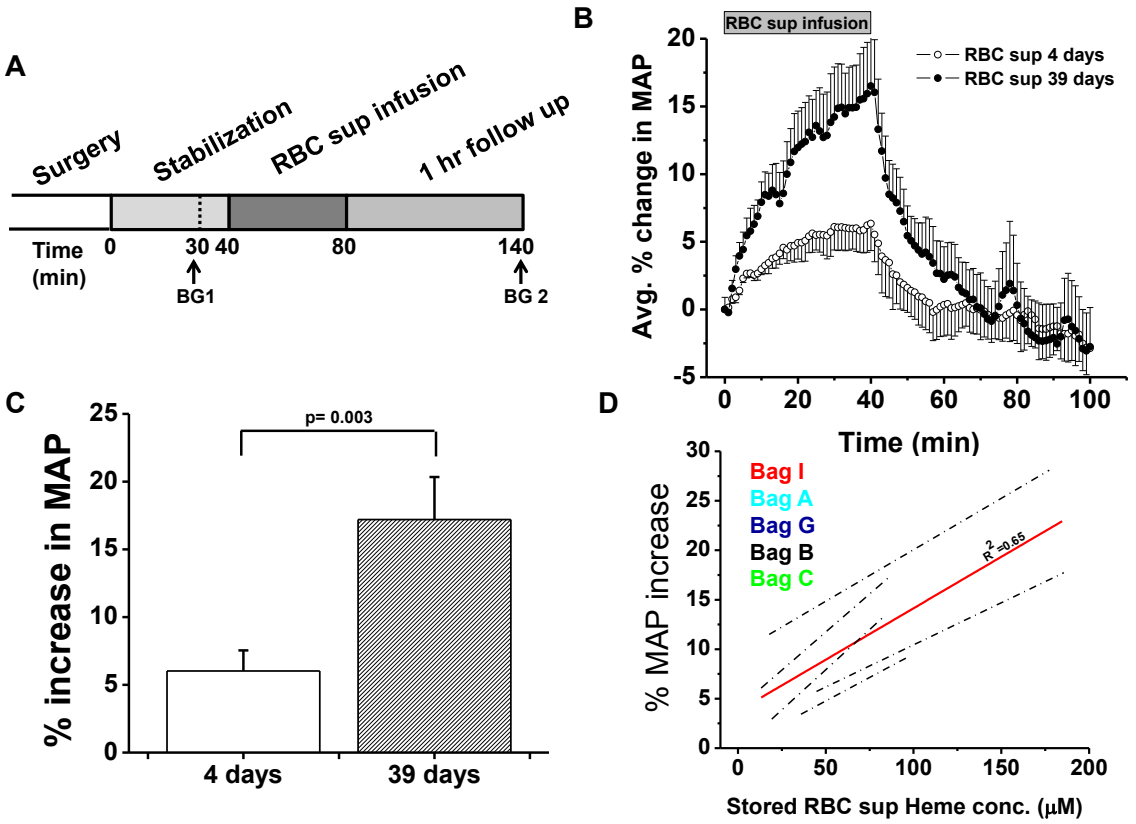


**Figure 4. Vasoactivity of infused packed red cell supernatant/plasma.** (A) Experimental time line for packed red cell supernatant infusions. Rats were stabilized for 30 minutes after surgery and blood gasses were drawn as indicated (BG 1 and 2). Supernatant (1.6 mL) of packed red blood cells stored either for 4 or 39 days was infused for 40 min, after which the rats were followed up for 1 hour (n=5). (B) Change in MAP over time after packed red blood cell supernatant infusion and 60 minute follow up. (C) Average percentage peak increase in MAP after infusion of packed red blood cell supernatants (P < 0.003). (D) Correlation (solid line) between the PRBC supernatant heme concentration and the percentage increase in MAP after a 40 minute infusion of either 4 days (●) or 39 days (■) stored PRBC supernatant ($r^2$ = 0.65). Each data point

was obtained from a separate rat infusion experiment (2 groups of n=5). All values are displayed as mean ± SEM.

**Microparticle Hemoglobin Content in Stored Blood Plasma Infused in Rat Experiments and Half-Life in Vivo**

To quantify the concentration of hemoglobin contained in microparticles in aged blood infused in our experiments we measured hemoglobin concentrations in microparticles in the 9 units of banked human blood at 6-weeks of storage. In these samples we evaluated the concentration of microparticles after centrifugation speeds of 2700 g, which was the protocol used to prepare the plasma. Note that quantification of microparticles by flow cytometry in Figure 2A and Figure 2B was measured in uncentrifuged stored units. The levels of microparticles were determined by measuring the hemoglobin concentration by Drabkin's reaction before and after centrifugation at 37,000 g to remove all microparticles. The median percentage of hemoglobin in the plasma contained in microparticles was 10.4 % (minimum = 3.2%, maximum = 23.7%). The mean ± SEM was 11.6% ± 2.2%. The hemoglobin concentration of these microparticles had a median of 9.1μM (minimum = 1.1μM, maximum = 17.2μM) and a mean ± SEM of 8.5 ±2.2μM. We also examined the amount of microparticles in 6 units of expired blood that was centrifuged at 750 x g and a median of 15% (minimum = 6%, maximum = 40%) of the plasma hemoglobin was contained in microparticles (mean ±SEM measured 17.9% ± 4.8%. The hemoglobin concentration of these microparticles had a median of 30.2μM ( minimum = 3.4 μM, maximum = 56.6 μM) and a mean ±SE of 31.9 ± 9.3μM.

Estimation of microparticle clearance rates for human microparticles infused into our *in vivo* rat model was achieved by infusing human RBC-derived microparticles into rats (n=2) and monitoring for human Hb in the rat plasma at selected time points (pre-infusion, 5, 10, 15, 20, 30 and 45 min). Microparticles were quantified by measuring the total human hemoglobin concentrations (ELISA) and by flow cytometry. We measured the double positive events (Glycophorin A-$PE^+$ Annexin V-$FITC^+$) in the microparticle size range, enumerated based upon their ratio to a known amount of Absolute Count Standard fluorescent microbeads in each sample. As shown in Figure 1 in the online-only Data Supplemental, the half-life of human microparticles in our rat model is less than 15-20 minutes, consistent with our observed drop in MAP after cessation of infusion of stored blood plasma. In aggregate these experiments suggest that the majority of hemoglobin in our rat experiments is in the form of free plasma hemoglobin. However, the effect of microparticles may be more after transfusion of packed red blood cell units as these have higher quantities of microparticles and the transfused red cells will continue to elaborate microparticles after infusion.

**Concentrations of Hemoglobin and Redox Status of Hemoglobin Necessary to Induce Vasoconstriction in the Rat Model**

Kinetic modeling suggests that levels of plasma hemoglobin as low as 1 μM can limit NO bioavailability.[43] These results notwithstanding, doubts have been expressed as to whether such low levels of plasma hemoglobin can significantly modulate in vivo vascular function.[44] Consistent with these theoretical studies, prior experiments have shown reduced NO responsiveness in rabbit tissues infused with as little as 6 μM hemoglobin (all concentrations in terms of heme), and we have found that vasodilator

responsiveness to NO donor (nitroprusside) are blunted by 80% in patients with sickle cell anemia who had plasma heme concentrations greater than or equal to 6 μM.[26] Despite these data, a number of investigators suggest that these low levels of plasma hemoglobin cannot modulate vascular function.[44] In order to directly test whether the low concentrations of cell-free plasma hemoglobin present in packed red blood cells are capable of producing vasoconstriction we infused a human hemoglobin solution over 10 minutes and evaluated the changes in MAP vs. the cell free plasma hemoglobin concentration. As shown in Figure 5A (and inset), infusion of human oxyhemoglobin produces a robust and immediate vasoconstrictive effect, even at levels below 10 μM. To determine if this is related to the NO dioxygenation reaction (eq. 1) versus a colloid osmotic property or the generation of ROS by the ferric form of hemoglobin (methemoglobin or ferryl-hemoglobin) we compared the infusions of oxyhemoglobin to the same concentration of methemoglobin and cyanomethemoglobin. The latter species is "locked" in a redox inactive form which cannot bind oxygen or participate in redox reactions, and represents a more rigorous control for colloid osmotic property effects. As shown in Figure 5B, there were no significant differences between methemoglobin and cyanomethemoglobin, while ferrous oxyhemoglobin produced a robust vasoconstriction. Finally, in separate experiments we infused oxyhemoglobin and serially sampled the plasma from the rat for measurement of NO consumption during continuous infusion. As shown in Figure 5C, the infusion of oxyhemoglobin produced a dose dependent increase in the NO consumption within plasma, which was of similar magnitude to the levels of plasma hemoglobin in the circulation, consistent with a mechanism mediated by rapid NO dioxygenation (scavenging). As indicated in reference 44 this concept is still very

controversial. Our results are the first to show that such low concentrations of heme (6 μM) scavenge NO and produce vasoconstriction, and the first to compare this response with an exact hemoglobin control, cyanomethemoglobin.

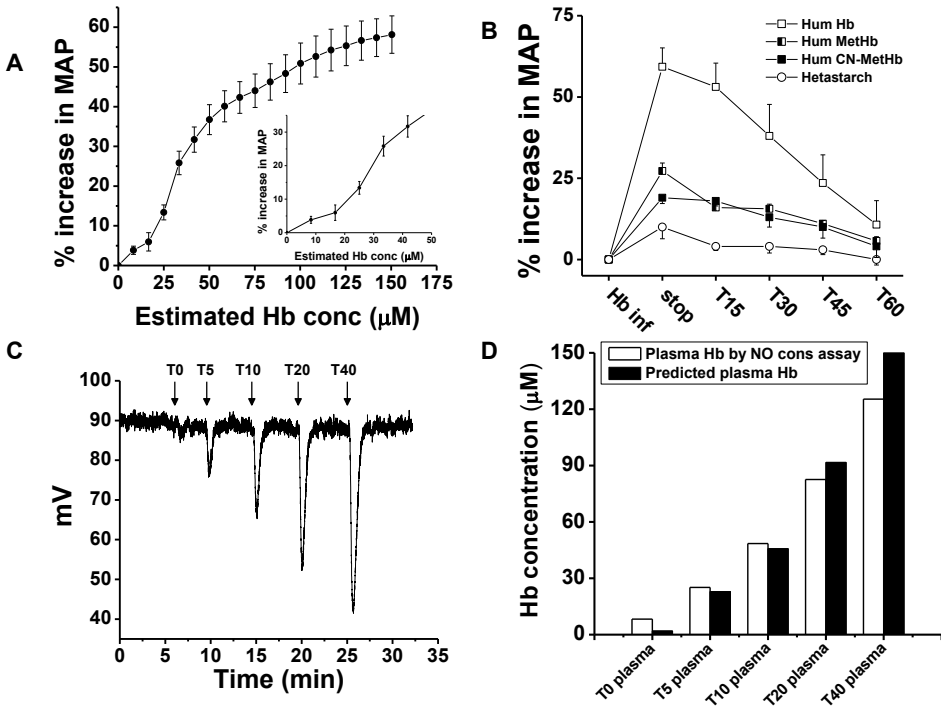


**Figure 5. Low concentrations of ferrous oxyhemoglobin increase MAP in rats.** (A) Percentage increase in MAP after infusion of human hemoglobin as a function of estimated rat plasma hemoglobin concentration (expressed as heme) as calculated from the dilution of infused hemoglobin in rat plasma volume over the 40-min infusion time. The inset shows a magnification of the data for a plasma hemoglobin concentration between 0 to 60 μM. (B) Percentage increase in MAP after infusion of unmodified human hemoglobin (□) and after modification of human hemoglobin to methemoglobin (◧) or cyanomethemoglobin (■) compared to infusion of the plasma expander hetastarch (○). (C) Rat plasma samples obtained before (T0), and after 5, 10, 20 and 40 min (T5-40) of infusion of human packed red blood cell supernatant and then were analyzed by tri-iodide chemiluminescence for NO consumption. (D) The area under the peaks (NO consumption) was quantified (open bars) and compared with the levels of cell free plasma hemoglobin.

**Discussion**

In these studies, we have examined the novel hypothesis that a component of the storage lesion is directly related to in vitro and in vivo hemolysis with dysregulation of redox pathways in NO signaling mediated by catabolism of NO and arginine. Previous studies have documented substantial hemolysis that increases cell free plasma hemoglobin as a function of time, reaching 28 μM (in heme) in packed red blood cells on average after 35 days of storage in citrate-phosphate-dextrose-adenine anticoagulant (CPDA).[20] Another study reported up to an average of 593 μM (in heme) after storage for 35 days in CPDA.[21] More recently, hemolysis was reported to be about 0.8% by day 50 of storage.[22] This is approximately 80 μM heme and consistent with our measurements in ADSOL. Given the low threshold for acceptable red blood cell viability (70% post-transfusion) in current guidelines, we suggest that intravascular hemolysis and elaboration of microparticles after transfusion may also be considerable.

A central problem with hemolysis in stored blood may involve the effects on NO bioavailability. Nitric oxide plays several major roles in human physiology. Nitric oxide functions as a neurotransmitter, a macrophage-derived host-defense molecule, inhibits platelet aggregation and endothelium adhesion molecule expression, is an antioxidant, and is a potent vasodilator. [45,46] To elicit its vasodilatory activity, NO must diffuse to the smooth muscle cells and activate sGC. In 1994, Lancaster suggested that the endothelium's proximity to millimolar concentrations of hemoglobin, would severely compromise the efficiency of the NO/sGC pathway.[47] Hemoglobin scavenges NO primarily through a classic dioxygenation reaction, where NO reacts with oxyhemoglobin to form methemoglobin (where the heme irons are ferric) and nitrate (Eq. 1). This

reaction, involving the oxidation of the ferrous heme iron ($Fe^{+2}$) to a ferric iron ($Fe^{+3}$), occurs at a rate of 6-8 × $10^7$ $M^{-1}s^{-1}$.[25,48] Because of the speed of this reaction, NO can only diffuse about 0.07 μm (assuming a diffusion constant of 3000 $\mu m^2$ $s^{-1}$ and 10 millimolar hemoglobin). Since NO is freely diffusible, the presence of hemoglobin on one side of the endothelium decreases the concentration of NO on the other side as well.

The reason that endothelial-derived NO does not undergo the dioxygenation reaction (Eq. 1) to the extent predicted, based purely on kinetic calculations, is that red blood cell-encapsulated hemoglobin reacts with NO much more slowly than does cell free plasma hemoglobin.[42,49-53] Three mechanisms contribute to reduced NO scavenging by red blood cells: (1) the rate of the reaction is largely limited by external diffusion of NO to the red blood cell; (2) NO diffusion is partially blocked by a physical barrier across the erythrocyte membrane; and (3) erythrocyte-encapsulated hemoglobin is efficiently compartmentalized in the lumen; it does not extravasate into the endothelium and interstitium. None of the three mechanisms responsible for reduced NO scavenging by hemoglobin encapsulated in intact red cells pertain to either free hemoglobin in plasma or to hemoglobin in microparticles, and all three of the mechanisms will break down upon hemolysis.

The enhanced ability of cell free plasma hemoglobin to scavenge NO has been widely attributed to the hypertension, increased systemic and pulmonary vascular resistance, and morbidity and mortality associated with administration of hemoglobin-based oxygen carriers (HbOCs or "blood substitutes").[54-58] Until recently, little attention has been paid to complications due to NO scavenging by cell free plasma hemoglobin in hemolytic disease, in part because the levels of plasma hemoglobin were so low.[26,59]

However, experiments show reduced NO responsiveness in rabbit tissues infused with as little as 6 μM hemoglobin (all concentrations in terms of heme) [60], and we found that vasodilator responsiveness to NO donor (nitroprusside) was blunted by 80% in patients with sickle cell anemia who had plasma heme concentrations greater than or equal to 6 μM.[26] We also demonstrated that intravascular hemolysis leads to vasoconstriction and impairs renal function in a canine intravascular hemolysis model.[61] Indeed, accumulating transgenic animal, large animal and human epidemiological evidence supports a role for hemolysis in the pathobiology of sickle cell disease and other hemolytic anemias.[29,30,61-65] In the current studies we confirm that levels of cell free plasma hemoglobin during acute infusions below 10 μM increased MAP. We further found that this effect was in large part mediated by ferrous oxyhemoglobin, rather than methemoglobin or protein-dependent increases in colloid osmotic pressure.

Our current studies suggest that a 3-4 unit packed red blood cell transfusion of aged blood has the potential to inhibit systemic NO signaling. The effects of cell free plasma ferrous oxyhemoglobin would be compounded by the delivery of red cell microparticles, and the latter may be more important owing to the fact that they would be resistant to clearance by the haptoglobin-CD163 clearance system and through the kidneys. In this study we hypothesized and confirmed using advanced reaction measurements that red cell microparticles scavenge NO rapidly, with the potential to inhibit NO bioavailability in transfused blood.

We recognize that the ongoing steady-state levels of plasma hemoglobin in patients with hemolytic anemias, such as sickle cell disease, likely differ markedly from the situation after red blood cell transfusion, where plasma hemoglobin levels may only

be transiently elevated following even substantial blood transfusions. Based on the relatively short half lives of both free hemoglobin and microparticles derived from transfused stored blood, the overall impact of transfusion on NO depletion and other effects of non-erythrocyte hemoglobin will be transient. Whether a transient inhibition in NO signaling is sufficient to increase the risk of multi-organ dysfunction or hemostatic activation in at-risk populations of patients remains to be determined.

Additional effects of hemolysis in stored blood were evaluated in our studies and may have contributed to the vasoactive effects we observed. One is the release of red cell arginase-1 into plasma. This enzyme converts arginine to ornithine, thus reducing arginine availability for NO synthesis.[29,63] Arginasemia has been correlated with hemolysis in a number of human diseases and high enzyme activity is associated with the development of pulmonary hypertension and increased prospective mortality. Previous work has shown that arginase levels increase in stored blood as a function of time.[66,67]

**Conclusions**

Based on these studies showing that even low levels of cell free plasma hemoglobin are sufficient to inhibit endothelial NO signaling and induce vasoconstriction and hypertension, we propose that hemolysis and microparticle formation, as well as arginase-1 release, during storage and after transfusion of aged erythrocytes contributes to decreased NO bioavailability and cardiovascular dysfunction. This effect may represent a contribution to organ injury in the susceptible host receiving multiple red blood cell transfusions. These studies suggest that new therapeutic avenues for red cell storage and transfusion should be studied. For example, methods to limit storage related hemolysis and microparticle formation using ATP sustaining preservation solutions, co-

transfusion of hemoglobin scavenger molecules like haptoglobin or hemoglobin-binding peptides, red cell membrane stabilizing agents, as well as NO signaling/donor agents.

**Acknowledgements**

We thank Zaharo Tsekouras for technical assistance.

**Sources of Funding**

Mark Gladwin and Daniel Kim-Shapiro receive research support from NIH grant RO1HL098032. Dr. Gladwin also receives research support from the Institute for Transfusion Medicine and the Hemophilia Center of Western Pennsylvania.

**Disclosures**

Drs. Gladwin and Kim-Shapiro are coauthors on patent applications related to treating hemolysis.

References


1. The 2007 National Blood Collection and Utilization Survey Report. In. Washington DC: US Dept of Health and Human Services; 2009.
2. Vincent JL, Baron JF, Reinhart K, et al. Anemia and blood transfusion in critically ill patients. JAMA 2002;288:1499-507.
3. Napolitano LM, Kurek S, Luchette FA, et al. Clinical practice guideline: red blood cell transfusion in adult trauma and critical care. Crit Care Med 2009;37:3124-57.
4. Corwin HL, Gettinger A, Pearl RG, et al. The CRIT Study: Anemia and blood transfusion in the critically ill--current clinical practice in the United States. Crit Care Med 2004;32:39-52.
5. Collins JA, James PM, Bredenberg CE, Anderson RW, Heisterkamp CA, Simmons RL. The relationship between transfusion and hypoxemia in combat casualties. Ann Surg 1978;188:513-20.
6. Fowler AA, Hamman RF, Good JT, et al. Adult respiratory distress syndrome: risk with common predispositions. Ann Intern Med 1983;98:593-7.
7. Martin AM, Jr., Simmons RL, Heisterkamp CA, 3rd. Respiratory insufficiency in combat casualties. I. Pathologic changes in the lungs of patients dying of wounds. Ann Surg 1969;170:30-8.
8. Koch CG, Li L, Sessler DI, et al. Duration of red-cell storage and complications after cardiac surgery. New Engl J Med 2008;358:1229-39.
9. de Watering LV, Lorinser J, Versteegh M, Westendord R, Brand A. Effects of storage time of red blood cell transfusions on the prognosis of coronary artery bypass graft patients. Transfusion 2006;46:1712-8.

10. Vandromme MJ, McGwin G, Jr., Marques MB, Kerby JD, Rue LW, 3rd, Weinberg JA. Transfusion and pneumonia in the trauma intensive care unit: an examination of the temporal relationship. J Trauma 2009;67:97-101.
11. Weinberg JA, McGwin G, Jr., Marques MB, et al. Transfusions in the less severely injured: does age of transfused blood affect outcomes? J Trauma 2008;65:794-8.
12. Leal-Noval SR, Rincon-Ferrari MD, Garcia-Curiel A, et al. Transfusion of blood components and postoperative infection in patients undergoing cardiac surgery. Chest 2001;119:1461-8.
13. Zallen G, Offner PJ, Moore EE, et al. Age of transfused blood is an independent risk factor for postinjury multiple organ failure. Am J Surg 1999;178:570-2.
14. Edgren G, Kamper-Jorgensen M, Eloranta S, et al. Duration of red blood cell storage and survival of transfused patients (CME). Transfusion 2010;50:1185-95.
15. Triulzi DJ, Yazer MH. Clinical studies of the effect of blood storage on patient outcomes. Transfus Apher Sci 2010;43:95-106.
16. Tinmouth A, Fergusson D, Yee IC, Hebert PC. Clinical consequences of red cell storage in the critically ill. Transfusion 2006;46:2014-27.
17. Tinmouth A, Chin-Yee I. The clinical consequences of the red cell storage lesion. Transfus Med Rev 2001;15:91-107.
18. Dumaswala UJ, Dumaswala RU, Levin DS, Greenwalt TJ. Improved red blood cell preservation correlates with decreased loss of bands 3, 4.1, acetylcholinestrase, and lipids in microvesicles. Blood 1996;87:1612-6.

19. Greenwalt TJ, Bryan DJ, Dumaswala UJ. Erythrocyte-Membrane Vesiculation and Changes in Membrane-Composition During Storage in Citrate-Phosphate-Dextrose-Adenine-1. Vox Sanguinis 1984;47:261-70.

20. Latham JT, Bove JR, Weirich FL. Chemical and Hematologic Changes in Stored Cpda-1 Blood. Transfusion 1982;22:158-9.

21. Aubuchon JP, Estep TN, Davey RJ. The Effect of the Plasticizer Di-2-Ethylhexyl Phthalate on the Survival of Stored Rbcs. Blood 1988;71:448-52.

22. Salzer U, Zhu R, Luten M, et al. Vesicles generated during storage of red cells are rich in the lipid raft marker stomatin. Transfusion 2008;48:451-62.

23. Greenwalt TJ, McGuinness CG, Dumaswala UJ. Studies in Red-Blood-Cell Preservation .4. Plasma Vesicle Hemoglobin Exceeds Free Hemoglobin. Vox Sanguinis 1991;61:14-7.

24. Lutz HU, Liu SC, Palek J. Release of Spectrin-Free Vesicles from Human Erythrocytes During Atp Depletion .1. Characterization of Spectrin-Free Vesicles. Journal of Cell Biology 1977;73:548-60.

25. Herold S, Exner M, Nauser T. Kinetic and mechanistic studies of the NO*-mediated oxidation of oxymyoglobin and oxyhemoglobin. Biochemistry 2001;40:3385-95.

26. Reiter CD, Wang X, Tanus-Santos JE, et al. Cell-free hemoglobin limits nitric oxide bioavailability in sickle-cell disease. Nat Med 2002;8:1383-9.

27. Greenwalt TJ. The how and why of exocytic vesicles. Transfusion 2006;46:143-52.

28. Willekens FL, Werre JM, Kruijt JK, et al. Liver Kupffer cells rapidly remove red blood cell-derived vesicles from the circulation by scavenger receptors. Blood 2005;105:2141-5.

29. Rother RP, Bell L, Hillmen P, Gladwin MT. The clinical sequelae of intravascular hemolysis and extracellular plasma hemoglobin - A novel mechanism of human disease. Jama-Journal of the American Medical Association 2005;293:1653-62.

30. Morris CR, Kato GJ, Poijakovic M, et al. Dysregulated arginine metabolism, hemolysis-associated pulmonary hypertension, and mortality in sickle cell disease. Jama-Journal of the American Medical Association 2005;294:81-90.

31. MacArthur PH, Shiva S, Gladwin MT. Measurement of circulating nitrite and S-nitrosothiols by reductive chemiluminescence. J Chromatogr B Analyt Technol Biomed Life Sci 2007;851:93-105.

32. Yang BK, Vivas EX, Reiter CD, Gladwin MT. Methodologies for the sensitive and specific measurement of S-nitrosothiols, iron-nitrosyls, and nitrite in biological samples. Free RadicRes 2003;37:1-10.

33. Huang Z, Louderback JG, Goyal M, Azizi F, King SB, Kim-Shapiro DB. Nitric oxide binding to oxygenated hemoglobin under physiological conditions. Biochim Biophys Acta 2001;1568:252-60.

34. Wang X, Tanus-Santos JE, Reiter CD, et al. Biological activity of nitric oxide in the plasmatic compartment. Proc Natl Acad Sci U S A 2004;101:11477-82.

35. Janka JJ, Koita OA, Traore B, et al. Increased pulmonary pressures and myocardial wall stress in children with severe malaria. J Infect Dis 2010;202:791-800.

36. Xiong Z, Cavaretta J, Qu L, Stolz DB, Triulzi D, Lee JS. Red blood cell microparticles show altered inflammatory chemokine binding and release ligand upon interaction with platelets. Transfusion 2010.

37. Azarov I, Huang KT, Basu S, Gladwin MT, Hogg N, Kim-Shapiro DB. Nitric oxide scavenging by red blood cells as a function of hematocrit and oxygenation. J Biol Chem 2005;280:39024-8032.

38. Tonomura B, Nakatani H, Ohnishi M, Yamaguchiito J, Hiromi K. Test Reactions for a Stopped-Flow Apparatus - Reduction of 2,6-Dichlorophenolindophenol and Potassium Ferricyanide by L-Ascorbic-Acid. Anal Biochem 1978;84:370-83.

39. Azarov I, He XJ, Jeffers A, et al. Rate of nitric oxide scavenging by hemoglobin bound to haptoglobin. Nitric Oxide-Biol Chem 2008;18:296-302.

40. Huang KT, Huang Z, Kim-Shapiro DB. Nitric Oxide Red Blood Cell Membrane Permeability at high and low Oxygen Tension. Nitric Oxide 2007;16:209-16.

41. Eich RF, Li TS, Lemon DD, et al. Mechanism of NO-induced oxidation of myoglobin and hemoglobin. Biochemistry 1996;35:6976-83.

42. Carlsen E, Comroe JH. The rate of uptake of Carbon Monoxide and of Nitric Oxide by normal and human erythrocytes and experimentally produced spherocytes. Journal of General Physiology 1958;42:83-107.

43. Jeffers A, Gladwin MT, Kim-Shapiro DB. Computation of plasma hemoglobin nitric oxide scavenging in hemolytic anemias. Free Radical Biology and Medicine 2006;41:1557-65.

44. Bunn HF, Nathan DG, Dover GJ, et al. Pulmonary hypertension and nitric oxide depletion in sickle cell disease. Blood;116:687-92.

45. Schmidt PM, Schramm M, Schroder H, Wunder F, Stasch JP. Identification of residues crucially involved in the binding of the heme moiety of soluble guanylate cyclase. J Biol Chem 2004;279:3025-32.

46. Patel RP, McAndrew J, Sellak H, et al. Biological aspects of reactive nitrogen species. Biochim Biophys Acta-Bioenerg 1999;1411:385-400.

47. Lancaster JR. Simulation of the Diffusion and Reaction of Endogenously Produced Nitric-Oxide. Proc Natl Acad Sci U S A 1994;91:8137-41.

48. Doyle MP, Hoekstra JW. Oxidation of nitrogen oxides by bound dioxygen in hemoproteins. J Inorg Biochem 1981;14:351-8.

49. Coin JT, Olson JS. Rate of Oxygen-Uptake by Human Red Blood-Cells. J Biol Chem 1979;254:1178-90.

50. Butler AR, Megson IL, Wright PG. Diffusion of nitric oxide and scavenging by blood in the vasculature. Biochim Biophys Acta-Gen Subj 1998;1425:168-76.

51. Vaughn MW, Kuo L, Liao JC. Estimation of nitric oxide production and reaction rates in tissue by use of a mathematical model. Am J Physiol-Heart Circul Physiol 1998;274:H2163-H76.

52. Vaughn MW, Huang KT, Kuo L, Liao JC. Erythrocyte consumption of nitric oxide: Competition experiment and model analysis (vol 5, pg 18, 2001). Nitric Oxide-Biol Chem 2001;5:425-.

53. Liu XP, Miller MJS, Joshi MS, Sadowska-Krowicka H, Clark DA, Lancaster JR. Diffusion-limited reaction of free nitric oxide with erythrocytes. J Biol Chem 1998;273:18709-13.

54. Vogel WM, Dennis RC, Cassidy G, Apstein CS, Valeri CR. Coronary Constrictor Effect of Stroma-Free Hemoglobin-Solutions. Am J Physiol 1986;251:H413-H20.

55. Hess JR, Macdonald VW, Brinkley WW. Systemic and Pulmonary-Hypertension after Resuscitation with Cell-Free Hemoglobin. J Appl Physiol 1993;74:1769-78.

56. Lee R, Neya K, Svizzero TA, Vlahakes GJ. Limitations of the Efficacy of Hemoglobin-Based Oxygen-Carrying Solutions. J Appl Physiol 1995;79:236-42.

57. Murray JA, Ledlow A, Launspach J, Evans D, Loveday M, Conklin JL. The Effects of Recombinant Human Hemoglobin on Esophageal Motor Function in Humans. Gastroenterology 1995;109:1241-8.

58. Ulatowski JA, Nishikawa T, MathesonUrbaitis B, Bucci E, Traystman RJ, Koehler RC. Regional blood flow alterations after bovine fumaryl beta beta-crosslinked hemoglobin transfusion and nitric oxide synthase inhibition. Critical Care Medicine 1996;24:558-65.

59. Reiter CD, Gladwin MT. An emerging role for nitric oxide in sickle cell disease vascular homeostasis and therapy. Curr Opin Hematol 2003;10:99-107.

60. Pohl U, Lamontagne D. Impaired Tissue Perfusion after Inhibition of Endothelium-Derived Nitric-Oxide. Basic Research in Cardiology 1991;86:97-105.

61. Minneci PC DK, Zhi H, Yuen PS, Star RA, Banks SM, Schechter AN, Natanson C, Gladwin MT, Solomon SB. Hemolysis-associated endothelial dysfunction mediated by accelerated NO inactivation by decompartmentalized oxyhemoglobin. J Clin Invest 2005;115:3409-17.

62. Gladwin MT. Unraveling the hemolytic subphenotype of sickle cell disease. Blood 2005;106:2925-6.

63. Kato GJ, McGowan VR, Machado RF, et al. Lactate dehydrogenase as a biomarker of hemolysis-associated nitric oxide resistance, priapism, leg ulceration, pulmonary hypertension and death in patients with sickle cell disease. Blood 2006;107:2279-85.

64. Nolan VG, Wyszynski DF, Farrer LA, Steinberg MH. Hemolysis-associated priapism in sickle cell disease. Blood 2005;106:3264-7.

65. Gladwin MT, Sachdev V, Jison ML, et al. Pulmonary hypertension as a risk factor for death in patients with sickle cell disease. New England Journal of Medicine 2004;350:886-95.

66. Bernard A, Meier C, Lopez N, et al. Packed red blood cell-associated arginine depletion is mediated by arginase. Journal of Trauma-Injury Infection and Critical Care 2007;63:1108-12.

67. Prins HA, Houdijk APJ, Nijveldt RJ, et al. Arginase release from red blood cells: Possible link in transfusion induced immune suppression? Shock 2001;16:113-5.

# CHAPTER III

# MECHANISMS OF SLOWER NITRIC OXIDE UPTAKE BY RED BLOOD CELLS AND OTHER HEMOGLOBIN-CONTAINING VESICLES

I. Azarov, C. Liu, H. Reynolds, Z. Tsekouras, J. S. Lee, M. T. Gladwin, D. B. Kim-Shapiro

The following manuscript was published in the Journal of Biological Chemistry, volume 286, pages 33567-33579, 2011, and is reprinted with permission. Stylistic variations are due to the requirements of the journal. I. Azarov, C. Liu, and H. Reynolds performed all experiments. I. Azarov and C. Liu analyzed experimental data. I. Azarov organized all experiments and conducted computational simulations. I. Azarov and D. B. Kim-Shapiro wrote the manuscript. C. Liu edited the manuscript.

# MECHANISMS OF SLOWER NITRIC OXIDE UPTAKE BY RED BLOOD CELLS AND OTHER HEMOGLOBIN-CONTAINING VESICLES

Ivan Azarov[1,2,3], Chen Liu[1], Hannah Reynolds[1], Zaharo Tsekouras[1], Janet S. Lee[3,4], Mark T. Gladwin[3,4] and Daniel B. Kim-Shapiro[1*]

From the Departments of [1]Physics and [2]Computer Science, Wake Forest University, Winston-Salem, NC 27109, [3]Vascular Medicine Institute, University of Pittsburgh, Pittsburgh, PA, 15213, [4]Department of Medicine, Division of Pulmonary, Allergy and Critical Care Medicine, University of Pittsburgh School of Medicine, Pittsburgh, PA, 15213

Running Head: NO Uptake by Membrane-Encapsulated Hemoglobin

Address correspondence to Daniel B. Kim-Shapiro, Department of Physics, Winston-Salem, NC 27109, Tel. 336-758-4993; Fax: 336-758-4973, Email: shapiro@wfu.edu

## ABBREVIATIONS

Hb, hemoglobin; MetHb, methemoglobin; NO, nitric oxide; RBC, red blood cell; CO, carbon monoxide; EPR, electron paramagnetic resonance spectroscopy; DPBS, Dubelco's phosphate buffered saline; PBS, phosphate buffered saline

## ABSTRACT

Nitric Oxide (NO) acts as a smooth muscle relaxation factor and plays a crucial role in maintaining vascular homeostasis. NO is scavenged rapidly by hemoglobin (Hb). However, under normal physiological conditions, the encapsulation of Hb inside red blood cells (RBCs) significantly retards this reaction, permitting NO to reach the smooth muscle. The rate limiting factors (diffusion of NO to the RBC surface, through the RBC membrane or inside of the RBC) responsible for this retardation have been the subject of much debate. Knowing the relative contribution of each of these factors is important for several reasons including optimization of the development of blood substitutes where Hb is contained within phospholipid vesicles. We have thus performed experiments of NO

uptake by erythrocytes and by microparticles derived from erythrocytes and conducted simulations of these data as well as that of others. We have included extracellular diffusion (that is, diffusion of the NO to the membrane) and membrane permeability, in addition to intracellular diffusion of NO, in our computational models. We find that all these mechanisms may modulate NO uptake by membrane-encapsulated Hb and that extracellular diffusion is the main rate limiting factor for phospholipid vesicles and erythrocytes. In the case of red cell microparticles, we find a major role for membrane permeability. These results are consistent with prior studies indicating that extracellular diffusion of several gas ligands is also rate limiting for erythrocytes, with some contribution of a low membrane permeability.

**INTRODUCTION**

Hemoglobin (Hb) encapsulated within red blood cells scavenges NO at a significantly slower rate than hemoglobin that is freely dissolved within blood plasma (cell-free Hb) (1-4). A similar effect is observed for the uptake of oxygen (5-7). This reduction in the scavenging rate allows NO that is produced in the endothelial cells within the walls of blood vessels to diffuse to the smooth muscle in sufficient concentrations to activate soluble guanylate cyclase (8-12), which would not be possible otherwise (13). NO thus effectively functions as a smooth muscle relaxant under normal physiological conditions. The reasons for the reduction of the rate of NO scavenging by red cell-encapsulated vs. cell-free Hb have been extensively investigated and yet this remains a debated subject. The difference in the scavenging rates has been attributed to four possible factors: (1) a red blood cell (RBC)-free zone adjacent to the endothelium due to the velocity gradient in laminar flow (2-4), (2) NO uptake being rate-limited by

diffusion of NO to the RBC, which contributes to the phenomenon of an unstirred layer around the RBC (1,6,14-16), (3) an intrinsic, physical RBC membrane barrier to NO diffusion (14,17-20), and (4) NO uptake being rate-limited by diffusion of NO within the RBC (intracellular diffusion) (17,21). Although there is no disagreement about the effect of the RBC-free zone along the endothelium on reducing NO reaction rates with red cell hemoglobin, the influence of the unstirred layer vs. membrane permeability vs. intracellular diffusion of NO is still disputed (21-24). There is, however, increasing evidence that the membrane of the RBC does provide some resistance to the passage of NO (14,19,20,22).

Disease states highlight the importance of the reduced rate of NO scavenging by red blood cells. The mechanisms of retardation of NO scavenging by red cell-encapsulated Hb are disrupted in hemolytic anemias due to intravascular hemolysis (25-33). This also occurs during administration of some hemoglobin-based oxygen carriers (34-48). Transfusion of banked blood of more than two weeks of age may show similar effects in vivo due to release of hemoglobin as the red cells degrade (49,50).

It is desirable to design blood substitutes that would not have the detrimental effects of cell-free hemoglobin. A potential candidate is hemoglobin encapsulated within phospholipid vesicles that are a few hundreds of nanometers in diameter (51-55). The vesicles are large enough to avoid extravasation into the endothelium and could potentially be affected by the radial pressure gradient within blood vessels so that NO consumption would be limited. Investigating the reaction kinetics of these vesicles with NO is therefore important to validate their functionality in place of red blood cells. Phospholipid vesicles of differing sizes and concentrations of intracellular hemoglobin

may be made (21). Measuring the dependence of their uptake rates of NO on size and on hemoglobin concentration may also provide insight into the relative importance of factors intrinsic to the erythrocyte that influence its scavenging rate of NO.

To elucidate the relative importance of factors that are intrinsic to red blood cells and phospholipid vesicles in their reactions with NO, another group of investigators (Sakai et al., (21)) performed stopped-flow experiments of the reaction of NO with vesicles of various sizes and with a number of different hemoglobin concentrations under anaerobic conditions. One great advantage of the elegant system developed by these authors is that it allows for modeling of well-characterized systems. The authors performed computer simulations of their experiments and also simulated reactions with smaller and larger vesicle diameters – from 50 nm up to that of a red cell (8000 nm). In their simulations the authors did not include either extracellular diffusion of NO (i.e. extravesicular, or diffusion to a vesicle through the bulk fluid up to (but not through) the membrane) or membrane permeability to NO (21). Only the diffusion of NO inside of a vesicle was simulated. The results obtained both experimentally and computationally showed that the bimolecular binding rate constant of NO decreases as intracellular hemoglobin concentration and vesicle diameter increase. The authors attributed these results to increasing viscosities of hemoglobin solutions and to increased diffusional distances of NO inside vesicles of larger diameters. This led them to conclude that the diffusion of NO inside a phospholipid vesicle is the rate limiting factor in the reaction and that this may also be the case for NO scavenging by red blood cells.

In contrast, we hypothesize that rapid mixing of NO and phospholipid vesicles does not eliminate rate limitations due to extracellular diffusion. Performing our own

computer simulations of the stopped-flow experiments with vesicles and NO, we show that the effective diffusion distance of NO through this extracellular space is not reduced sufficiently by the rapid mixing in stopped-flow. In fact, it is the rate limiting factor in the reaction.

In support of our simulations, we conducted stopped-flow absorption measurements of NO uptake by red blood cells under oxygenated and deoxygenated conditions. To explore the role of external diffusion, we employed a viscous and non-viscous buffer. We found that the viscosity of the buffer had a substantial effect on external diffusion, supporting our computational simulations and previous reports that demonstrate the importance of external diffusion in limiting oxygen uptake by red blood cells (6,7).

In addition, we have simulated our own kinetics measurements of NO uptake by microparticles derived from aged red blood cells under aerobic conditions (50). Unlike phospholipid vesicles, these microparticles still have lipid raft proteins and other components characteristic of red cells in their membrane (56). Our simulations show that, in our fast time-resolved kinetic measurements of NO scavenging by red cell microparticles under aerobic conditions, membrane permeability mostly likely limits the reaction rate.

We also performed competition experiments that support the notion that in the case of these red cell microparticles, membrane permeability plays a substantial role in limiting NO uptake. These results support our previous data, showing that NO uptake by oxygenated red blood cells is mostly limited by extracellular diffusion, with a smaller

contribution of reduced membrane permeability under aerobic conditions (14,20).

**EXPERIMENTAL PROCEDURES**

*Computational model development* – We have constructed a three-dimensional model to simulate stopped-flow experiments of the anaerobic reaction between phospholipid vesicle-encapsulated hemoglobin and NO within the software package COMSOL Multiphysics (Comsol Inc., Burlington, MA; version 3.5), a partial differential equation-based finite element modeling environment. In these experiments deoxygenated hemoglobin within vesicles binds NO to form a ferrous heme-NO complex ($Fe^{II}$-NO). We have assumed that vesicles are distributed homogeneously within the reaction volume. The reaction may then be simulated with a spherically symmetric model consisting of two spheres. The inner sphere represents a vesicle and the outer sphere represents the reaction volume, such that the difference between its radius and the radius of the vesicle is an average half-distance between any two vesicles in a real experiment (Figure 6A). To sufficiently resolve both the reaction volume and vesicles with enough finite elements we exploited the spherical symmetry of our model. The reaction was simulated solely over a 20×20 degree square cone cut out of the two-sphere system (Figure 6A). This reduced the number of degrees of freedom that had to be solved for to between 20,000 and 30,000 while allowing a sufficient number of finite elements (Figure 6B).

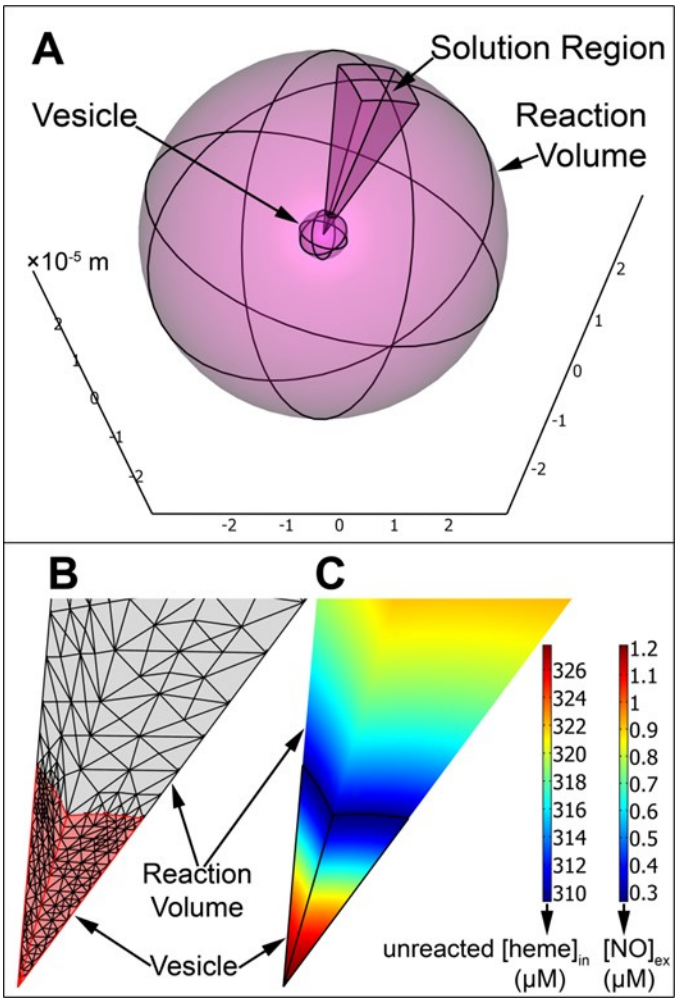


**Figure 6. Three-dimensional model of NO uptake by phospholipid vesicles.** A. The two-sphere model of a stopped-flow experiment between NO and 0.62 mM of deoxygenated hemoglobin encapsulated within a phospholipid vesicle with a diameter of 8000 nm. The radius of the large outer sphere represents the half-distance between the centers of any two vesicles in a real experiment. The axes are marked in units of 10-5 meters. On this scale the vesicle diameter is 0.8×10-5 m and the outer sphere diameter is 6×10-5 m. The 20×20 degree square cone is the region over which we have solved our system of equations. B. A zoom-in to the finite element mesh of the cone solution region shown in panel A. The vesicle domain is the bottom section colored in pink and part of the extracellular volume domain is the gray section above. The border between the vesicle domain and the extracellular volume domain is the membrane of the vesicle. Each straight edge of the vesicle domain is the 4000 nm vesicle radius. C. The simulated concentrations in micromolar of unreacted hemoglobin inside the vesicle and NO in the extracellular space (Reaction Volume) at the half-life of the reaction. The domains are displayed with the same zoom as in panel B and the vesicle domain is outlined in black. The same color code is applied to both domains, but maps the concentration of unreacted hemoglobin inside the vesicle ([heme]in) and NO outside of the vesicle ([NO]ex).

*Model-governing equations* – The general mass-transport equation governing the reaction was as follows:

$$\frac{\partial C}{\partial t} + \nabla \cdot (-D\nabla C) = S - R \qquad \text{(Eq. 1)}$$

Here C represents the concentration of NO or hemoglobin. The extra terms S and R refer to the rate of reactant production and consumption, respectively. In our case neither reactant was being produced so S was zero, and inside a vesicle

$$R = k_{Hb}[Hb][NO], \qquad \text{(Eq. 2)}$$

where [*NO*] and [*Hb*] are time dependent concentrations and $k_{Hb}$ is the known bimolecular rate constant for the reaction of cell-free deoxygenated hemoglobin with NO (20,57,58). We used the value given in the recent work on phospholipid vesicles (21) ($2.7\times10^7$ $M^{-1}s^{-1}$, Table II). *D* is the diffusion rate constant of the particular diffusing species described by the equation (NO outside or inside or hemoglobin inside of a vesicle, Table II). The boundary condition employed on the surface of the outer sphere was:

$$-\hat{\boldsymbol{n}} \cdot (-D\nabla C) = 0, \qquad \text{(Eq. 3)}$$

and at the surface of the vesicle, the inward flux of NO was defined as:

$$-\hat{\boldsymbol{n}} \cdot (-D\nabla C) = P_m(C_{ex} - C_{in}) \qquad \text{(Eq. 4)}$$

Here $C_{ex}$ and $C_{in}$ represent the concentrations of NO on the outside (**ex**tracellular region) and on the inside (intracellular region) of the vesicle, respectively, $\hat{n}$ is the unit vector normal to the sphere surface pointing in the radial direction and $P_m$ is the lipid membrane permeability coefficient of NO (Table II).

**TABLE II. Simulation parameters for phospholipid vesicles**

| **Parameter** | **Value** | | | | **Units** |
|---|---|---|---|---|---|
| Vesicle diameter | 50, 100, 200, 250, 500, 1000, 2000, 8000 | | | | nm |
| Total [heme] in solution | 1.5 | | | | μM |
| Initial [NO] in solution | 1.9 | | | | μM |
| $k_{Hb}$ (aerobic reaction) | $2.7\times10^{7}$ | | | | $M^{-1}\ s^{-1}$ |
| Physiological $D_{ex}$ of NO | 3300 | | | | $\mu m^2\ s^{-1}$ |
| Physiological $P_m$ of NO | $9\times10^{5}$ | | | | $\mu m\ s^{-1}$ |
| **$[heme]_{in}$ →** | **0.62** | **6.2** | **12.4** | **21.7** | mM |
| Physiological $D_{in}$ of NO | 2080 | 1590 | 1160 | 706 | $\mu m^2\ s^{-1}$ |
| Physiological $D_{in}$ of Hb | 77 | 53 | 29 | 7.4 | $\mu m^2\ s^{-1}$ |
| Hematocrit | 0.242 | 0.024 | 0.012 | 0.007 | % |
| Effectively infinite values of diffusion and permeability | $\infty\times(D_{ex}, D_{in}) \equiv 33\times10^{8}$ | | | | $\mu m^2\ s^{-1}$ |
| | $\infty\times P_m \equiv 9\times10^{8}$ | | | | $\mu m\ s^{-1}$ |
| Tested ranges of diffusion and permeability | $(D_{ex}, D_{in}, P_m)\times$ $(10^{-5, -4, -3, -2, -1}, ⅓, ½, 1, 2, 3, 10^{1, 2, 3, 4, 5})$ | | | | |

[a] The bimolecular rate constant for the NO reaction with free deoxygenated hemoglobin is represented by $k_{Hb}$. $D_{ex}$ is the diffusion rate constant of NO in saline (in the **ex**tracellular space) and $D_{in}$ refers to the diffusion rate constants of both NO and hemoglobin inside a vesicle (in the **in**tracellular space).

$P_m$ is the phospholipid membrane permeability of NO. The bottom row shows factors by which physiological parameter values were multiplied to test how this affects reaction kinetics.

*Simulation parameters for NO uptake by phospholipid vesicles* – Each reaction was simulated until half of the intracellular hemoglobin had reacted with NO and this

time was taken as the half-life ($t_{½}$) of the reaction. Figure 6C shows an example of simulated concentration profiles of unreacted hemoglobin inside a vesicle and NO outside of the vesicle at the half-life of the reaction. The apparent bimolecular reaction rate constant, $k'_{on}$, was calculated at 5 ms of reaction time, as in the recent publication on vesicles, from the following formula:

$$\ln\left(\frac{[Hb](t)}{[Hb](0)}\right) = -k'_{on}[NO](0) \times t, \qquad \text{(Eq. 5)}$$

which assumes pseudo first order initial kinetics with a constant concentration of NO equal to the initial concentration. The model parameters we used in our simulations are summarized in Table II. To properly simulate the stopped-flow experiment we included physiological values for the diffusion of NO in the extracellular region ($D_{ex}$, 3300 $\mu m^2 s^{-1}$) and the lipid membrane permeability of NO ($P_m$, $9\times10^5$ $\mu m\, s^{-1}$) which we have previously used (20,59). In the intracellular region we have used the diffusion constants for both NO and hemoglobin cited in the work on phospholipid vesicles (21), which increase with decreasing concentration of hemoglobin inside a vesicle. The total hemoglobin (in heme) used in our simulations was 1.5 μM and the initial concentration of NO in the whole reaction volume was 1.9 μM, as in the publication on vesicles (21). To assess whether extra or intracellular diffusion of NO or the membrane permeability of NO is rate limiting we have performed simulations where each of these parameters was varied over a range of fifteen different values by multiplying the physiological value of a parameter by fifteen different factors (from as small as $10^{-5}$ to as large as $10^5$, Table II, bottom row) while maintaining the other parameters constant at either physiological values (data not shown) or at very high values. The very high values were selected to make the corresponding parameters effectively infinite so that they would not contribute to the reaction rate (Table

II, bottom row). These simulations were performed for intracellular hemoglobin concentrations of 0.62, 12.4 and 21.7 mM and for vesicle radii of 50, 500 and 8000 nm (Table II). For simulations where intracellular diffusion was varied while extracellular diffusion and membrane permeability were constant the NO and hemoglobin diffusion coefficients were both multiplied by the same factor. Because these two parameters were always varied synchronously together they are both referred to by the same symbol, $D_{in}$ (intracellular or intravesicular diffusion). To fit all of the experimental and computational data presented in the recent work on phospholipid vesicles (21), we have also performed some simulations with vesicle diameters of 100, 200, 250, 1000 and 2000 nm. The experimental and simulated data in the recent work on phospholipid vesicles by Sakai et al. (21) have been obtained by precisely estimating the values from the graphs of their publication in order to compare it to our own. Some values explicitly given in the publication were also estimated from the graphs and these deviated by a maximum of 1.4% from the exact values.

*Computational model validation for simulations of NO uptake by phospholipid vesicles* – Several approaches were taken to confirm the validity of our computational approach. Normally the mesh of our 3D model had been created with a fine setting and further refined twice in the extracellular domain and five times in the intracellular (vesicle) domain (Figure 6B). Comparing these to simulations performed with a coarser mesh, we have identified that models with the largest vesicle diameter and the highest concentration of intracellular hemoglobin need the most number of mesh refinements to be properly resolved. To make sure that our chosen number of mesh refinements provided a sufficient number of finite elements the simulations requiring the most number of

refinements were also performed with three and six refinements for the intra and extracellular domains respectively. The average percent difference from simulations with lower, normally used, number of mesh refinements at physiological parameter values (Table II) was 0.16% ± 0.19% for the apparent rate constants and 18% ± 4% for the reaction half-lives (n = 2). When parameter values one tenth of physiological values and higher were included the percent difference was 1.65% ± 4.45% for initial rates and 12% ± 8% for half-lives (n = 26). All of the simulations performed in three dimensions have also been performed in one dimension in spherical coordinates with only a radial dependence (data not shown). It was determined that to appropriately simulate apparent bimolecular rate constants for the smallest values of extra and intracellular diffusion used ($10^{-5}\times D_{ex}$ and $10^{-5}\times D_{in}$, Table II) the number of mesh refinements in 1D had to be increased to 10 for the extracellular space and 12 for the intracellular space, so that our three-dimensional model was not resolved enough at low diffusion rates (below one tenth of physiological values presented in Table II). However, the simulated half-lives had little dependence on the mesh size and gave qualitatively the same results for both one and three-dimensional simulations. Importantly, the mesh size in three dimensions resolved the model sufficiently for accurate simulations of both initial rates and half-lives at physiological parameter values. We are confident that our conclusions about mechanistic issues surrounding NO uptake by Hb containing vesicles could not be due to any deficiencies in the grid size or other model parameter.

*Computational model settings & data analysis* – Normally simulations were performed with three application modes – two for diffusion of NO in the extra and intracellular regions and one for the diffusion of hemoglobin in the intracellular region. In

some cases formation and diffusion of the product of the reaction, iron-nitrosyl hemoglobin ($Fe^{II}$-NO), was simulated with a fourth application mode and the results were found to be insignificantly different from that of a system of NO and hemoglobin only. Some simulations were also performed to completion, until all of the intracellular hemoglobin had reacted. Mass conservation of reactants and products was observed in all cases. The direct, UMFPACK, linear system solver was used by COMSOL Multiphysics during the simulations and the time stepping was performed by the default, Backward Differentiation Formula, method. To perform a large number of simulations in series, a Matlab code was used to control COMSOL Multiphysics. This included setting up the geometry of each model, creating and refining the mesh, collecting simulation data and calculating the apparent reaction rate constant of each simulation.

*Measurements of NO reactions with red blood cells.* Stopped-flow time-resolved absorption measurements were conducted using a Molecular Kinetics three-syringe mixer (Indianapolis, IN) coupled to an Olis RSM spectrometer (Bogart, GA) using similar methods as described previously (14,50). Red blood cells were suspended in either Dubelco's phosphate buffered saline (DPBS) (14) or a viscous buffer. The viscous buffer was made by first dissolving 50 g of dextran in 34 mL of water, 200 mL of DPBS and 10 mL Optiprep (Sigma Aldrich) and then mixing this solution with the non-viscous buffer (DPBS) in a ratio of 3 to 1 under aerobic or anaerobic conditions. Anaerobic conditions were maintained using sodium dithionite at a maximum concentration of 5 mM. The NO donor PROLINONOate (Cayman Chemicals) was prepared in 0.0.1M NaOH at a concentration of 35 mM. These two solutions were loaded in two of the syringes and the third contained either the viscous or non-viscous buffer. The viscosity of the viscous

buffer used in our experiments (after dilutions) was measured to be 7.7 centistokes. In the first mix, the NO donor was diluted into the one containing buffer and then this mixture was aged for twenty seconds so that the NO would be released. Afterward, the NO buffer was rapidly mixed with the red cells. This two-step mixing procedure was performed to avoid degradation of the NO either from reactions with air or dithionite, as the donor is quite stable in 0.01 M NaOH. Time-resolved absorption spectra were collected and analyzed using Specfit software (Boston, MA) through singular value decomposition and global analysis as previously described (14,50).

*Measurements of NO uptake by red blood cell microparticles* – We also simulated our own photolysis experiments measuring the very fast uptake of NO by red blood cell microparticle-encapsulated hemoglobin under aerobic conditions (50). In these experiments oxygenated hemoglobin inside microparticles reacts with NO to form methemoglobin (MetHb, $Fe^{III}$). Microparticles were obtained from outdated packed red blood cell units with ACD anticoagulant purchased from Interstate Blood Bank, Inc. (Memphis, TN). The microparticles were prepared as previously described (50,60). The preparation was confirmed to contain only microparticle encapsulated hemoglobin via microscopy and absorbance measurements (50). We used dynamic light scattering to estimate the size of our microparticles. Samples were measured in a Zetasizer series instrument by Malvern Instruments Ltd and analyzed with Malvern software to obtain a size average by number. We found the diameter to be 200 ± 10 nm (from 4 separate microparticle preparations). The internal hemoglobin concentration was determined by measuring the total hemoglobin concentration in a resuspended microparticle pellet.

Hemoglobin was purified as described previously (61). All chemicals were purchased from Sigma (St. Louis, MO) unless stated otherwise. Measurements of NO dioxygenation by microparticles via the time-resolved photolysis method were performed similarly to those described previously (50,62). NO was photolyzed off of the donor compound potassium pentachloronitrosyl-ruthenate (II) in the presence of microparticle-encapsulated or cell-free Hb and absorbance of the reaction mixture was simultaneously recorded by a CCD camera. A quantum yield of NO in each experiment was calculated from each observed reaction rate between cell-free Hb and NO and a $5\times10^{7}$ $M^{-1}$ $s^{-1}$ bimolecular rate constant for the same reaction, a lower bound which we have previously established (20). Each obtained value for the yield of NO was used to calculate a corresponding bimolecular rate constant for every observed reaction rate between microparticle-encapsulated hemoglobin and NO. Microparticles were confirmed to have remained intact during an experiment by measuring the absorbance in the Soret and visible ranges of the supernatant (after sedimention at 30,000 g for 90 minutes) after photolysis, which showed no detectable amount of freely dissolved hemoglobin. The age of blood used for preparation of microparticles for photolysis experiments was 28 or 33 days old.

*Competition Experiments* - Competition experiments were performed similarly to those described previously (14,17). Cell-free Hb at a concentration of 50 or 800 μM was mixed with red cell microparticles (prepared as described above) at a similar concentrations in heme (50 or 800 μM) in Phosphate buffered saline (PBS). The NO donor DEANONOate was added to a final concentration of 12.5 μM for the low heme concentration experiments and 200 μM for the high heme concentration experiments.

After 150 minutes the mixtures were centrifuged at 37,000 g for 60 minutes to sediment the microparticles. The amount of reacted NO in each fraction was determined by absorption and electron paramagnetic resonance spectroscopy as previously described (14,17). Experiments were performed under aerobic conditions. Control experiments were performed as described previously to account for any auto-oxidation or MetHb reductase activity (14).

The ratio of the bimolecular rate constants for NO uptake by cell-free Hb compared to that encapsulated by red cell microparticles, $k_f / k_{mp}$ is given by

$$\ln\left(1 - \frac{[MetHb]_f(t)}{[HbO_2]_f(0)}\right) = \frac{k_f}{k_{mp}} \ln\left(1 - \frac{[MetHb]_{mp}(t)}{[HbO_2]_{mp}(0)}\right) \quad \text{(Eq. 6)}$$

where the subscript f refers to cell-free Hb and mp to red cell microparticles Hb. The natural log terms on both sides of the equation derive from the fact that the total amount of oxygenated hemoglobin in the free and microparticle fractions may decrease with time from its initial amount (18).

*Simulations of NO uptake by red blood cell microparticles* – Photolysis experiments were simulated with the same computational model that we used to simulate the experiments with phospholipid vesicles. The different parameter values for these simulations are summarized in Table III. For simulations of each experiment the measured average NO yield was used as the initial concentration of NO (Table III). The total amount of oxygenated hemoglobin in each experiment was 19.8 μM. Our simulations focused on our own measured values of vesicle diameter and internal Hb concentration, but also included the full range of microparticle diameters that have been

reported by Kriebardis et al. (56) based on measurements of microparticle preparations similar to ours. Based on our measurements of the volume of a pellet of microparticles after sedimentation and on absorbance of the same microparticles suspended in buffer, we have estimated the average hemoglobin concentration inside microparticles to be approximately 12.7 mM. The diffusion rate constants of NO and hemoglobin inside solutions of various concentrations of internal Hb (Table III) were obtained by extrapolating the diffusion coefficients provided in the recent publication on phospholipid vesicles (21) (Table III) with a third degree polynomial. For each initial concentration of NO, total hemoglobin and microparticle diameter, the experiment was simulated with 25 to 28 different microparticle membrane permeability values of NO, from $1\times10^{3}$ to $9\times10^{5}$ $\mu ms^{-1}$. Some simulations were also performed when only one parameter (diffusion of NO outside, diffusion of NO and hemoglobin inside, or membrane permeability to NO) had a physiological value while the other two were assigned effectively infinite values (Table III), as in the simulations of vesicles. The time of each simulation at which Equation 5 was used to compute a bimolecular rate constant was changed from 5 ms to 0.05 ms, because under the given conditions the reaction proceeds much faster and is complete within approximately 1 ms. The reported bimolecular rate constants are an average of three identical simulations but with different initial concentrations of NO (Table III).

**TABLE III. Simulation parameters for red blood cell microparticles.**

| **Parameter** | **Value** | | | | **Units** |
|---|---|---|---|---|---|
| Vesicle diameter | 50, 150, **200**, 210 | | | | nm |
| Total [heme] in solution | 20 | | | | μM |
| Initial [NO] in solution | 99, 130, 160 | | | | μM |
| $k_{Hb}$ (anaerobic reaction) | $5\times10^{7}$ | | | | $M^{-1}\ s^{-1}$ |
| Physiological $D_{ex}$ of NO | 3300 | | | | $\mu m^2\ s^{-1}$ |
| Physiological $P_m$ of NO | $1\times10^{3}$ - $9\times10^{5}$ | | | | $\mu m\ s^{-1}$ |
| **$[heme]_{in}$ →** | **8** | **12.7** | **15** | **21.7** | mM |
| Physiological $D_{in}$ of NO | 1453 | 1142 | 1010 | 706 | $\mu m^2\ s^{-1}$ |
| Physiological $D_{in}$ of Hb | 45.6 | 28 | 21 | 7.4 | $\mu m^2\ s^{-1}$ |
| Hematocrit | 0.25 | 0.156 | 0.13 | 0.007 | % |
| Effectively infinite values of diffusion and permeability | $\infty\times(D_{ex}, D_{in}) \equiv 33\times10^{8}$ | | | | $\mu m^2\ s^{-1}$ |
| | $\infty\times P_m \equiv 9\times10^{8}$ | | | | $\mu m\ s^{-1}$ |

[a] The bimolecular rate constant for the NO reaction with free oxygenated hemoglobin is represented by $k_{Hb}$. $D_{ex}$ is the diffusion rate constant of NO in saline (in the **ex**tracellular space) and $D_{in}$ refers to the diffusion rate constants of both NO and hemoglobin inside a microparticle (in the **in**tracellular space).

$P_m$ is the microparticle membrane permeability of NO.

## RESULTS

*Extracellular diffusion limits the uptake rate of NO by phospholipid vesicles more than intracellular diffusion.* The effect of different parameters (extracellular vs. intracellular diffusion vs. membrane permeability) on the apparent bimolecular reaction rate constant is compared with values obtained experimentally and with simulated data from the recent work on phospholipid vesicles (21) in Figure 7. The bimolecular rate

constant for a solution of cell-free Hb is shown on the y-axes (white squares). Figure 7A & B display apparent reaction rate constants vs. intracellular hemoglobin concentrations at a vesicle diameter of 250 nm. In Figure 7A the experimental results of Sakai et al. (21) are plotted along with their simulations that only include internal diffusion of NO as a rate-limiting factor. Our simulations, where we include extra and intracellular diffusion and membrane permeability of NO set to physiological values (Table II) are also plotted. It is evident that the rate constants obtained from our simulations where we have included physiological values of all parameters fit the experimental data of Sakai et al. more closely than their simulations which only include internal diffusion as a rate-limiting factor.

Figure 7B shows the effect of each individual rate-limiting mechanism in our simulations on the apparent reaction rate constant. We also include results from the simulation where all three parameters (intracellular diffusion constant, extracellular diffusion constant, and membrane permeability) are kept at their physiological values (as also plotted in Figure 7A). We display results from when only extracellular diffusion was set to its physiological value and the intracellular diffusion (of both NO and Hb) and membrane permeability of NO were effectively infinite. In addition the panel displays results from simulations where we have set diffusion parameters only inside a vesicle (both of NO and Hb) to physiological values while letting extracellular diffusion and membrane permeability be effectively infinite. Finally, the case where only membrane permeability of NO had a physiological value (for a phospholipid vesicle) while diffusion rate constants inside and outside of a vesicle were effectively infinite is also shown, and the effect of this single factor alone is not great. The fact that including only extracellular

diffusion as a rate limitation reduces the rate constants more than including only intracellular diffusion as a rate limitation, demonstrates that diffusion of NO through the extracellular space limits the reaction rate more than diffusion inside of the vesicle. In addition, although extracellular diffusion by itself is not sufficient to explain the observed rate, it gives a better approximation to experimental data than when only intracellular diffusion is included in our simulations.

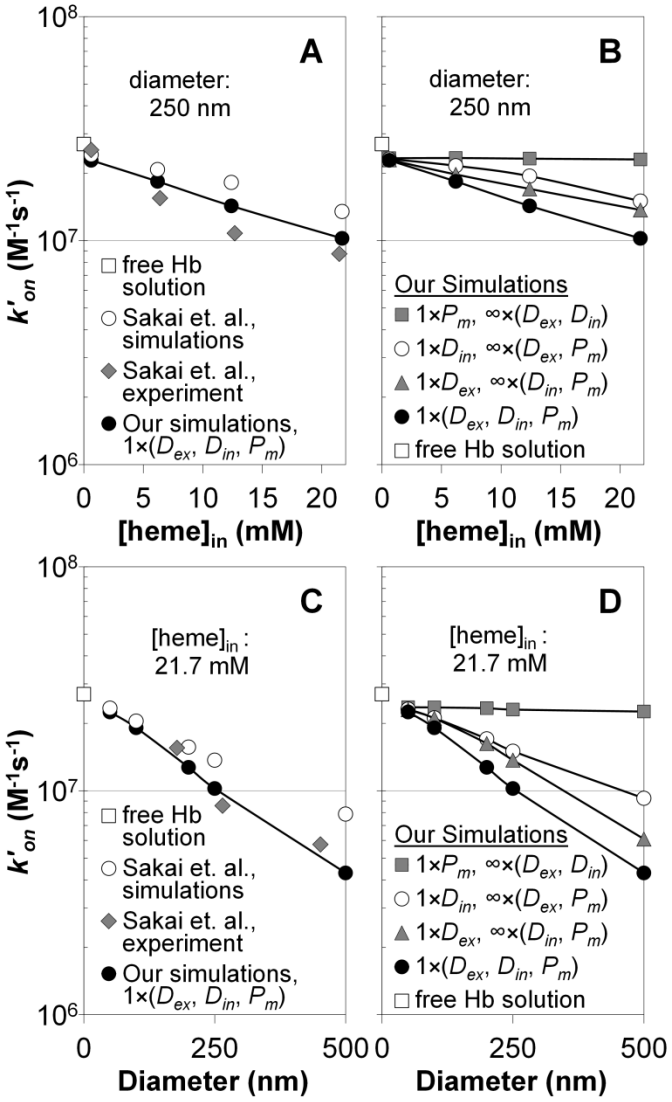


**Figure 7. Apparent bimolecular binding rate constants for NO uptake by phospholipid vesicles under anaerobic conditions.** A. The apparent bimolecular rate constant (y-axis, logarithmic scale) plotted vs. intracellular hemoglobin (Hb) concentration for a vesicle with a diameter of 250 nm. Our simulations which included

physiological values of NO diffusion outside (Dex), diffusion of NO and Hb inside (Din) and of membrane permeability of NO (Pm) are shown as black circles. The multiplication factor of one used in the legend indicates that these parameters retained physiological values presented in Table II. The simulated rate constants of Sakai et al. are displayed as white circles and their experimentally measured rate constants are shown as gray rhombuses. The rate constant for NO binding by a solution of free deoxygenated Hb is shown with the white square on the y-axis. B. Our simulated rate constants plotted vs. intracellular Hb concentration for a vesicle of 250 nm in diameter when all parameters had physiological values (black circles, the same data as in panel A), when only diffusion rate of NO outside a vesicle had a physiological value while the other parameters were effectively infinite (gray triangles), when only diffusion rate inside (of both NO and Hb) had a physiological value (white circles) and when only membrane permeability of NO had a physiological value (gray squares). For each set of simulations, the parameter that was assigned its physiological value presented in Table II is indicated with a multiplication factor of one in the legend. The parameters which were assigned effectively infinite values (Table II) are indicated with a multiplication factor of infinity in the legend. For example, 1×Pm refers to the physiological phospholipid membrane permeability of $9\times105$ μm $s^{-1}$ and $\infty\times$(Dex, Din) indicates the very high diffusion rate constants of $33\times108$ $\mu m^2$ $s^{-1}$ for both diffusion of NO outside (Dex) and diffusion of NO and Hb inside (Din). C. Rate constants analogous to those of panel A, but plotted vs. vesicle diameter at an intracellular Hb concentration of 21.7 mM. D. Rate constants analogous to those of panel B, but plotted vs. vesicle diameter at an intracellular Hb concentration of 21.7 mM.

The data displayed in Figure 7C & D are analogous to those of Figure 7A & B, but here the apparent bimolecular rate constant is plotted vs. vesicle diameter at the highest concentration of intracellular hemoglobin of 21.7 mM. In Figure 7C, again, we overlay our simulated rates when physiological values of all parameters were included with the experimental and simulated data from the recent work with phospholipid vesicles (21). As before, our simulations using all three physiological parameters agree best with the experimental data. Figure 7D shows a similar pattern to Figure 7B where diffusion of NO to a vesicle through the extracellular space limits the reaction rate more than diffusion inside of a vesicle. Membrane permeability has little additional effect. Importantly, our simulations in which physiological values of intracellular diffusion only

were included (Figure 7B & D, white circles) agree well with the similar simulations presented in the recent work with vesicles (21). (Figure 7A & C, white circles). These and other data are overlaid for better comparison in Figure 9.

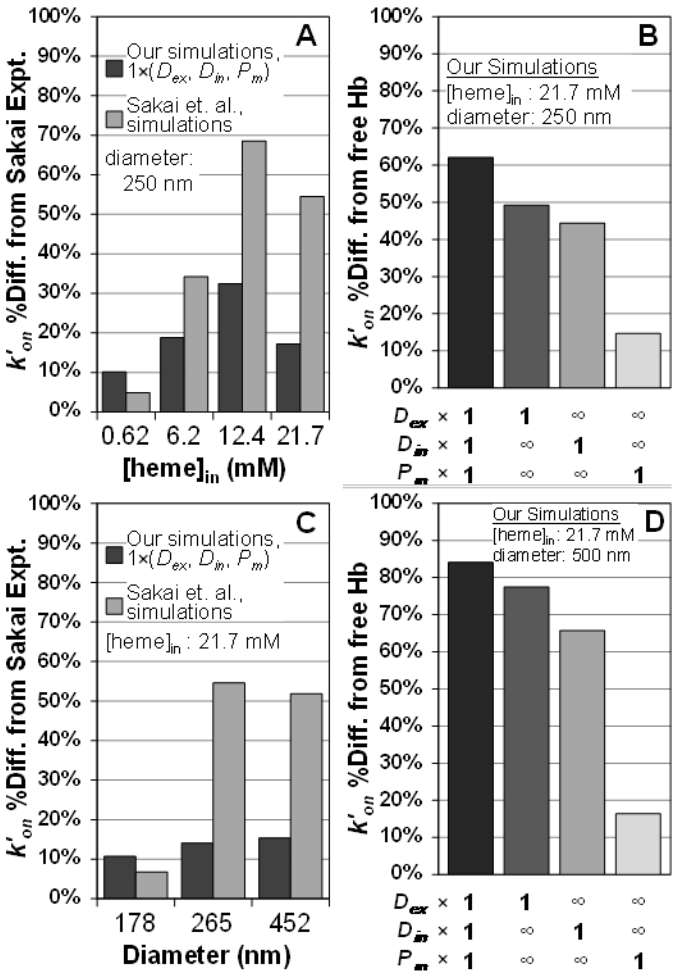


**Figure 8. Comparisons of bimolecular rate constants for NO uptake by phospholipid vesicles.** A. The percent difference between experimentally obtained rate constants by Sakai et al. and simulated rate constants plotted vs. intracellular Hb concentration from the data in Figure 7A (250 nm vesicle diameter). A multiplication factor of 1 in the legend for extracellular Diffusion of NO (Dex), intracellular diffusion of NO and Hb (Din) and for membrane permeability of NO (Pm) indicates that the physiological values of these parameters were used in our simulations (Table II). B. The percent difference between the cell-free Hb uptake rate constant of NO and our simulated rate constants for a vesicle of 250 nm in diameter and with 21.7 mM of intracellular hemoglobin from Figure 7B. Employed parameter values for extra (Dex) and intracellular diffusion (Din) and membrane permeability (Pm) are indicated below the x-axis. A multiplication factor of 1 refers to the physiological value presented in Table II and the infinity symbol signifies the effectively infinite parameter value from Table II C. Percent

difference between simulated rate constants and the experimentally measured rate constants of Sakai et al. from the data of Figure 7C (intracellular hemoglobin concentration of 21.7 mM) plotted vs. vesicle diameter. Our simulated data and that of the other authors was extrapolated with a third degree polynomial to the average vesicle diameters (x-axis) in the experiments of the other authors. D. Percent difference between the NO uptake rate of cell-free Hb and our simulated NO uptake rate constants for a vesicle of 500 nm in diameter and with 21.7 mM of intracellular Hb plotted, analogous to data in panel B, from the data in Figure 7D. Parameter values in each simulation are indicated below the x-axis.

In Figure 8 A and C, the percent difference between the data and the theoretical simulations are shown. The comparisons support the notion that simulations which include all three potential rate-limiting factors set at their physiological levels fit the data substantially better than when only intracellular diffusion is included. In addition, as shown in Figure 8B and D, when any single one of the three potential rate-limiting factors is included, external diffusion has the largest effect. The data shown in Figure 7 and Figure 8 compare rate constants for the reactions under certain conditions and simulation parameters, as expected, similar results are obtained when comparing half-lives of the reactions.

*Effect of extracellular diffusion on NO uptake by phospholipid vesicles increases with vesicle size and with concentration of encapsulated hemoglobin.* We summarize the differences between the simulations presented in the recent work with phospholipid vesicles (21) and our simulations which best approximate the experimental data of the same authors in Figure 9. This figure displays the bimolecular reaction rate constant calculated by Equation 5 vs. vesicle diameter at the lowest (0.62 mM, light colors) and highest (21.7 mM, dark colors) concentrations of hemoglobin inside a vesicle. The bimolecular rate constant for a reaction of cell-free Hb with NO ($2.7 \times 10^7$ $M^{-1}$ $s^{-1}$) is shown on the y-axis as a white square. We have already pointed out that our simulations

where only intracellular diffusion is rate limiting (light blue and blue squares) appropriately agree with the simulations of Sakai et al. (light green and green triangles). Our simulations where physiological values of all parameters (extracellular diffusion of NO and intracellular diffusion of NO and Hb, as well as membrane permeability to NO, Table II) were used are plotted as light blue circles (0.62 mM intracellular Hb) and blue circles (21.7 mM intracellular Hb). With 0.62 mM of intracellular hemoglobin, only one experimentally measured bimolecular rate constant for a vesicle diameter of 305 nm (pink rhombus) was provided (21). At this diameter and hemoglobin concentration all of the data converge to the bimolecular rate constant of the cell-free Hb reaction. However, experimental data of the other authors at 21.7 mM of intracellular hemoglobin (red rhombuses) agrees best with our simulations where both diffusion inside and outside and membrane permeability were included. The results of these simulations indicate that, at high concentrations of intracellular hemoglobin and large vesicle diameters, the reaction is limited by diffusion of NO through the extracellular space and suggest that intracellular diffusion alone is not sufficient to explain the decrease in the reaction rate compared with cell-free Hb. This conclusion and the relationships between vesicle diameter and the extent of rate limitations shown in Figure 9 were previously demonstrated for the case of oxygen uptake by red cells of various sizes and artificial vesicles (7).

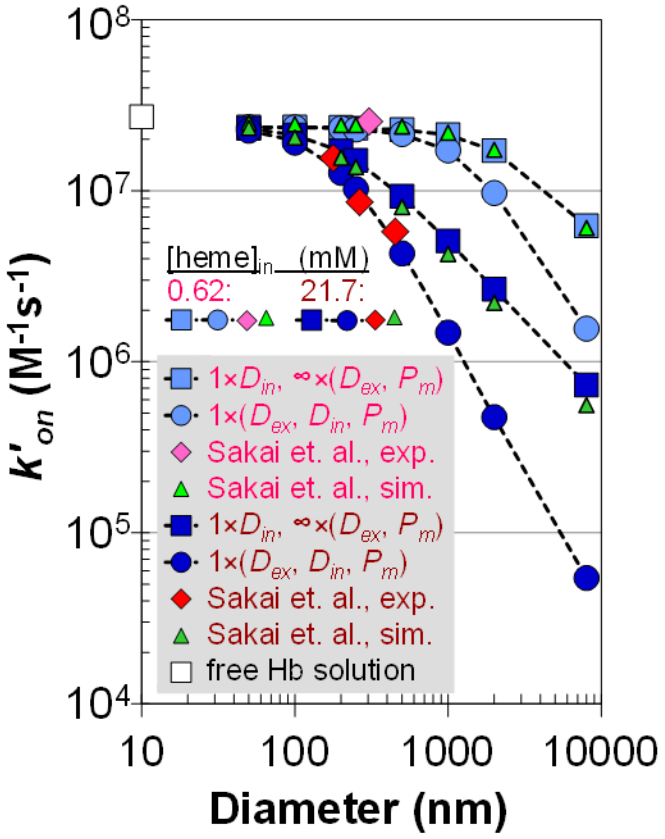


**Figure 9. Simulated apparent bimolecular rate constants for NO uptake by deoxygenated phospholipid vesicles compared with the experimentally measured constants.** The bimolecular rate constant (y-axis, logarithmic scale) is plotted vs. vesicle diameter (x-axis, logarithmic scale) for two different concentrations of intracellular hemoglobin (Hb) (0.62 mM, pink legend items and 21.7 mM, dark red legend items). Experimentally obtained rate constants (21) are shown as red rhombuses (21.7 mM [heme]in) and as the pink rhombus (0.62 mM [heme]in). The simulated rate constants of Sakai et al. are represented by light green triangles (0.62 mM [heme]in) and by dark green triangles (21.7 mM [heme]in). Our simulations mimicking the simulations of the other authors, when NO (and Hb) diffuses only inside of a vesicle, are shown in light blue (0.62 mM [heme]in) and dark blue squares (21.7 mM [heme]in). That the physiological rate constant presented in Table II was used for intracellular diffusion of NO (Din) is indicated by multiplying this parameter with a factor of one in the legend. The diffusion rate outside (Dex) and the membrane permeability of NO (Pm) were assigned effectively infinite values (Table II, second-to-bottom row), this is indicated by multiplying these parameters with a factor of infinity in the legend. Finally, our simulations with physiological values of extra (Dex) and intracellular (Din, both NO and Hb) diffusion and membrane permeability (Pm) of NO are displayed as light blue circles (0.62 mM [heme]in) and dark blue circles (21.7 mM [heme]in). These parameters are multiplied with a factor of one in the legend to indicate that they have the same physiological values as presented in Table II. The rate constant for the reaction of NO with free deoxygenated Hb is plotted as a white square on the y-axis.

*Experimental support of contribution by external diffusion for large vesicles.* In order to provide experimental support for our conclusion that extracellular diffusion is a major contributor to rate limitations in NO reactivity with large vesicles with high hemoglobin concentrations, we performed stopped-flow absorption experiments with red blood cells (Figure 10). In these experiments we varied the viscosity of the buffers similar to experiments published previously examining the reaction of red blood cells and oxygen (6). If external diffusion is not a major factor in limiting NO reactivity, we would expect the viscosity of the buffer not to have any effect on the kinetics of the reaction. Figure 10A shows typical spectra for the reaction of NO and red blood cells under anaerobic conditions in non-viscous buffer and that in Figure 10B shows analogous data for when viscous buffer is used. These data represent the binding of NO to deoxygenated Hb to form the nitrosyl (NO bound) species. Figure 10C shows kinetic traces and their fits for the reaction of NO and red cells for the viscous and non-viscous buffers. The average rate constant was $4.2 \pm 1.0 \times 10^3$ $M^{-1}s^{-1}$ for viscous buffer and $20.9 \pm 8.1 \times 10^3$ $M^{-1}s^{-1}$ for non-viscous buffer (from greater than 25 mixes from three separate sample preparations on different days). Analogous data for the reaction of NO with red blood cells under aerobic conditions are shown in Figure 10D and E. Here, NO reacts with oxygenated Hb to form MetHb and then can bind to the ferric heme to form a NO bound MetHb species. Thus, the data were fit to a bi-exponential process to properly represent these two reactions. Figure 10F shows kinetic traces and their fits for the reaction of NO and red cells for the viscous and non-viscous buffers under aerobic conditions (from greater than 25 mixes from three separate sample preparations on different days). The average rate constant for MetHb formation in viscous buffer was $8.5 \pm 1.3 \times 10^3$ $M^{-1}s^{-1}$

and 29.8 ± 10.4 × $10^3$ $M^{-1}s^{-1}$ for non-viscous buffer. The large deviations in the data for non-viscous buffer are due to the reaction being very fast for the instrumentation employed. However, the data under both aerobic and anaerobic conditions clearly demonstrate that the reaction is retarded when a viscous buffer is employed ($P < 10^{-6}$), supporting a major role for external diffusion in limiting NO uptake by red blood cells as similarly observed in the case of oxygen uptake (6,7).

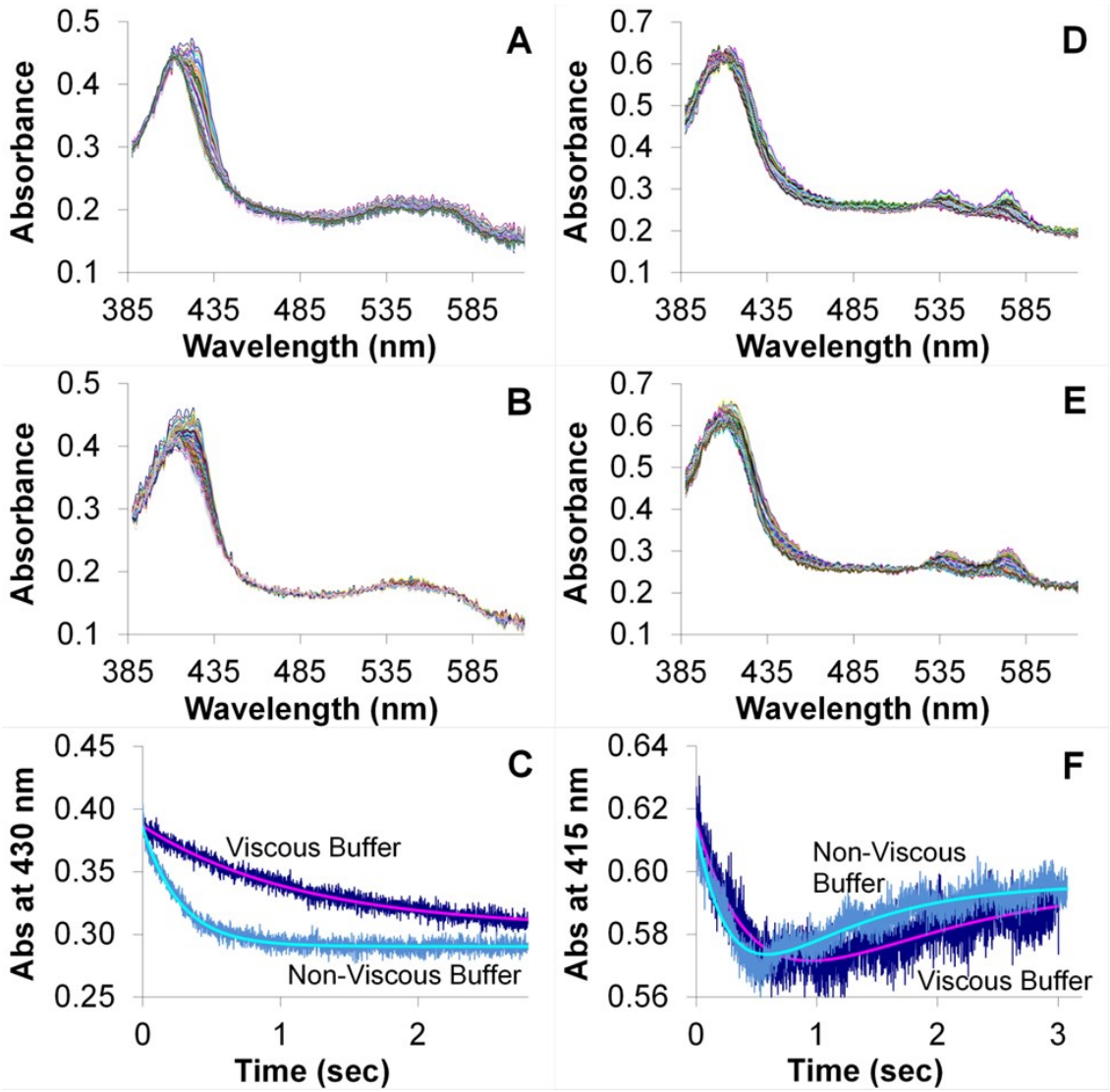

**Figure 10. Stopped-flow absorption of red blood cells in viscous and non-viscous buffer.** Red blood cells were diluted into NO-containing buffer and absorption spectra were collected as a function of time. A. A subset of absorption spectra collected every millisecond are shown after a mixture in non-viscous buffer under anaerobic conditions. The final mixture contained Hb at a concentration 50 μM and NO at a concentration of 200 μM. The data show NO binding to deoxygenated Hb and analysis yielded an observed rate constant of 3.7 1/sec. B. A subset of absorption spectra collected every millisecond are shown after a mixture in viscous buffer under anerobic conditions. The final mixture contained Hb at a concentration 50 μM and NO at a concentration of 200 μM. The data show NO binding to deoxygenated Hb and analysis yielded an observed rate constant of 0.86 1/sec. C. The kinetics of the absorption at 430 nm are shown for both viscous and non-viscous buffers for data collected under anaerobic conditions. Both the raw data (noisy) and the fits from singular value decomposition and global analysis are shown. D. A subset of absorption spectra collected every millisecond are shown after a mixture in non-viscous buffer under aerobic conditions. The final mixture contained Hb at a concentration 59 μM and NO at a concentration of 180 μM. The data show NO reacting with oxygenated Hb to form MetHb with subsequent NO binding to the MetHb and analysis yielded an observed rate constant of 3.1 1/sec for the initial reaction. E. A subset of absorption spectra collected every millisecond are shown after a mixture in viscous buffer under aerobic conditions. The final mixture contained Hb at a concentration 64 μM and NO at a concentration of 190 μM. The data show NO reacting with oxygenated Hb to form MetHb with subsequent NO binding to the MetHb and analysis yielded an observed rate constant of 1.5 1/sec for the initial reaction. F. The kinetics of the absorption at 415 nm are shown for both viscous and non-viscous buffers for data collected under aerobic conditions. Both the raw data (noisy) and fit from singular value decomposition and global analysis are shown.

*Bimolecular reaction rate constants in simulations of NO uptake by red blood cell microparticles.* The bimolecular reaction rate constants obtained in simulations of our photolysis experiments under aerobic conditions are presented in Figure 11. The experimentally measured bimolecular rate constant for NO dioxygenation by microparticle-encapsulated hemoglobin was $1.81 \pm 0.40 \times 10^7$ $M^{-1}$ $s^{-1}$ (n = 301, 3 separate experiments) (50). This number is shown as a continuous black line in the panels of Figure 11 and the standard deviation is displayed as the two dotted horizontal lines. The bimolecular rate constant for the cell-free Hb reaction is represented by the gray square with a black cross on the y-axis of the panels in Figure 11 ($5\times10^7$ $M^{-1}$ $s^{-1}$). Figure 11A

shows simulated bimolecular rate constants (y-axes) for microparticles with the average intracellular Hb concentration of 12.7 mM and a diameter of 200 nm, as determined experimentally. In these simulations 26 different values of membrane permeability (x-axes, logarithmic scale) were used while extra and intracellular diffusion were assigned physiological values (Table III). The simulated rate constant which is most similar to the experimentally observed bimolecular rate constant for NO uptake by microparticles is marked as a black circle. This gives an estimate of the microparticle membrane permeability to NO (marked on the x-axis). The extent to which this permeability value limits the reaction rate is compared to the effects of extra and intracellular diffusion of NO in Figure 11B. The physiological membrane permeability value is that obtained from Figure 11A. The results from simulations where all three mechanistic parameters are included are compared to simulations where only one of the parameters has its physiological value while others are effectively infinite. We find that for these red cell microparticles, including membrane permeability alone yields a theoretical bimolecular rate constant that is closer to the experimental value than when either external or internal diffusion are included by themselves. The contribution of internal diffusion is the smallest. These data suggest that in the case of red blood cell microparticles, membrane permeability plays the largest role in limiting NO uptake.

In Figure 11 we have used the values for red cell microparticle diameter and internal Hb concentration that we determined experimentally. However, both of these values could be a source of error in our simulations, particularly that of the internal Hb concentration as our sedimentation technique assumes that there is no empty volume in the red cell microparticles pellet. Thus, we have also conducted simulations over a range

of diameters and internal Hb concentrations (Table III and supplementary Figure 7). In all these simulations, we find that membrane permeability plays a substantial, in fact the largest, role in limiting NO uptake by red cell microparticles except for conditions where the highest internal Hb concentration (21 mM) and highest diameter (210 nm) is used.

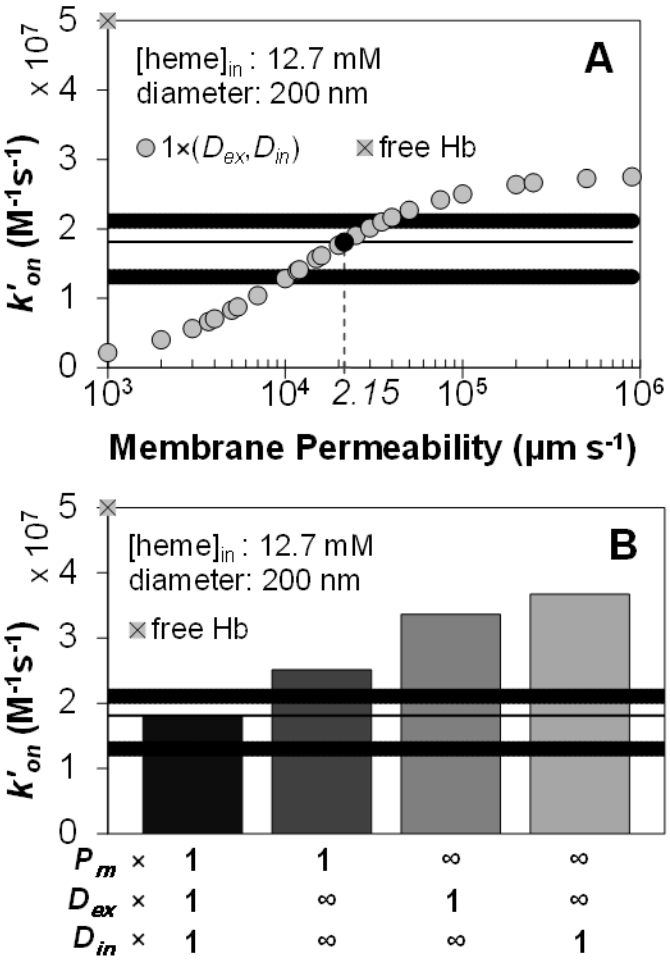


**Figure 11. Computer simulations of the apparent bimolecular rate constants for NO uptake by oxygenated red blood cell microparticles.** A. Our simulated bimolecular rate constant is plotted for 26 different values of membrane permeability to NO (x-axis). As indicated in the legend with a multiplication factor of 1, extracellular diffusion of NO (Dex) as well as intracellular diffusion of NO and Hb (Din) were set to the physiological values from Table III. The rate constant for NO uptake by a solution of freely dissolved oxygenated Hb is shown on the y-axis as a gray square with a black cross. The experimentally measured bimolecular rate constant ($1.81 \pm 0.40 \times 107$ $M^{-1}$ $s^{-1}$) appears as a horizontal black line (in all panels) and its standard deviation as two dotted horizontal black lines. The simulated rate constant which is the same as that obtained experimentally is shown as a black circle, the corresponding membrane permeability is indicated on the

x-axis below. B. Effect of membrane permeability determined in panel A (2.15×104 μm $s^{-1}$) compared with diffusion effects in limiting the NO uptake rate. Four simulated rate constants are shown as bars. The left-most represents the same simulation as the black circle in panel A, where extra (Dex) and intracellular (Din) diffusion were set to the physiological values given in Table III and membrane permeability was set to the value determined in panel A, as indicated with a multiplication factor of 1 for all of these parameters below the x-axis. In each of the remaining three simulations the parameter with a multiplication factor of 1 (as indicated below the x-axis) was set to its physiological value, while the other two were effectively infinite (indicated by the infinity symbols).

*Experimental support for membrane limitation of NO uptake by red cell microparticles.* In order to provide experimental support for our conclusions based on theoretical modeling of photolysis-based measurements of NO uptake by red cell microparticles, we conducted competition experiments involving the red cell microparticles and cell-free Hb similar to those described previously (14,17). In these experiments red cell microparticles are mixed with cell-free Hb in the presence of the NO donor DEA NONOate at two different concentrations of Hb. When the Hb concentration of the red cell microparticles is increased, this effectively increases the "hematocrit", decreases the average distance between microparticles, and hence should lead to a decrease in the average time for external diffusion of NO to the microparticle. Thus, at the higher concentration, external diffusion should have a diminished effect on limiting the rate of NO uptake. At a "hematocrit" of 100% there is no external diffusion and thus no limitation due to this process on the kinetics of NO uptake. In previous experiments using this approach, we demonstrated the importance of external diffusion on the rate of NO uptake by oxygenated red blood cells (14).

Typical spectra from electron paramagnetic resonance (EPR) and visible absorption (insets) are shown in Figure 12. Spectra are shown for the supernatants (cell-

free Hb) and re-suspended pellets (red cell microparticles) after sedimentation for experiments at high (800 μM, Figure 12A) and low (50 μM, Figure 12B) Hb concentrations. There is no obvious effect of Hb concentration. The average and standard deviation of the ratio of the bimolecular rate constants for NO uptake by cell-free Hb ($k_f$) compared to that by red cell microparticles ($k_{mp}$) are plotted in Figure 12C for the case when the hemoglobin concentrations in each fraction are high and low. Note that for each experiment, the concentration of cell-free Hb and that contained in microparticles are equal. For each experiment, the amount of NO reacted with each fraction was determined by separating the cell-free Hb from the microparticles by sedimentation and then determining reacted Hb (MetHb) using absorption and electron paramagnetic resonance spectroscopy. Overall, he EPR data are more reliable because in the case of absorption we are looking for a small signal from the reacted Hb (MetHb) in the background of absorption that is due to unreacted Hb (oxygenated Hb) while in EPR spectra, oxygenated Hb is silent and the entire signal is due to MetHb. In addition, the absorption spectra include scattering from microparticles that could lead to some error in fitting the data. We find that the red cell microparticles scavenge NO only about 3 to 5 times slower than cell-free Hb, consistent with our previously reported measurements based on time-resolved absorption experiments (50). Unlike what was previously observed for red cells under aerobic conditions (14), we do not observe a significant effect of hematocrit on $k_f/k_{mp}$.

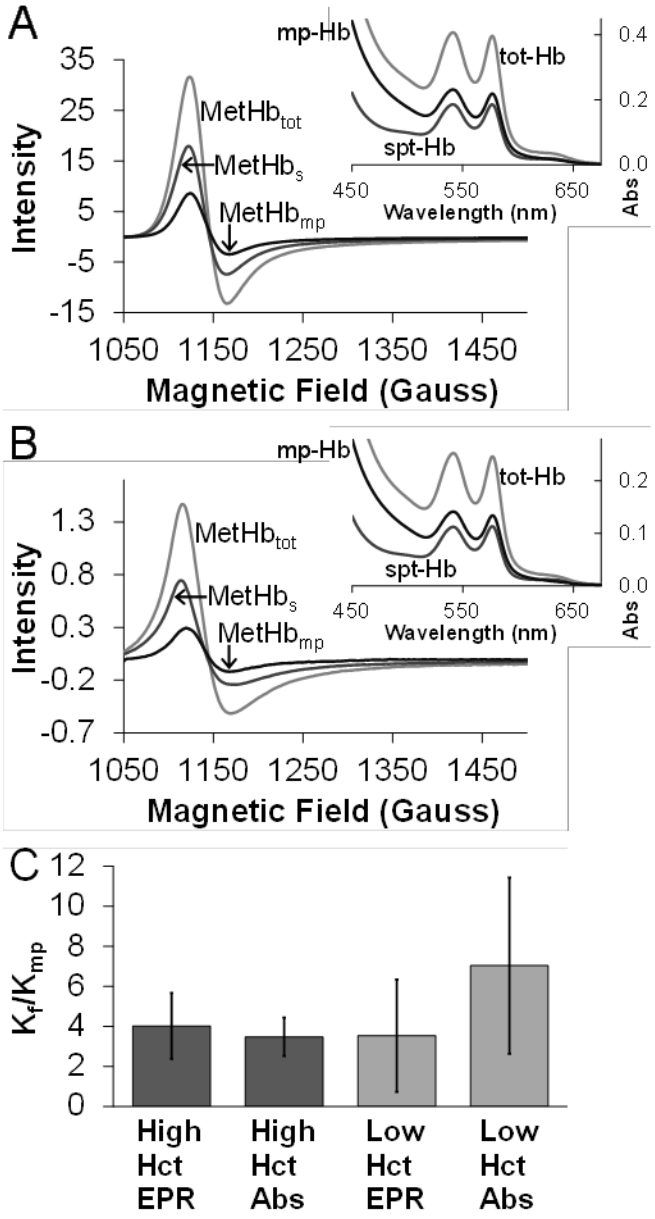


**Figure 12. Competition experiments between red cell microparticles and cell-free Hb for reaction with NO.** A. Typical EPR and absorbance (inset) spectra collected after the competition of low concentrations (50 μM, ~0.3% microparticle Hct) of microparticle-encapsulated and cell-free Hb for NO. The main panel shows the EPR signal from the product of the reaction, methemoglobin, in the microparticle fraction (MetHbmp) (after spinning, supernatant removal, and re-suspension), in the supernatant after spinning out the microparticles (MetHbs) and in the whole mixture (MetHbtot) plotted vs. magnetic field. In the inset, absorbance in the visible wavelength range of the microparticle encapsulated Hb (mp-Hb), the Hb in the supernatant (spt-Hb) and hemoglobin in the whole mixture (tot-Hb) is presented. A shoulder due to the formation of methemoglobin (seen with EPR) is visible around 630 nm in each of the spectra. B. Data analogous to those in panel A, but from a competition experiment of high

concentrations (800 μM, ~6.3% microparticle Hct) of microparticle-encapsulated and cell-free Hb for NO. C. The ratio of the bimolecular rate constant for NO uptake by cell-free Hb to that for NO uptake by microparticle-encapsulated Hb calculated using equation 6 with data obtained from the competition experiments. The ratios obtained by analysis of the EPR and Absorbance data are shown for the high and low microparticle-encapsulated and cell-free Hb amounts. By EPR, the amounts of MetHb formed during competition were obtained by fitting to a standard MetHb EPR spectrum, double integrating, and comparing to a standard curve. The absorbance data was analyzed for MetHb by fitting to standard oxygenated Hb and MetHb spectra.

## DISCUSSION

We have simulated the uptake of NO by deoxygenated hemoglobin encapsulated in phospholipid vesicles (as in the recent experiments carried out by another group of researchers (21)) and by oxygenated hemoglobin encapsulated in red blood cell microparticles, and conducted experiments on NO uptake by red blood cells and the red cell microparticles. Generally, we find that all of the factors considered, diffusion to the vesicle, inside the vesicle, and permeability through the vesicle can (in principle) affect the NO uptake rates. We found that in the experiments of Sakai et al. (21) and in our experiments with red cells, extracellular diffusion of NO to the encapsulated Hb is the major rate limiting factor, whereas, in our experiments with red cell microparticles, membrane permeability of NO appears to be rate limiting.

The best fit to the experimental data with phospholipid vesicles was obtained when physiological values of NO diffusion rate outside and inside of a vesicle and of membrane permeability to NO have been used (Table II), as shown in Figure 7A & C. From our simulations we may safely conclude that, in the stopped-flow experiments performed by Sakai et al., both diffusion of NO to a vesicle and inside of a vesicle contributed to the rate of the reaction, but that diffusion of NO through the extracellular space was the major rate limiting factor.

To confirm that external diffusion plays the major role in limiting NO uptake by red blood cells, we conducted stopped-flow absorption experiments where we modulated the viscosity of the external buffer. We found that increasing the buffer viscosity decreased the rate of NO uptake under both aerobic and anaerobic conditions. These data support our simulations which show that as particle diameter and internal heme concentration increases, NO uptake rates decrease and this is dominated by the effect of external diffusion. These results are analogous to those reported previously in the case of oxygen uptake (7).

We have previously estimated (20) that the red blood cell membrane under aerobic conditions may be at least 12.5 times less permeable to NO ($4.4\times10^3$ – $5.1\times10^3$ $\mu m\ s^{-1}$) than under anaerobic conditions ($64\times10^3$ – $900\times10^3$ $\mu m\ s^{-1}$). The effect of oxygen was hypothesized to be due to binding of deoxygenated Hb to Band 3 tetramers in the cytoskeleton thereby displacing ankyrin (14,20), similar to a previously proposed mechanism involving intracellular HbNO modulation of RBCs (24). However, it is also possible that the perceived change in membrane permeability is actually due to reactions of NO that occur specifically or preferentially in the membrane, such as the accelerated reaction of NO with oxygen due to the high solubility of these molecules in the lipid phase (63). In such a case, it would not be a real effect of membrane permeability in limiting the rate of NO diffusion from the exterior to the interior of the red cell, but rather competing NO reactions in the membrane that lead to an apparent effect of membrane permeability.

The results from simulations of our photolysis experiments indicate that membrane permeability may contribute substantially to slower NO uptake by

microparticles derived from red blood cells under aerobic conditions. The membrane of these microparticles is known to contain many of the same components as the membrane of red blood cells, including lipid raft proteins (56). In our fast time-resolved photolysis experiments of NO uptake by red cell microparticles, we have measured that they scavenge NO approximately 3 times slower ($1.81\times10^{7}$ $M^{-1}$ $s^{-1}$) than cell-free Hb ($5\times10^{7}$ $M^{-1}$ $s^{-1}$). These experiments, unlike those with phospholipid vesicles, were performed with higher excess amounts of NO of 5 to 8 times as much as total hemoglobin concentration, and at slightly higher hematocrits. Using our best estimate for the average concentration of hemoglobin inside a microparticle of 12.7 mM and our measured diameter of 200 nm, our simulations suggest a larger role for membrane permeability than other factors in limiting NO uptake by these red cell microparticles.

Generally, it is seen that whereas particle size and internal Hb concentration greatly affect the degree of rate limitation by diffusion mechanisms, membrane permeability is independent of particle size and internal Hb concentration in its ability to limit the rate. Thus, if membrane permeability is to have an effect, we might expect it to be most noticeable with small particles. It is worth noting that the overall decrease in the rate of NO uptake by red cell microparticles compared to that by intact red cells is very small (a factor of about 3 vs cell-freeHb compared to a factor of up to 1000 vs cell-free Hb). In the case of red blood cells, the effect of membrane permeability is washed out by the effect of external diffusion. However, in the case of the much smaller red cell microparticles, one would expect the relative role of membrane permeability in limiting the rate of NO uptake to be greater than in the case of red cells, due to the fact that the effects of external and internal diffusion decrease as particle size decreases.

One would not expect a simple phospholipid membrane to limit NO uptake as NO is more soluble in the membrane than in aqueous solution. The difference between red cell microparticles and the phospholipid vesicles is that the former are likely to contain membrane proteins previously hypothesized to decrease membrane permeability (17,18) whereas the latter do not.

Our results from competition experiments between red cell microparticles and cell-free Hb did not show a significant effect of hematocrit. Although there was a trend in data collected by absorption spectroscopy that support a role of external diffusion in limiting NO uptake by the red cell microparticles, this was not shown in EPR data and did not reach significance. Thus, these data suggest major roles of other rate-limiting factors such as membrane permeability or internal diffusion. Our results, as well as previous analogous experiments on oxygen uptake (7), show that as diameter of the Hb containing particles decreases, limitations on NO uptake decrease. As shown in Figure 7, the effect of diameter is seen in diffusion, but not in membrane permeability. Thus, to the extent that membrane permeability does play a role, it should be expected to do so in the smallest vesicles. Overall, these data suggest that, for the case of red cell microparticles that likely maintain membrane proteins and other structures that may partially obstruct NO, the small decrease in NO uptake compared to cell-free Hb could be due to decreased membrane permeability. However, several caveats should be considered. Firstly, the difference in NO uptake between these red cell microparticles and cell-free Hb is much smaller than that between red blood cells and cell-free Hb, so the cause of the rate limitation is harder to draw firm conclusions on. In addition, the physical and chemical make-up of red cell microparticles could be complex and involve a wider size and shape

distribution as well as free hemin or degradation products that our computational modeling did not account for. Finally, our simulations for a range of microparticle sizes (Supplementary Figure 7) show a smaller effect of membrane permeability for dense, larger particles.

In vivo we would expect NO diffusion to a phospholipid vesicle to contribute even more to the slow uptake rate of NO than in stopped-flow experiments due to the cell-free (or vesicle-free) zone. There should still be a plasma layer of some thickness next to the wall of a blood vessel that is mostly free of vesicles due to the radial pressure gradient in laminar flow, similar to the red blood cell free zone. Under physiological conditions the fraction of NO that reacts with Hb is very small, so NO would never have to diffuse very far into a vesicle before reacting. Thus, NO would only have to diffuse through the membrane of a vesicle before being scavenged by hemoglobin. Therefore, even if there is no vesicle-free zone as with red blood cells, the NO diffusion distance inside a phospholipid vesicle might be negligible. The same argument can be applied to NO uptake by red blood cells in vivo. So, intracellular diffusion of NO is not likely to limit the rate at which it is scavenged by red blood cells or by phospholipid vesicles in vivo. Our work also suggests that, in addition to the main rate limiting factor of extracellular diffusion, the erythrocyte membrane permeability could be low enough to partially modulate its uptake of NO under aerobic conditions as also suggested by others (14,18-20,22). Our results have important implications regarding the mechanism of increased NO scavenging by cell-free hemoglobin or red cell microparticles that form in pathological conditions or in older stored blood (27,49,50). The results of our work on NO reactivity with red blood cells and other membrane-encapsulated Hb could also

potentially have implications in other biological situations where a signaling molecule or drug must diffuse through a reactive medium such as oxygen, HNO, or hydrogen sulfide.

In summary, we have found that data obtained by Sakai et al. on NO reactions with phospholipid vesicles can be explained by several mechanisms. Thus, agreement with a model where only intracellular diffusion is included does not prove that this is the only rate-limiting factor. In fact we found that extracellular diffusion is likely to play a larger role in limiting NO uptake by phospholipid vesicles used in those experiments, and that inclusion of this as well as some permeability barrier of the membrane best fits the data. Overall, our data support the concept that extracellular diffusion is the main rate-limiting factor for NO reactions with red cells or phospholipid vesicles in vivo. Similar conclusions have been drawn based on experiments examining oxygen uptake by red cells from different species and artificial vesicles (6,7). We have also demonstrated that membrane permeability to NO may play a major role in limiting NO uptake by microparticles derived from red blood cells under aerobic conditions. Thus, which mechanism is the main factor in limiting NO uptake by membrane-encapsulated Hb depends on many factors including particle size, intracellular Hb concentration, and hematocrit.

**ACKNOWLEDGEMENTS**

This work was supported by National Institutes of Health Grants HL058091 and HL098032.

REFERENCES


1. Liu, X. P., Miller, M. J. S., Joshi, M. S., Sadowska-Krowicka, H., Clark, D. A., and Lancaster, J. R. (1998) *J. Biol. Chem.* **273**, 18709-18713
2. Butler, A. R., Megson, I. L., and Wright, P. G. (1998) *Biochim. Biophys. Acta* **1425**, 168-176
3. Liao, J. C., Hein, T. W., Vaughn, M. W., Huang, K. T., and Kuo, L. (1999) *Proc. Natl. Acad. Sci. USA* **96**, 8757-8761
4. Vaughn, M. W., Kuo, L., and Liao, J. C. (1998) *Am. J. Physiol.-Heart Circ. Physiol.* **43**, H1705-H1714
5. Huxley, V. H., and Kutchai, H. (1981) *J. Physiol. (London)* **316**, 75-83
6. Coin, J. T., and Olson, J. S. (1979) *J. Biol. Chem.* **254**, 1178-1190
7. Vandegriff, K. D., and Olson, J. S. (1984) *J. Biol. Chem.* **259**, 2619-2627
8. Furchgott, R. F., and Zawadzki, J. V. (1980) *Nature* **288**, 373-376
9. Ignarro, L. J., Byrns, R. E., Buga, G. M., and Wood, K. S. (1987) *Circ. Res.* **61**, 866-879
10. Katsuki, S., Arnold, W., Mittal, C., and Murad, F. (1977) *J. Cyclic Nucleotide Res.* **3**, 23-35
11. Palmer, R. M. J., Ferrige, A. G., and Moncada, S. (1987) *Nature* **327**, 524-526
12. Ignarro, L. J. (2000) *Nitric Oxide Biology and Pathobiology*, Academic press, San Diego
13. Lancaster, J. R. (1994) *Proc. Natl. Acad. Sci. USA* **91**, 8137-8141
14. Azarov, I., Huang, K. T., Basu, S., Gladwin, M. T., Hogg, N., and Kim-Shapiro, D. B. (2005) *J. Biol. Chem.* **280**, 39024-39032

15. Liu, X. P., Samouilov, A., Lancaster, J. R., and Zweier, J. L. (2002) *J. Biol. Chem.* **277**, 26194-26199

16. Vandegriff, K. D., and Olson, J. S. (1984) *Biophys. J.* **45**, 825-835

17. Vaughn, M. W., Huang, K. T., Kuo, L., and Liao, J. C. (2000) *J. Biol. Chem.* **275**, 2342-2348

18. Vaughn, M. W., Huang, K. T., Kuo, L., and Liao, J. C. (2001) *Nitric Oxide-Biol Ch* **5**, 18-31

19. Huang, K. T., Han, T. H., Hyduke, D. R., Vaughn, M. W., Van Herle, H., Hein, T. W., Zhang, C. H., Kuo, L., and Liao, J. C. (2001) *Proc. Natl. Acad. Sci. USA* **98**, 11771-11776

20. Huang, K. T., Huang, Z., and Kim-Shapiro, D. B. (2007) *Nitric Oxide* **16**, 209-216

21. Sakai, H., Sato, A., Masuda, K., Takeoka, S., and Tsuchida, E. (2008) *Journal of Biological Chemistry* **283**, 1508-1517

22. Han, T. H., and Liao, J. C. (2005) *Biochim. Biophys. Acta* **1723**, 135-142

23. El-Farra, N. H., Christofides, P. D., and Liao, J. C. (2003) *Ann Biomed Eng* **31**, 294-309

24. Han, T. H., Qamirani, E., Nelson, A. G., Hyduke, D. R., Chaudhuri, G., Kuo, L., and Liao, J. C. (2003) *Proc. Natl. Acad. Sci. U. S. A.* **100**, 12504-12509

25. Reiter, C. D., and Gladwin, M. T. (2003) *Curr. Opin. Hematol.* **10**, 99-107

26. Reiter, C. D., Wang, X. D., Tanus-Santos, J. E., Hogg, N., Cannon, R. O., Schechter, A. N., and Gladwin, M. T. (2002) *Nat. Med.* **8**, 1383-1389

27. Gladwin, M. T. (2005) *Blood* **106**, 2925-2926

28. Nolan, V. G., Wyszynski, D. F., Farrer, L. A., and Steinberg, M. H. (2005) *Blood* **106**, 3264-3267

29. Rother, R. P., Bell, L., Hillmen, P., and Gladwin, M. T. (2005) *Jama-J Am Med Assoc* **293**, 1653-1662

30. Morris, C. R., Vichinsky, E. P., Kato, G. J., Gladwin, M. T., Hazen, S., and Morris, S. M. (2005) *Jama-J Am Med Assoc* **294**, 2433-2434

31. Gladwin, M. T., Sachdev, V., Jison, M. L., Shizukuda, Y., Plehn, J. F., Minter, K., Brown, B., Coles, W. A., Nichols, J. S., Ernst, I., Hunter, L. A., Blackwelder, W. C., Schechter, A. N., Rodgers, G. P., Castro, O., and Ognibene, F. P. (2004) *New Engl J Med* **350**, 886-895

32. Minneci, P. C., Deans, K. J., Zhi, H., Yuen, P. S. T., Star, R. A., Banks, S. M., Schechter, A. N., Natanson, C., Gladwin, M. T., and Solomon, S. B. (2005) *J. Clin. Invest.* **115**, 3409-3417

33. Kato, G. J., McGowan, V. R., Machado, R. F., Little, J. A., Taylor VI, J., Morris, C. R., Nichols, J. S., Wang, X., Poljakovic, M., Morris, J., Sidney M, and Gladwin, M. T. (2006) *Blood* **107**, 2279-2285

34. Doherty, D. H., Doyle, M. P., Curry, S. R., Vali, R. J., Fattor, T. J., Olson, J. S., and Lemon, D. D. (1998) *Nat. Biotechnol.* **16**, 672-676

35. Patel, R. P. (2000) *Free Radical Bio Med* **28**, 1518-1525

36. Vogel, W. M., Dennis, R. C., Cassidy, G., Apstein, C. S., and Valeri, C. R. (1986) *Am. J. Physiol.* **251**, H413-H420

37. Hess, J. R., Macdonald, V. W., and Brinkley, W. W. (1993) *J Appl Physiol* **74**, 1769-1778

38. Lee, R., Neya, K., Svizzero, T. A., and Vlahakes, G. J. (1995) *J Appl Physiol* **79**, 236-242

39. Murray, J. A., Ledlow, A., Launspach, J., Evans, D., Loveday, M., and Conklin, J. L. (1995) *Gastroenterology* **109**, 1241-1248

40. Ulatowski, J. A., Nishikawa, T., MathesonUrbaitis, B., Bucci, E., Traystman, R. J., and Koehler, R. C. (1996) *Crit Care Med* **24**, 558-565

41. Sloan, E. P., Koenigsberg, M., Gens, D., Cipolle, M., Runge, J., Mallory, M. N., and Rodman, G. (1999) *Jama-J Am Med Assoc* **282**, 1857-1864

42. Dou, Y., Maillett, D. H., Eich, R. F., and Olson, J. S. (2002) *Biophys Chem* **98**, 127-148

43. Olson, J. S., Foley, E. W., Rogge, C., Tsai, A. L., Doyle, M. P., and Lemon, D. D. (2004) *Free Radic. Biol. Med.* **36**, 685-697

44. Gulati, A., Barve, A., and Sen, A. P. (1999) *J. Lab. Clin. Med.* **133**, 112-119

45. Abassi, Z., Kotob, S., Pieruzzi, F., Abouassali, M., Keiser, K. R., Fratantoni, J. C., and Alayash, A. I. (1997) *J. Lab. Clin. Med.* **129**, 603-610

46. Sharma, A. C., Singh, G., and Gulati, A. (1995) *Am. J. Physiol.-Heart Circul. Physiol.* **38**, H1379-H1388

47. Thompson, A., McGarry, A. E., Valeri, C. R., and Lieberthal, W. (1994) *J Appl Physiol* **77**, 2348-2354

48. Sampei, K., Ulatowski, J. A., Asano, Y., Kwansa, H., Bucci, E., and Koehler, R. C. (2005) *Am. J. Physiol.-Heart Circul. Physiol.* **289**, H1191-H1201

49. Gladwin, M. T., and Kim-Shapiro, D. B. (2009) *Curr. Opin. Hematol.* **16**, 515-523

50. Donadee, C., Raat, N. J. H., Kanias, T., Tejero, J., Lee, J. S., Kelley, E. E., Zhao, X., Liu, C., Reynolds, H., Azarov, I., Frizzell, S., Meyer, M., Donnenberg, A. D., Qu, L., Triulzi, D., Kim-Shapiro, D. B., and Gladwin, M. T. (2011) *Circulation*, Accepted

51. Rudolph, A. S., Sulpizio, A., Hieble, P., MacDonald, V., Chavez, M., and Feuerstein, G. (1997) *J. Appl. Physiol.* **82**, 1826-1835

52. Alayash, A. I. (1999) *Nat. Biotechnol.* **17**, 545-549

53. Sou, K., Klipper, R., Goins, B., Tsuchida, E., and Phillips, W. T. (2005) *J. Pharmacol. Exp. Ther.* **312**, 702-709

54. Kim, H. W., and Greenburg, A. G. (2004) *Artif. Organs* **28**, 813-828

55. Chang, T. M. S. (2006) *Artif. Cells Blood Substit. Biotechnol.* **34**, 551-566

56. Kriebardis, A. G., Antonelou, M. H., Stamoulis, K. E., Economou-Petersen, E., Margaritis, L. H., and Papassideri, I. S. (2008) *Transfusion* **48**, 1943-1953

57. Kim-Shapiro, D. B. (2004) *Free Radic. Biol. Med.* **36**, 402-412

58. Eich, R. F., Li, T. S., Lemon, D. D., Doherty, D. H., Curry, S. R., Aitken, J. F., Mathews, A. J., Johnson, K. A., Smith, R. D., Phillips, G. N., and Olson, J. S. (1996) *Biochemistry-US* **35**, 6976-6983

59. Jeffers, A., Gladwin, M. T., and Kim-Shapiro, D. B. (2006) *Free Radical Biology and Medicine* **41**, 1557-1565

60. Xiong, Z., Cavaretta, J., Qu, L., Stolz, D. B., Triulzi, D., and Lee, J. S. *Transfusion* **51**, 610-621

61. Huang, Z., Louderback, J. G., Goyal, M., Azizi, F., King, S. B., and Kim-Shapiro, D. B. (2001) *Biochim. Biophys. Acta* **1568**, 252-260

62. Azarov, I., He, X. J., Jeffers, A., Basu, S., Ucer, B., Hantgan, R. R., Levy, A., and Kim-Shapiro, D. B. (2008) *Nitric Oxide-Biology and Chemistry* **18**, 296-302

63. Liu, X. P., Miller, M. J. S., Joshi, M. S., Thomas, D. D., and Lancaster, J. R. (1998) *Proc. Natl. Acad. Sci. USA* **95**, 2175-2179

# CHAPTER IV

## NITRIC OXIDE SCAVENGING BY RED CELL MICROPARTICLES

C. Liu, W. Zhao, G. J. Christ, M. T. Gladwin, D. B. Kim-Shapiro

The following manuscript was published in Free Radical Biology & Medicine, volume 65, pages 1164-1173, 2013, and is reprinted with permission. Stylistic variations are due to the requirements of the journal. C. Liu performed all experiments and computational simulations. W. Zhao helped to isolate branches of mesenteric artery from rats and set up the instrument for myography experiments. D. B. Kim-Shapiro originally designed the experiments and wrote and edited most of the manuscript. C. Liu prepared all figures and wrote the sections of the Methods & Materials and Results. G. J. Christ and M. T. Gladwin edited the manuscript.

# Nitric Oxide Scavenging by Red Cell Microparticles

**Chen Liu[a], Weixin Zhao[b], George J. Christ[b], Mark T. Gladwin[c,d], Daniel B. Kim-Shapiro[a,*]**

[a]Department of Physics, Wake Forest University, Winston-Salem, NC 27109, USA
[b]Institute for Regenerative Medicine, Wake Forest University School of Medicine, Winston-Salem, NC 27101, USA
[c]Vascular Medicine Institute, University of Pittsburgh, Pittsburgh, PA 15213, USA
[d]Department of Medicine, Division of Pulmonary, Allergy and Critical Care Medicine, University of Pittsburgh School of Medicine, Pittsburgh, PA 15213, USA

[*] Corresponding author. Fax: +1 336 758 6142.

E-mail address: shapiro@wfu.edu (D.B. Kim-Shpairo).

## ABSTRACT

Red cell microparticles form during the storage of red blood cells and in diseases associated with red cell breakdown and asplenia, including hemolytic anemias such as sickle cell disease. These small phospholipid vesicles that are derived from red blood cells have been implicated in the pathogenesis of transfusion of aged stored blood and hemolytic diseases, via activation of the hemostatic system and effects on nitric oxide (NO) bioavailability. Red cell microparticles react with the important signaling molecule NO almost as fast as cell-free hemoglobin, about one-thousand times faster than red cell encapsulated hemoglobin. The degree to which this fast reaction with NO by red cell microparticles impacts NO bioavailability depends on several factors that are explored here. In the context of stored blood preserved in ADSOL, we find that both cell-free hemoglobin and red cell microparticles increase as a function of duration of storage and the proportion of extra erythrocytic hemoglobin in the red cell microparticles fraction is

about 20% throughout storage. Normalized by hemoglobin concentration, the NO scavenging ability of cell-free hemoglobin is slightly higher than red cell microparticles as determined by a chemiluminescent NO scavenging assay. Computational simulations show that the degree to which red cell microparticles scavenge NO will depend substantially on whether they enter the cell-free zone next to the endothelial cells. Single microvessel myography experiments performed under laminar flow conditions demonstrate that microparticles significantly enter the cell-free zone and inhibit acetylcholine, endothelial-dependent and NO-dependent vasodilation. Taken together, these data suggest that as little as five micromolar hemoglobin in red cell microparticles, an amount formed after the infusion of one unit of aged stored packed red blood cells, has the potential to reduce NO bioavailability and impair endothelial-dependent vasodilation.

**Keywords:**

Nitric oxide, Blood storage, Red cell microparticles, Cell-free hemoglobin

## INTRODUCTION

Nitric oxide (NO)[*] is an important signaling molecule that functions as the endothelial derived relaxing factor (EDRF which modulates vascular tone), reduces platelet activation and cellular vascular adhesion, is anti-inflammatory, is used in host defense mechanisms, and functions as a neurotransmitter [1-5]. Low NO bioavailability contributes to several pathological conditions [6-10]. A clue to the identification of NO as the EDRF which is synthesized in endothelial cells and then diffuses to smooth muscle to effect vasodilation was that both the endothelial relaxing factor and NO are scavenged by hemoglobin (Hb) [11]. In fact, given that there is so much Hb in the blood (10 mM in

[*] Abbreviations: NO, nitric oxide; EDRF, endothelial derived relaxing factor; Hb, hemoglobin; OxyHb, oxygenated hemoglobin; RBC, red blood cell; MPs, microparticles; ACD, acid citrate dextrose; CFZ, cell-free zone; ACh, acetylcholine; PE, phenylephrine; Hct, hematocrit

heme), the ability of NO to function as the EDRF, diffusing to smooth muscle without being scavenged by Hb was seen as a paradox [12].

Oxygenated Hb (OxyHb) reacts with NO to form nitrate and methemoglobin. This reaction, which is rate-limited by the time it takes for NO to diffuse to the heme pocket of Hb ($k = 107\text{-}108\ M^{-1}s^{-1}$), essentially destroys the ability of NO to signal, as nitrate is relatively inert [13-15]. Nitric oxide can also reversibly bind to the vacant deoxygenated heme of hemoglobin, but the binding is very tight and even when the NO does come off, it is still likely to be inactivated by its reaction with OxyHb [16]. Thus, Hb effectively scavenges NO and computer simulations showed that the amount of NO that would be capable of diffusing to the smooth muscles and effecting vasodilation when there is so much Hb in blood would not be sufficient to affect vasodilation; leaving a paradox as to how NO could function as the EDRF.

The paradox of how NO can function to effect vasodilation without being scavenged by Hb is resolved by the fact that when Hb is encapsulated inside of a red blood cell (RBC), it scavenges NO up to one-thousand times slower than when the Hb is not encapsulated (referred to as cell-free Hb) [17-26]. One mechanism that accounts for the reduced rate of NO scavenging by red cell encapsulated Hb compared to when it is free in solution is the formation of a cell-free zone [18, 21]. Due to effects of flow within the blood vessel, red blood cells are pushed inward away from the endothelium forming a cell-free zone next to the endothelium. Computational analysis showed that the existence of a cell-free zone could resolve the paradox of how NO functions as the EDRF [18]. In addition, experiments with single arteriole vessels showed that flowing red cells (in which there would be a cell-free zone) inhibited vasodilation less than when there was no

flow and the effect of flow was not observed using cell-free Hb instead of red cells (since cell-free Hb enters the cell-free zone) [21].

Nitric oxide scavenging by Hb is observed to be several orders of magnitude slower when the Hb is encapsulated in red cells compared to when it is free in solution even when the Hb and NO are rapidly mixed in a turbulent mixer such as in stopped-flow experiments [17, 19, 22, 27]. Since there is no cell-free zone in this geometry, other factors must further account for the slower NO scavenging by red cells. One such mechanism involves the unstirred layer that forms around the red blood cells [19, 24, 27-29]. Since NO reacts so fast with Hb, any NO that is close to a red blood cell after mixing is rapidly scavenged. On the other hand, the rate that NO that is further away is scavenged is rate-limited by the time for the NO to diffuse to the red blood cell. Thus, shortly after mixing, the concentration of NO around a red cell is no longer uniform and there is an "unstirred layer". The rate of NO scavenging by a red cell is thus limited by the time for external diffusion to the red blood cell.

Another mechanism that has been proposed to account for slower NO scavenging by red blood cells compared to cell-free Hb is that the red cell membrane has a finite permeability to NO, so that there is a physical barrier to NO diffusion across the membrane [22, 23]. This notion has gained support from experiments in which chemical or physical disruption of the protein layer next to the membrane is disrupted whereupon NO uptake by red cells is increased [26]. Overall, the relative role of each mechanism in limiting NO uptake by red cells continues to be elucidated but the fact that red cells do scavenge NO much slower than cell-free Hb is clear.

We have recently shown that red cell microparticles (MPs) also scavenge NO many times faster than red blood cells[8]. Red cell microparticles are 50 to 200 nm diameter phospholipid vesicles that are derived from red blood cells and contribute to pathology in a variety of conditions including sickle cell disease, hereditary spherocytosis, and transfusion of older stored blood [30]. Along with other RBC changes during blood storage, red cell fragmentation and formation of these microparticles has been measured [31-37]. The microparticle formation is associated with lipid loss secondary to ATP depletion [36, 37]. The microparticles have been shown to contain substantial amounts of Hb [31, 33, 37], and one study found that the majority of plasma Hb was actually contained in these microparticles [31]. While still controversial, a recent meta-analysis of twenty-one studies suggested that transfusion of older stored blood is associated with a significantly higher risk of death [38]. We have hypothesized that disruption of NO homeostasis, secondary to NO scavenging by cell free hemoglobin and red cell microparticles contributes to the blood storage lesion [8], as it does to sickle cell disease and other conditions characterized by red cell breakdown [6].

We have shown that, as in the case of oxygen uptake by Hb containing vesicles, NO scavenging by red cell microparticles increases as the size of the particles decreases and the concentration of intravascular Hb increases [28, 39]. In this work, we further explore factors that would determine the extent to which red cell microparticles contribute to NO scavenging, such as the ability of these microparticles to concentrate in the cell free zone. These findings are considered in the context of transfusion of older stored blood and in hemolytic diseases.

## MATERIALS AND METHODS

Microparticles were obtained from outdated packed red blood cell units in acid citrate dextrose (ACD) and ADSOL storage solution purchased from the Interstate Blood Bank, Inc. (Memphis, TN). The microparticles were prepared as previously described [8]. The preparation was confirmed to contain only microparticle-encapsulated hemoglobin via microscopy and absorbance measurements [8]. Other chemicals were purchased from Sigma unless otherwise stated.

*Packed Red Blood Cells*

Five randomly selected packed red blood cell units were obtained from the Interstate Blood Bank, Inc. (Memphis, TN) to examine the percentages of cell-free and microparticle encapsulated hemoglobin formed in blood units during storage. These units were not leukoreduced and preserved in ADSOL. The five packed red blood cell units were stored in a refrigerator at 4 ℃ for 40 days and hemoglobin concentrations in cell free hemoglobin and microparticles were examined at three timepoints (7, 27, and 40 days). In addition, packed red blood cell units stored in ACD were also examined at three different lengths of time (7, 18, and 26 days) as well. These units were not leukoreduced. At each storage time, the supernatant was collected by sedimentation of the red blood cells and cell-free hemoglobin and microparticles were separated from the supernatant as previously described [8]. Absorption spectra were collected in the visible range ( 450 – 700nm) on a Cary 100 Bio spectrometer (Varian Inc.) equipped with an integrating sphere to collect scattered light from the RBCs and MPs suspensions as described previously [39, 40]. Some spectra that did not contain RBCs and MPs were taken on a Cary 50 Bio spectrometer (Varian Inc.).

*Nitric Oxide Consumption*

NO consumption was measured using a Nitric Oxide Analyzer (Sievers) as described previously [8]. A glass vessel with 120 μM DETA NONOate in PBS was purged with Helium in-line with a chemiluminescent Nitric Oxide Analyzer. A steady NO signal of 40 to 60 mV was generated by the decay of DETA NONOate and the release of NO. After the signal became stable, 25 μl or 50 μl samples containing known concentrations of hemoglobin (standards) or plasma fractions were injected into the solution and the NO signal decreased because of NO consumption. The areas above the decreased NO signal curve and below baseline were linearly related to the concentrations of hemoglobin standards or plasma fractions. The standard curve was obtained by injecting 5 different concentrations of hemoglobin and calculating the areas. The amounts of NO consumed by plasma fractions was quantified by calculating the areas of the decreased curves caused by injecting plasma fractions and comparing to the standard curve.

*2D Computational Simulation*

The computational simulation (Figure 13) was based on a two dimensional model for NO availability within a blood vessel as described previously [41, 42]. The model computed the production, diffusion, and consumption of NO in various compartments within the vascular area, including the intracellular space of the red blood cells and red cell microparticles, the extracellular space of the RBCs and MPs, a RBC cell-free zone (CFZ) within the lumen, the endothelium around the blood vessel wall, and the surrounding smooth muscle cells. The end result was a steady-state NO concentration computed as a function of position. The symmetry of the geometry was taken advantage

of and the NO concentrations obtained at each fixed radius from the center were averaged. NO scavenging by Hemoglobin both encapsulated by RBCs and MPs was studied in this model with a presence of a RBC cell-free zone. The steady-state NO concentration was calculated with MPs either allowed to diffuse into the cell-free zone or restricted to the lumen that does not include the cell-free zone. Both 45% and 30% hematocrit were studied in the model. The parameters, based on previous work [39, 41], that were used in the simulations are listed in Table IV. Modeling work was performed using COMOSOL 4.0a software.

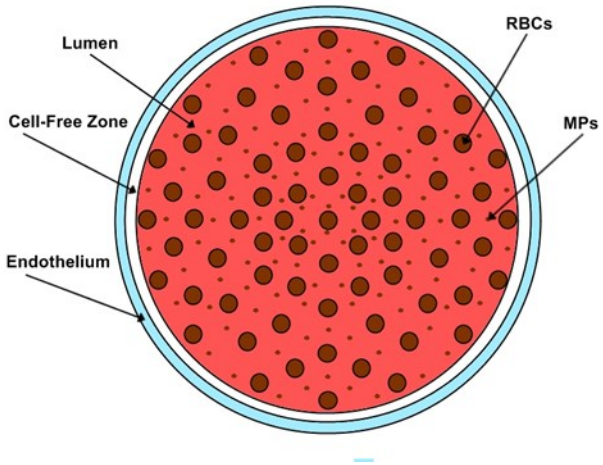


**Figure 13. Illustration of regions modeled. Red blood cells and microparticles are in the lumen of the blood vessel, which includes a red blood cell-free zone.** NO is produced in the endothelium which is on the exterior of the blood vessel. The smooth muscle is the outermost layer around the blood vessel. The rate of NO production, scavenging, and diffusion is defined separately for each compartment as described previously. This schematic of the modeled regions is drawn to scale.

**TABLE IV. List of symbols, their meanings, and values used in simulations.**

| Parameter | Value |
|---|---|
| Extracellular NO diffusion coefficient | $3300\ \mu m^2 s^{-1}$ |
| Intracellular NO diffusion coefficient | $1142 \mu m^2 s^{-1}$ |
| RBC membrane permeability of NO-low | $450\ \mu m\ s^{-1}$ |
| RBC membrane permeability of NO-high | $9 \times 10^5\ \mu m\ s^{-1}$ |
| MP membrane permeability of NO | $2.15 \times 10^4\ \mu m\ s^{-1}$ |
| NO reaction rate constant in smooth muscle | $0.05\ \mu M^{-1} s^{-1}$ |
| OxyHb-NO reaction rate constant | $8.9 \times 10^7\ M^{-1} s^{-1}$ |
| Total NO production rate | $42.4\ \mu M\ s^{-1}$ |
| Hb concentration in RBC | $23\ mM$ |
| Hb concentration in MP | $12.7\ mM$ |
| Hct | 30%, 45 % |
| Blood vessel radius | $50\ \mu m$ |
| Cell-free zone thickness | $2.5\ \mu m$ |
| Endothelium thickness | $2.5\ \mu m$ |
| Radius of RBC | $3.39\ \mu m$ |
| Radius of MP | $0.2\ \mu m$ |
| RBC membrane thickness | $0.0078\ \mu m$ |

*Microvessel Myographic Bioassay*

Male Lewis rats (6–8 weeks) were used. Rodents were purchased from commercial vendors (Harlan and Jackson Laboratories). All animal procedures were approved by the Wake Forest University IACUC and were in accordance with animal use guideline set by the American Physiological Society. Rats were euthanized with carbon dioxide. The mesenteric bed was quickly removed and placed in a chilled oxygenated Krebs-Ringers bicarbonate solution (containing, in mmol/L: NaCl 118.3, KCl 4.7, $CaCl_2$ 2.5, $MgSO_4$ 1.2, $KH_2PO_4$, 1.2, $NaHCO_3$ 25, and dextrose 11.1). Second-order branches of the superior mesenteric artery were isolated and removed for functional studies. The segments of cleaned arterial segments were mounted in a Pressure Myograph System (Danish Myo Technology). In brief, each segment was cannulated between 2 glass cannulas with tip diameters <100 μm in a chamber filled with 8 mL of Krebs solution bubbled by 20% $O_2$, 5% $CO_2$, and 75% $N_2$, and maintained at 37°C (pH 7.4). After one end of the segment was secured on a cannula with two 10-0 nylon sutures, the luminal content was flushed through with Krebs solution using a perfusion device at a pressure difference <20 mm Hg. The other end was then cannulated. Glass cannulas were pulled on a micropipette puller model P-97 (Shutter Instrument Company, Novato, CA). Both cannulating pipettes were connected to independent reservoir systems that controlled the flow rate and intraluminal pressure. The in and out intraluminal pressure were measured by a pressure transducer on each side of the pressure myograph system (model 110P, DMT). A video camera attached to a light-inverted microscope (Zeiss Axiovert 40 Microscope, model 110P) was used to visualize changes in the diameter of

cannulated arteries. The outer diameter and luminal pressure were recorded simultaneously using Myo-View software (version 1.2P, Photonics Engineering).

After a blood vessel was cannulated, the chamber was placed on the stage of the pressure myograph system. The vessel was set to its in situ length with 8 mL of Krebs solution in the vessel bath, the absence of leaks was confirmed, and the artery segment was equilibrated for 60 minutes during which the vessel developed spontaneous tone at 60 cm $H_2O$ luminal pressure without flow [21]. The experimental interventions were performed after the tone was developed. Samples of Hb, RBCs, or MPs were infused through the vessel which was bathed entirely in Krebs solution during the experiment. No more than two infusions were performed on one vessel due to vessel sensitivity. Bubbling of the bath insured homogeneity of the solution.

The effects of Hb, RBCs, and MPs on NO-mediated vasodilation were studied. Each of these was infused intravascularly, and was thus not present outside the vessel. We used Acetylcholine (ACh) to induce NO production by endothelial cells [43-45]. The vessels were first pressurized to 60 cm $H_2O$ luminal pressure without flow by setting both reservoirs to the same hydrostatic level. Although it has been shown that vessels of similar size to those employed herein may not develop myogenic tone, we let the vessels equilibrate for a half hour and recorded basal tone (T1) [46-48]. The average basal tone in the study was 229±14 μm. Subsequently, 0.5 μM Phenylephrine (PE) was added to the vessel bath and the vessel reached a new steady state (after at least ten minutes), constricting to tone two (T2). Relaxation was induced with 0.5 μM Acetylcholine added into the vessel bath after a complete vessel contraction due to PE. At least ten minutes were required to allow the relaxation to become stable and tone three (T3) was reached.

The vessel contraction and dilation were examined in the absence or presence of luminal Hb, RBCs, or MPs. The percentage change was calculated by: (T3-T2)/(T1-T2).

After tone three was reached, the flow effects of Hb, RBCs, and MPs on NO-mediated vasodilation were studied on these same vessels. Using the same vessels for all these interventions allowed proper calculation of percent changes. When ACh induced vasodilation was fully achieved, the vascular response to a luminal flow driven by a pressure gradient of 60 cm $H_2O$ across the length of vessel was examined. A period of 3-5 minutes was applied to obtain a stable dilation and tone four (T4) was recorded. Previous work has shown that flow can induce NO mediated vasodilation on similar sized rat mesenteric vessels as employed herein [49, 50]. The luminal flow was produced by simultaneously moving the reservoirs in opposite directions of the same magnitude. The average luminal flow rate at 60 cm $H_2O$ was 4.46 µl/sec. T4 was recorded when the outer diameter became stable and this took at least three minutes. The flow effect was calculated by: (T4-T3)/(T1-T2).

*Statistical Analysis*

Analysis was performed with Microsoft Office Excel 2010 (Redland, OR), GraphPad Prism (GraphPad Software, Inc., La Jolla, CA). The hemoglobin concentrations of cell-free Hb and MPs at 40 days and 7 days for ADSOL and 26 days and 7days for ACD were compared by a paired two-sample student's t-test. Statistical significance in myography experiments was evaluated by one-way ANOVA. Results were considered significant when $P < 0.05$. All values are presented as mean ± SD.

## RESULTS

*Cell-Free Hemoglobin and Microparticles during Storage*

To explore the relative role of cell-free and microparticle encapsulated hemoglobin formed during blood storage in scavenging NO, we measured the concentration and percentages of cell-free hemoglobin and microparticles separated from the supernatant of packed red blood cells stored in ADSOL or ACD by UV-visible spectroscopy and least-squares spectral deconvolution. For the red blood cells stored in ADSOL, we found that both cell-free hemoglobin and red cell microparticles increase as a function of duration of storage, and the proportion of hemoglobin in red cell microparticles remained approximately 20% during storage (Figure 14). The concentrations of hemoglobin in cell-free hemoglobin and microparticles were significantly increased in blood units of 40 days compare to those of 7 days ($n=5$, $P<0.05$). Cell-free hemoglobin concentration ranged from an average of $10.6 \pm 5.4$ μM at 7 days to $79.8 \pm 29.6$ μM at 40 days and microparticles ranged from an average of $3.3 \pm 3.5$ μM at 7 days to $14.4 \pm 3.9$ μM at 40 days. Similar to ADSOL, when the red blood cells were stored in ACD, both cell-free hemoglobin and red cell microparticles increased during storage (data not shown). However, the proportion of hemoglobin in red cell microparticles increases relative to cell-free hemoglobin when ACD storage solution was used. A significant increase was observed for both the concentrations of hemoglobin in cell-free hemoglobin and microparticles in blood units of 26 days compare to those of 7 days ($n=5$, $P<0.05$). Cell-free hemoglobin concentration was an average of $28.2 \pm 8.7$ μM at 7 days and $88.2 \pm 41.5$ μM at 26 days. The hemoglobin concentration in microparticles was an average of $4.3 \pm 3.0$ μM at 7 days and $111.0 \pm 57.4$ μM at 26 days.

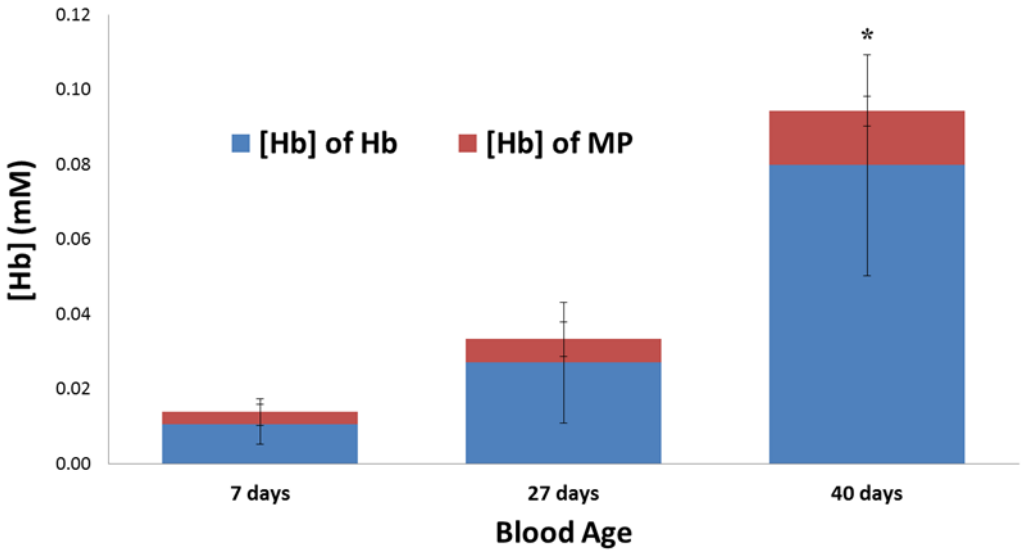


**Figure 14. Extracellular hemoglobin as a function of length of storage in ADSOL.** Both hemoglobin concentrations of cell-free Hb and MPs increase along with blood aging. The proportion of hemoglobin concentration in MPs is about 20% (n=5). *, a paired two-sample Student's t-Test, $P < 0.05$ for both hemoglobin concentrations of cell-free Hb and MPs at 40 days compare to 7 days.

*Cell-Free Hemoglobin and Microparticles NO-Scavenging Activity*

Previous work has demonstrated that cell-free hemoglobin consumes NO with a 1:1 ratio [8]. We employed a NO consumptions assay using hemoglobin to quantify NO consumed (Figure 15A). Typical result from injection of 10 μM of Hb or microparticles is shown in Figure 15B. Overall, we observed a ratio of 0.7 from the plot of the amount of NO consumed by microparticles vs. its heme concentration (Figure 15D) and a ratio of 1 from the plot of the amount of NO consumed by free hemoglobin vs. heme concentration (Figure 15C) (n=9). We found that the NO scavenging ability of red cell microparticles is about 70% of that of cell-free Hb on a molar basis. This reduction in NO scavenging efficiency of microparticles is likely due to the slightly reduced rate of NO

scavenging by microparticles that we have previously reported [8], competing with NO being purged into the Nitric Oxide Analyzer.

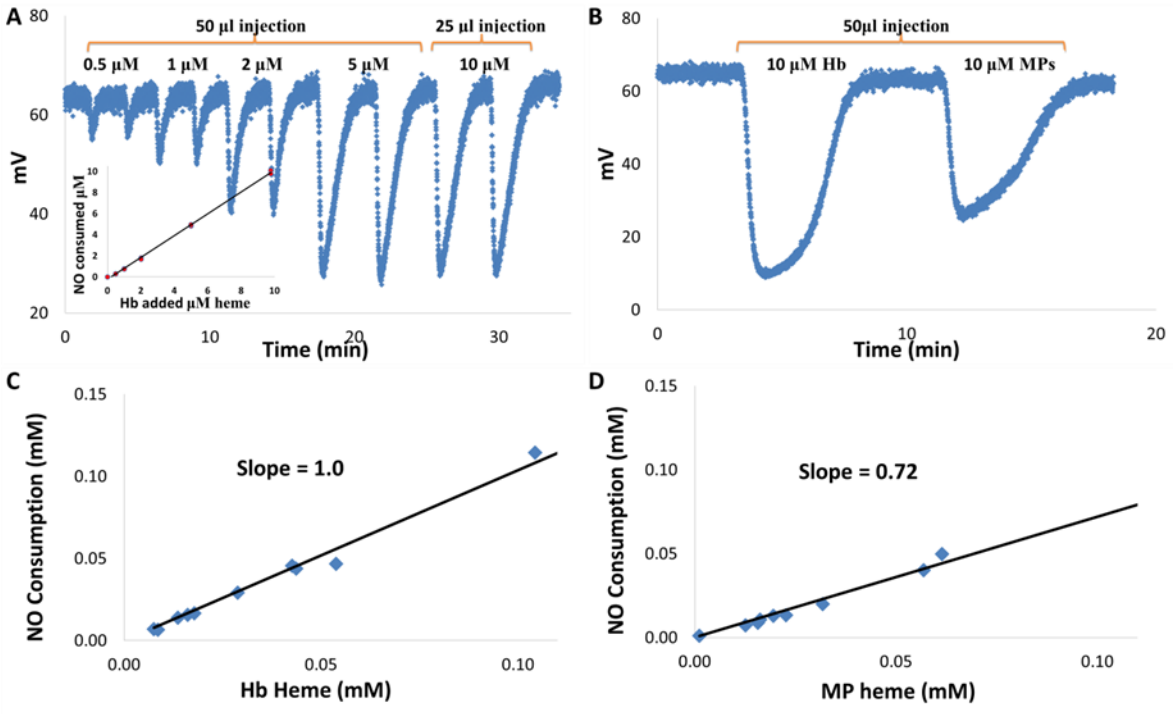


**Figure 15. Nitric Oxide consumption assay.** (A) Standard curves were generated by injections of 50 or 25 µl cell-free hemoglobin (Hb from 0-10 µM heme) diluted in PBS produced concentration-dependent, transient decreases in the baseline NO signal (NO consumption, mV) generated by 120 µM DETA NONOate in PBS, which was purged with a helium stream in-line with an NO analyzer. Inset: A plot of the NO consumed in response to the hemoglobin added. (B) Raw data showing NO consumption by 10 µM Hb and MPs. (C, D) The plasma fractions heme concentrations were plotted against the amounts of NO consumption of the fractions, quantified by the standard curve with a $R^2$ of 0.989 for Hb and a $R^2$ of 0.977 for MP. NO scavenging ability of red cell microparticles (D) is about 70% of that of cell-free Hb on a molar (C) (n=9).

*Simulations show 5 µM of MP-encapsulated Hb can significantly reduce bioavailable NO*

Using computer simulations, the effects of MPs on NO bioavailability were examined in terms of Hematocrit (Hct), permeability, and the absence or presence of MPs in the cell-free zone. (Figure 16 and Figure 17). The concentrations of NO are plotted against the distance from the center of a 100-$\mu m$-diameter vessel. In all the results, the

NO concentration in the lumen is almost zero and it increases rapidly at the endothelial layer where NO is produced. As the distance from the center of the vessel increases further, the NO concentration decreases. The NO concentration versus the distance from the center of the blood vessel when the hematocrit is 45% and 30% are plotted in Figure 16 and Figure 17 respectively. The permeability of membranes from MPs used in our simulations was set equal to that determined previously [39] while the permeability of red cell membranes to NO (which has not been defined precisely) was given values at the extreme of previous publications [41]. When red cell permeability to NO is low, steady state NO is higher which is reasonable as it is harder for NO to get into the red cells to be consumed (compare panels A and B to panels C and D). We found that the effects of microparticles are larger when they enter the cell-free zone and in these cases just 5 μM microparticle encapsulated Hb can affect NO bioavailability (compare panels B and D to panels A and C). As hematocrit increases, NO bioavailability in the absence of MPs decreases due to increased scavenging by red blood cells (compare Figure 16 and Figure 17). However, the relative effect of microparticles is greater for lower Hct (30%, Figure 17) compared to the higher Hct (45%, Figure 16).

The percentage reduction in NO concentration at the endothelium layer (52.5 μm from the vessel center) is illustrated in Figure 18. The percentage reduction was calculated by subtracting the NO concentration with MPs from the NO concentration with no MPs and dividing by the NO concentration without MPs. The results consistently show that the presence of MPs reduces NO concentration more significantly when the red cell permeability is low, MPs enter the cell-free zone, or the Hct is 30%.

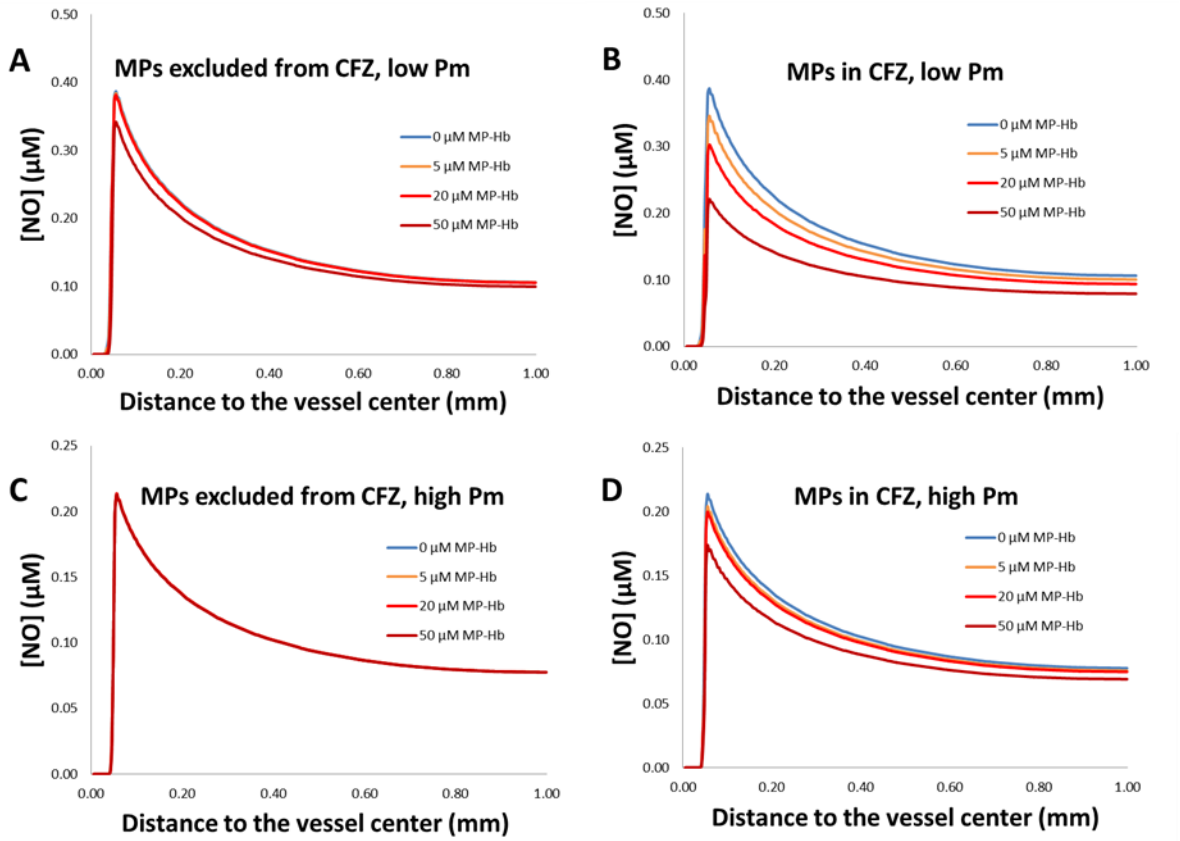


**Figure 16. NO bioavailability dependence on cell-free zone, membrane permeability (PM), and MP-encapsulated Hb concentration at 45% Hct.** The label of MP-Hb in the figure refers to MP encapsulated Hb. (A) NO concentrations along the distance are plotted when MPs are excluded from the CFZ and red cell membrane permeability is low. (B) MPs appear in the CFZ and membrane permeability is low. (C) MPs are excluded from the CFZ and membrane permeability is high. (D) MPs appear in the CFZ and membrane permeability is high.

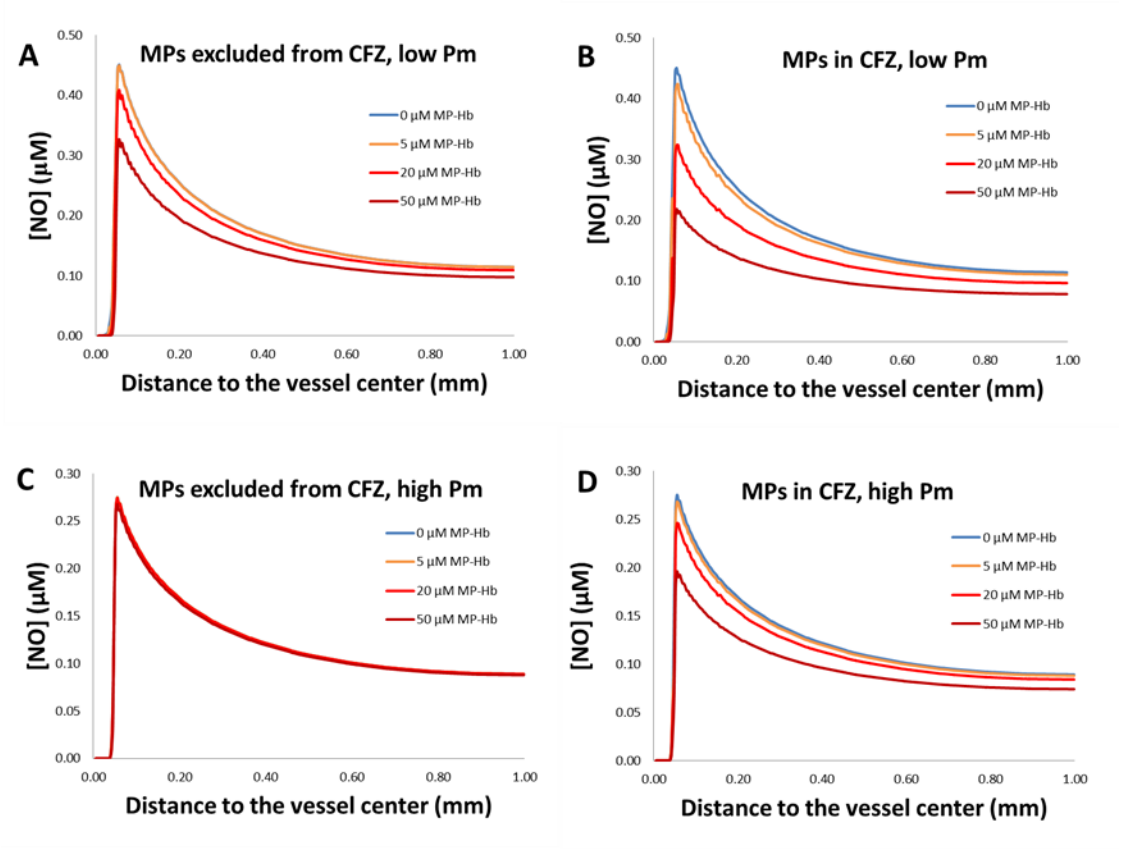


**Figure 17. NO bioavailability dependence on cell-free zone, membrane permeability, and MP-encapsulated Hb concentration at 30% Hct.** (A) NO concentrations along the distance are plotted when MPs are excluded from the CFZ and red cell membrane permeability is low. (B) MPs appear in the CFZ and membrane permeability is low. (C) MPs are excluded from the CFZ and membrane permeability is high. (D) MPs appear in the CFZ and membrane permeability is high.

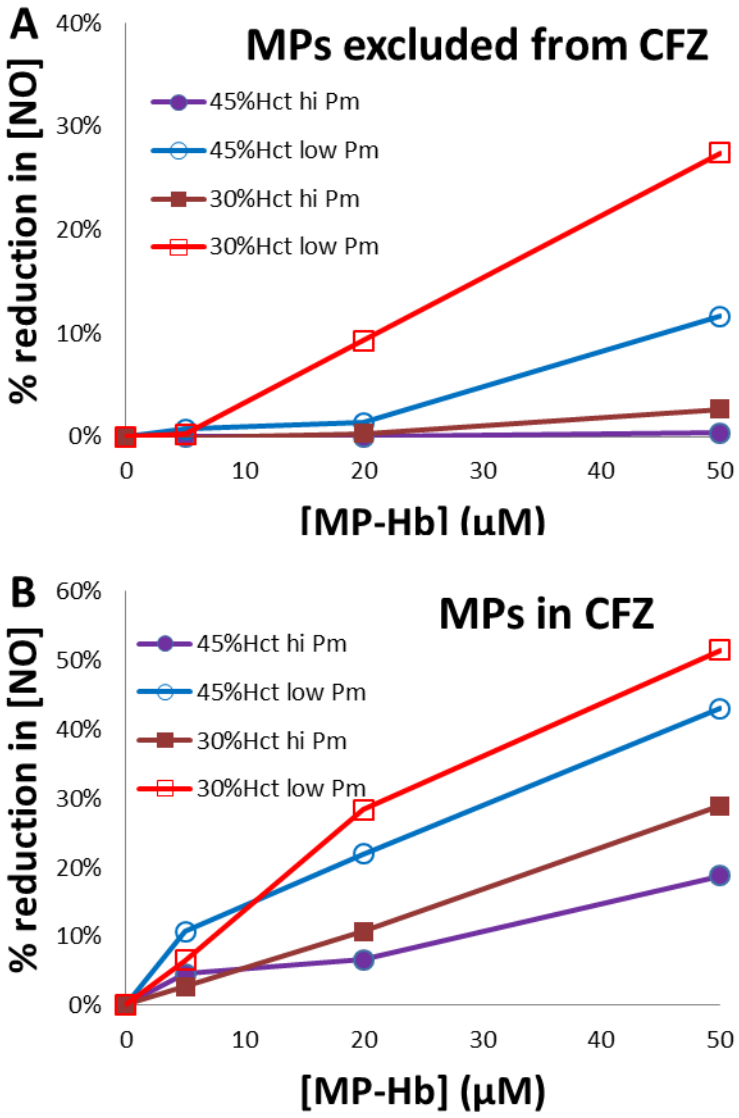


**Figure 18. Percentage reduction in NO concentration at the point of endothelium layer.** The percentage reduction was calculated by subtracting the NO concentration with MPs from the NO concentration with no MPs and dividing by the NO concentration without MPs. The x-axis shows MP-encapsulated Hb concentration. (A) Percentage reduction in NO concentration when MPs are excluded from the CFZ. (B) Percentage reduction in NO concentration when MPs appear in the CFZ.

*Red Cell Microparticles Enter the Cell-Free Zone*

Experiments were conducted to examine whether red cell microparticles do indeed enter the cell-free zone, following an experimental approach employed by others studying cell-free Hb, red cells, and the cell-free zone [21]. Measurements and calculations of the outer diameters at tone 1,2,3,4 in the absence or presence of luminal Hb, RBCs, or MPs are shown in Table V. A single mesenteric arteriole with red blood cells present at 45% hematocrit was observed by an inverted microscope (Zeiss Axiovert 40, DMT) with the absence and presence of flow (Figure 19). A cell-free zone is clearly formed with the presence of flow and a larger vessel diameter is obtained as shown in Figure 19B.

To compare the effect of free Hb, MPs and RBCs on NO-mediated dilation without flow, the vessel was dilated by ACh after a complete contraction caused by PE. Acetylcholine can affect vasodilation by activation of endothelial NO production. Our results show that a hemoglobin concentration of 30 μM in free Hb and MPs had similar effect as RBCs with 45% hematocrit (10mM Hb) on the vasodilation (shown in Table V and Figure 20A). A combined solution of MPs and RBCs was examined as well but had no additional constrictive effect, perhaps due the vessel already being fully constricted. Overall, these results are consistent with the fact that cell-free Hb and red cell microparticles scavenge NO much more efficiently than red cells.

To investigate whether MPs enter the cell-free zone we studied the effects of flow on NO-mediated vasodilation as flow would induce a cell-free zone. Previous work has shown that flow increases NO-mediated vasodilation in the presence of red cells, but flow has no effect on vasodilation in the presence of cell-free Hb [21], indicating that cell-free

Hb remains in the cell-free zone. To investigate the flow effect on NO-mediated dilation in the presence of MPs, the vascular response to flow ($\Delta P$=60 cm $H_2O$) in the absence and presence of luminal Hb, RBCs, and MPs was examined (shown in Table V and Figure 20B). No significant hemolysis was observed by examining cell-free hemoglobin concentration in red blood cell solution after the solution flew out the system.

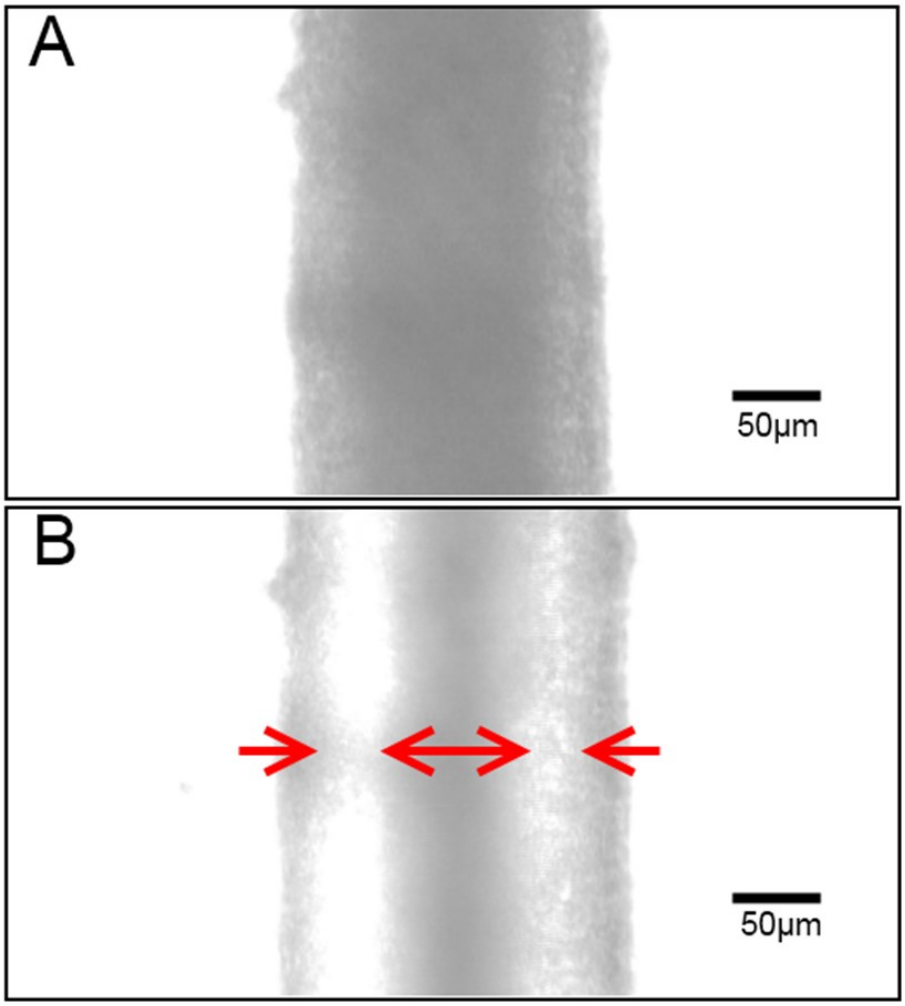


**Figure 19. Observation of a cell-free zone.** A single mesenteric arteriole (about 210 μm diameter when fully dilated) is shown with red blood cells present at 45% hematocrit after 0.5 μM ACh was added in the absence of flow giving a diameter of about 178 μm (A) and in the presence of flow giving a diameter of about 200 μm (B) where a cell-free zone is apparent (cell-free zone indicated by red arrows, bars are 50μm in length).

Surprisingly, intravascular flow induced no vascular response in the absence of luminal Hb, RBCs, and MPs (when only buffer was in the vessel). One would expect vessel dilation to occur in response to flow due to shear induced NO production. We hypothesized that the lack of dilation when buffer was flowing in the vessel was due to the vessels being already fully extended at the concentration of Ach used. Thus, the effect of flow under the control conditions was further explored. A lower concentration of ACh (0.1 μM) was applied to the vessel after a complete contraction caused by PE and the vessel dilated about 33% (compared to a mean of 97% when the usual 0.5 μM ACh was used). The flow effect was tested after dilation became stable and an average of 29% (n=4) additional vasodilation due to flow was observed (Figure 20B). This vasodilation observed when using a lower ACh concentration suggests that flow has an effect in the presence of buffer alone as long as the vessel is not already at its maximum diameter. When the vessel was at its maximum diameter (when 0.5 μM ACh was added), NO induced by shear cannot further dilate the vessel.

**TABLE V. The outer diameters of vessel wall at tone 1,2,3,4 in the absence or presence of luminal Hb, RBCs, or MPs (unit of μm)[*].**

| | **T1 Basal Tone** | **T2 + PE** | **T3 + ACh** | **T4 With Flow** | $\frac{T3-T2}{T1-T2}$ | $\frac{T4-T3}{T1-T2}$ |
|---|---|---|---|---|---|---|
| Control | 235 ± 7.44 | 185 ± 11.90 | 233 ± 6.95 | 234 ± 4.73 | 97% ± 3% | 1% ± 4% |
| Hb(30μM) | 230 ± 1.15 | 145 ± 19.63 | 177 ± 10.08 | 190 ± 8.91 | 39% ± 6% | 15% ± 2% |
| MP(30μM) | 228 ± 20.21 | 167 ± 12.29 | 188 ± 12.20 | 196 ± 12.75 | 35% ± 4% | 14% ± 3% |
| RBC(45%Hct) | 224 ± 22.46 | 148 ± 26.76 | 172 ± 19.60 | 209 ± 22.33 | 32% ± 9% | 48% ± 10% |
| RBC+MP | 231 ± 18.61 | 165 ± 18.61 | 188 ± 9.76 | 201 ± 1.50 | 35% ± 7% | 20% ± 5% |

Values are means ± SD. * These values are not normalized by the initial diameters.

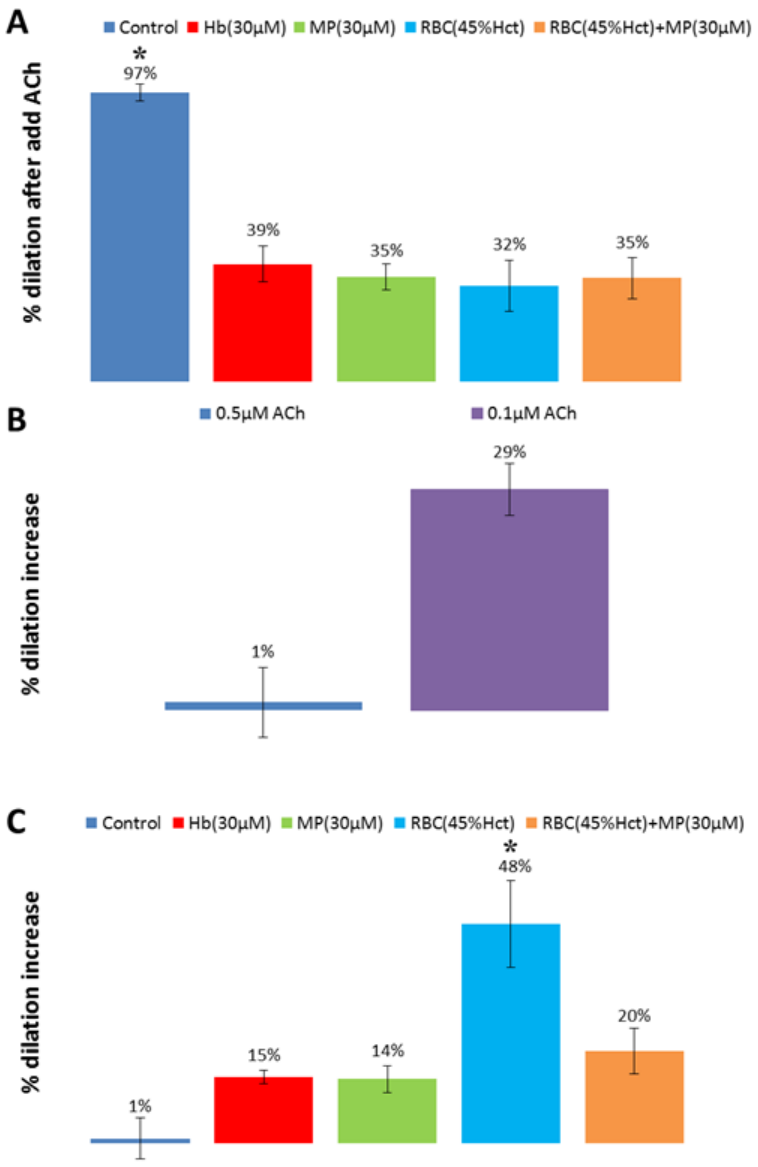


**Figure 20. Single vessel myography.** (A) NO scavenging ability of Hb, MPs, RBCs, and mixture of MPs and RBCs in single arterioles at 60 cm H2O luminal pressure. The results indicate that cell-free Hb and red cell derived MPs scavenge NO much more efficiently than RBCs (n=4). *, one-way ANOVA, P<0.01, control versus all samples. (B) Intravascular flow effect on NO-mediated vasodilation with only buffer in the vessel after either 0.5 μM or 0.1 μM ACh added to the vessel bath. (C) Intravascular flow effect on NO-mediated vasodilation in the absence or presence of luminal Hb, MPs, and RBCs (ΔP=60 cm H2O). Percent dilation increase was calculated as described in the methods section. These data suggest that red cell microparticles enter the cell-free zone (n=4). *, one-way ANOVA, P<0.01, RBCs versus all other samples.

Since Hb, RBCs, and MPs cause vessel contraction, experiments studying the cell-free zone employed the larger Ach concentration (0.5 μM). In this case, in the presence of Hb, RBCs, and MPs, intravascular flow resulted in vasodilation. The flow effect was greater in the presence of RBCs than in the presence of Hb and MPs (n=4, $P<0.05$, Figure 20C). The flow effect was observed with a mixed solution of MPs and RBCs in the lumen and the effect was less than that with luminal RBCs. These data suggest that, like cell-free Hb, red cell microparticles enter the cell-free zone.

**DISCUSSION**

In this study our major findings were that (1) both cell-free Hb and Hb contained in red cell microparticles increase over time; (2) NO scavenging by red cell microparticles is slightly less efficient than by cell-free Hb as measured on a heme basis; (3) MPs enter the cell-free zone, and (4) as little as 5 μM Hb in MPs can affect NO bioavailability. These results suggest that NO scavenging by red cell MPs, that form during blood storage or otherwise, could contribute to pathological consequences.

Our results are consistent with previous ones showing that extraerythrocytic Hb increases as a function of storage duration [8]. Others have also previously found that a substantial portion of extracellular Hb that is found during blood storage is contained within microparticles as compared to cell-free Hb [31, 33, 37] including one that found that 2/3 or more of the Hb was contained in microparticles [31]. In addition to confirming these earlier results we show here that the percentage of Hb in microparticles remained approximately 20% during storage when the red blood cells were stored in ADSOL and increases relative to cell-free hemoglobin when ACD preservation solution is used. Our earlier work showed that there is no difference in total extraerythrocytic Hb (free Hb plus

that in microparticles) that accumulates in blood that is leukoreduced vs. that which not leukoreduced [8]. However, the effect of leukoreduction on the percentage of extraerythrocytic Hb in microparticles vs free Hb has not been established. One should consider that our preparation of MPs, like other preparations, only yields MPs of a certain size range. However, flow cytometry analysis shows that particles of a very large size range can form and larger particles would sediment along with red cells. However, these larger red cell particles are not likely to scavenge NO as efficiently as the smaller ones [39].

Our previous work showed that MP encapsulated Hb reacts with NO with a rate constant of $1.8 \times 10^7$ $M^{-1}s^{-1,}$ which is only about three times slower than that for cell-free Hb and still about 1000 faster than red cell encapsulated Hb [8]. In Figure 14 we presented results from experiments where the relative rate of NO scavenging is determined by a competition between its reaction with Hb and it being purged into the chemiluminescent NO detector. We observed a slightly lower efficiency for NO scavenging by microparticle encapsulated Hb which is consistent with its slightly lower bimolecular rate constant. We also showed that the ability of red cell microparticle encapsulated Hb to inhibit NO mediated vasodilation in a single arterial vessel is similar to that of cell-free Hb in the absence of flow, both of which were substantially more efficient than red cells. These data are all consistent with the notion that red blood microparticles scavenge NO almost as fast as cell-free Hb.

One mechanism that influences the degree of NO scavenging is whether or not the Hb enters the cell-free zone. Velocity and consequent pressure gradients push red cells towards the center of vessels when there is laminar flow while cell-free Hb is not pushed

inward and thus remains in the cell-free zone [21]. As MPs are intermediate in size compared to molecular Hb and red cells, it is a priori unclear whether they would enter the cell-free zone or not. Our experiments examining the effect of flow on inhibition of NO scavenging by red cells vs cell-free Hb vs MPs suggest that MPs do enter the cell-free zone similar to Hb. The similarity of MPs and Hb and the dissimilarity of MPs and RBCs support our conclusion that MPs do enter the cell-free zone. It should be noted, however, that the width of a cell-free zone and likely the degree to which different sized particles are compartmentalized in flow, depends on the rate of flow and size of the vessel. The vessels we studied were on the large size for resistance vessels (second order of rat mesenteric vessels with an average outer diameter of 229±14 μm). In our experiments, the vehicle flow was driven by a pressure gradient of 60 cm $H_2O$ which corresponds to that found in arterioles of similar sizes in the beating heart and is similar to conditions employed previously [21].

With red cell microparticles entering the cell-free zone, as little as 5 μM microparticle encapsulated Hb was seen to reduce NO bioavailability in our computer simulations. The absolute effect was greater in the background of 45% Hct which is a normal Hct, but the percentage change was larger for 30% Hct which is most relevant for transfusion. The extent of the effect was seen to be dependent on the value of the red cell permeability employed in the simulations. With a low permeability, the red cells contribute less to NO scavenging, so the effect of MPs is greater. Literature values of the NO permeability of red blood cells range from $4 \times 10^{-4}$ m $s^{-1}$ to 0.9 m $s^{-1}$ (= 400 μm/s to 900,000 μm/s) [23, 51-53], and we conducted our simulation at the extremes of these values. Interestingly, some of our previous work has suggested that the permeability of

the red cell membrane is modulated by oxygen tension so that the permeability of RBCs to NO under oxygenated conditions is between 4,400 μm/s and 5,100 μm/s while the permeability under deoxygenated conditions is greater than 64,000 μm/s [54]. Throughout circulation, conditions are mostly oxygenated, in terms of Hb saturation, so that the low permeability values of around 5,000 μm/s would be most relevant and the impact of red cell microparticles on NO bioavailability would be substantial.

Based on our data presented here showing how much cell-free hemoglobin and red cell microparticle hemoglobin accumulate over time in storage along with our data showing the effects on vasodilation, as well as our previous working showing just 6 μM extraerythrocytic Hb reduces blood pressure in a rodent model [8], it is clear that transfusion of 3-4 units of older stored blood would increase red cell microparticle and cell-free Hb concentrations to a level where they would affect NO bioavailability. The relative contribution of red cell microparticles vs cell-free Hb in lowering NO bioavailability could have important implications in designing therapeutic strategies. Clearly, any strategy designed to increase clearance of cell-free Hb such as increasing haptoglobin concentrations [55] would have no effect on pathology associated with MPs as MPs are not cleared by haptoglobin. Red cell microparticles have been reported to be cleared from plasma within the thirty minutes but end up in the liver and other tissues [56]. The plasma concentration of MPs may be substantial after transfusion even after thirty minutes due to red cell breakdown of older transfused blood when it is in circulation. We propose that transfusion of older stored results in an acute loss of NO bioavailability that could also be sustained due to subsequent intravascular hemolysis.

The loss of NO bioavailability could contribute to increased inflammation, thrombosis, and other negative consequences that underlie the blood storage lesion.

**ACKNOWLEDGEMENTS**

This work was supported by NIH Grants HL098032 (D.K.-S.) and the Graduate Fellowship from the Center for Molecular Communication and Signaling at Wake Forest University.

REFERENCES

[1] Furchgott, R. F.; Zawadzki, J. V. The Obligatory Role of Endothelial-Cells in the Relaxation of Arterial Smooth-Muscle by Acetylcholine. *Nature* **288:**373-376; 1980.

[2] Ignarro, L. J.; Byrns, R. E.; Buga, G. M.; Wood, K. S. Endothelium-Derived Relaxing Factor from Pulmonary-Artery and Vein Possesses Pharmacological and Chemical-Properties Identical to Those of Nitric-Oxide Radical. *Circ. Res.* **61:**866-879; 1987.

[3] Katsuki, S.; Arnold, W.; Mittal, C.; Murad, F. Stimulation of Guanylate Cyclase by Sodium Nitroprusside, Nitroglycerin and Nitric-Oxide in Various Tissue Preparations and Comparison to Effects of Sodium Azide and Hydroxylamine. *J. Cyclic Nucleotide Res.* **3:**23-35; 1977.

[4] Palmer, R. M. J.; Ferrige, A. G.; Moncada, S. Nitric-Oxide Release Accounts for the Biological-Activity of Endothelium-Derived Relaxing Factor. *Nature* **327:**524-526; 1987.

[5] Ignarro, L. J. *Nitric Oxide Biology and Pathobiology.* San Diego: Academic press; 2000.

[6] Rother, R. P.; Bell, L.; Hillmen, P.; Gladwin, M. T. The clinical sequelae of intravascular hemolysis and extracellular plasma hemoglobin: a novel mechanism of human disease. *Jama* **293:**1653-1662; 2005.

[7] Kunz, J. Initial lesions of vascular aging disease (arteriosclerosis). *Gerontology* **46:**295-299; 2000.

[8] Donadee, C.; Raat, N. J. H.; Kanias, T.; Tejero, J.; Lee, J. S.; Kelley, E. E.; Zhao, X. J.; Liu, C.; Reynolds, H.; Azarov, I.; Frizzell, S.; Meyer, E. M.; Donnenberg, A. D.;

Qu, L. R.; Triulzi, D.; Kim-Shapiro, D. B.; Gladwin, M. T. Nitric Oxide Scavenging by Red Blood Cell Microparticles and Cell-Free Hemoglobin as a Mechanism for the Red Cell Storage Lesion. *Circulation* **124:**465-476; 2011.

[9] Knott, A. B.; Bossy-Wetzel, E. Impact of nitric oxide on metabolism in health and age-related disease. *Diabetes Obesity & Metabolism* **12:**126-133; 2010.

[10] Allen, J. D.; Miller, E. M.; Schwark, E.; Robbins, J. L.; Duscha, B. D.; Annex, B. H. Plasma nitrite response and arterial reactivity differentiate vascular health and performance. *Nitric Oxide-Biol Ch* **20:**231-237; 2009.

[11] Ignarro, L. J.; Buga, G. M.; Wood, K. S.; Byrns, R. E.; Chaudhuri, G. Endothelium-Derived Relaxing Factor Produced and Released from Artery and Vein Is Nitric-Oxide. *Proc. Natl. Acad. Sci. USA* **84:**9265-9269; 1987.

[12] Lancaster, J. R. Simulation of the Diffusion and Reaction of Endogenously Produced Nitric-Oxide. *Proc. Natl. Acad. Sci. USA* **91:**8137-8141; 1994.

[13] Doyle, M. P.; Hoekstra, J. W. Oxidation of Nitrogen-Oxides by Bound Dioxygen in Hemoproteins. *J Inorg Biochem* **14:**351-358; 1981.

[14] Eich, R. F.; Li, T. S.; Lemon, D. D.; Doherty, D. H.; Curry, S. R.; Aitken, J. F.; Mathews, A. J.; Johnson, K. A.; Smith, R. D.; Phillips, G. N.; Olson, J. S. Mechanism of NO-induced oxidation of myoglobin and hemoglobin. *Biochemistry-US* **35:**6976-6983; 1996.

[15] Herold, S.; Exner, M.; Nauser, T. Kinetic and mechanistic studies of the NO center dot-mediated oxidation of oxymyoglobin and oxyhemoglobin. *Biochemistry-US* **40:**3385-3395; 2001.

[16] Cassoly, R.; Gibson, Q. H. Conformation, Co-Operativity and Ligand-Binding in Human Hemoglobin. *J. Mol. Biol.* **91:**301-313; 1975.

[17] Coin, J. T.; Olson, J. S. Rate of Oxygen-Uptake by Human Red Blood-Cells. *J. Biol. Chem.* **254:**1178-1190; 1979.

[18] Butler, A. R.; Megson, I. L.; Wright, P. G. Diffusion of nitric oxide and scavenging by blood in the vasculature. *Biochim. Biophys. Acta* **1425:**168-176; 1998.

[19] Liu, X. P.; Miller, M. J. S.; Joshi, M. S.; Sadowska-Krowicka, H.; Clark, D. A.; Lancaster, J. R. Diffusion-limited reaction of free nitric oxide with erythrocytes. *J. Biol. Chem.* **273:**18709-18713; 1998.

[20] Vaughn, M. W.; Kuo, L.; Liao, J. C. Effective diffusion distance of nitric oxide in the microcirculation. *Am. J. Physiol.-Heart Circul. Physiol.* **43:**H1705-H1714; 1998.

[21] Liao, J. C.; Hein, T. W.; Vaughn, M. W.; Huang, K. T.; Kuo, L. Intravascular flow decreases erythrocyte consumption of nitric oxide. *Proc. Natl. Acad. Sci. USA* **96:**8757-8761; 1999.

[22] Vaughn, M. W.; Huang, K. T.; Kuo, L.; Liao, J. C. Erythrocytes possess an intrinsic barrier to nitric oxide consumption. *J. Biol. Chem.* **275:**2342-2348; 2000.

[23] Vaughn, M. W.; Huang, K. T.; Kuo, L.; Liao, J. C. Erythrocyte consumption of nitric oxide: Competition experiment and model analysis. *Nitric Oxide-Biol Ch* **5:**18-31; 2001.

[24] Liu, X. P.; Samouilov, A.; Lancaster, J. R.; Zweier, J. L. Nitric oxide uptake by erythrocytes is primarily limited by extracellular diffusion not membrane resistance. *J. Biol. Chem.* **277:**26194-26199; 2002.

[25] Huang, K. T.; Han, T. H.; Hyduke, D. R.; Vaughn, M. W.; Van Herle, H.; Hein, T. W.; Zhang, C. H.; Kuo, L.; Liao, J. C. Modulation of nitric oxide bioavailability by erythrocytes. *Proc. Natl. Acad. Sci. USA* **98:**11771-11776; 2001.

[26] Han, T. H.; Liao, J. C. Erythrocyte nitric oxide transport reduced by a submembrane cytoskeletal barrier. *Biochim. Biophys. Acta* **1723:**135-142; 2005.

[27] Azarov, I.; Huang, K. T.; Basu, S.; Gladwin, M. T.; Hogg, N.; Kim-Shapiro, D. B. Nitric oxide scavenging by red blood cells as a function of hematocrit and oxygenation. *J. Biol. Chem.* **280:**39024-38032; 2005.

[28] Vandegriff, K. D.; Olson, J. S. Morphological and Physiological Factors Affecting Oxygen-Uptake and Release by Red-Blood-Cells. *J. Biol. Chem.* **259:**2619-2627; 1984.

[29] Vandegriff, K. D.; Olson, J. S. A Quantitative Description in 3 Dimensions of Oxygen-Uptake by Human Red-Blood-Cells. *Biophys. J.* **45:**825-835; 1984.

[30] Piccin, A.; Murphy, W. G.; Smith, O. P. Circulating microparticles: pathophysiology and clinical implications. *Blood Reviews* **21:**157-171; 2007.

[31] Greenwalt, T. J.; McGuinness, C. G.; Dumaswala, U. J. Studies in Red-Blood-Cell Preservation .4. Plasma Vesicle Hemoglobin Exceeds Free Hemoglobin. *Vox Sanguinis* **61:**14-17; 1991.

[32] Izzo, P.; Manicone, A.; Spagnuolo, A.; Lauta, V. M.; Di Pasquale, A.; Di Monte, D. Erythrocytes stored in CPD SAG-mannitol: evaluation of their deformability. *Clin Hemorheol Micro* **21:**335-339; 1999.

[33] Aubuchon, J. P.; Estep, T. N.; Davey, R. J. The Effect of the Plasticizer Di-2-Ethylhexyl Phthalate on the Survival of Stored Rbcs. *Blood* **71:**448-452; 1988.

[34] Dumaswala, U. J.; Dumaswala, R. U.; Levin, D. S.; Greenwalt, T. J. Improved red blood cell preservation correlates with decreased loss of bands 3, 4.1, acetylcholinestrase, and lipids in microvesicles. *Blood* **87:**1612-1616; 1996.

[35] Greenwalt, T. J.; Bryan, D. J.; Dumaswala, U. J. Erythrocyte-Membrane Vesiculation and Changes in Membrane-Composition During Storage in Citrate-Phosphate-Dextrose-Adenine-1. *Vox Sanguinis* **47:**261-270; 1984.

[36] Haradin, A. R.; Weed, R. I.; Reed, C. F. Changes in Physical Properties of Stored Erythrocytes. *Transfusion* **9:**229-235; 1969.

[37] Lutz, H. U.; Liu, S. C.; Palek, J. Release of Spectrin-Free Vesicles from Human Erythrocytes During Atp Depletion .1. Characterization of Spectrin-Free Vesicles. *Journal of Cell Biology* **73:**548-560; 1977.

[38] Wang, D.; Sun, J.; Solomon, S. B.; Klein, H. G.; Natanson, C. Transfusion of older stored blood and risk of death: a meta-analysis. *Transfusion*; 2012.

[39] Tiso, M.; Tejero, J.; Basu, S.; Azarov, I.; Wang, X. D.; Simplaceanu, V.; Frizzell, S.; Jayaraman, T.; Geary, L.; Shapiro, C.; Ho, C.; Shiva, S.; Kim-Shapiro, D. B.; Gladwin, M. T. Human Neuroglobin Functions as a Redox Regulated Nitrite Reductase. *Faseb J* **25**; 2011.

[40] Huang, Z.; Louderback, J. G.; Goyal, M.; Azizi, F.; King, S. B.; Kim-Shapiro, D. B. Nitric oxide binding to oxygenated hemoglobin under physiological conditions. *Bba-Gen Subjects* **1568:**252-260; 2001.

[41] Jeffers, A.; Gladwin, M. T.; Kim-Shapiro, D. B. Computation of plasma hemoglobin nitric oxide scavenging in hemolytic anemias. *Free Radic. Biol. Med.* **41:**1557-1565; 2006.

[42] El-Farra, N. H.; Christofides, P. D.; Liao, J. C. Analysis of nitric oxide consumption by erythrocytes in blood vessels using a distributed multicellular model. *Ann. Biomed. Eng.* **31:**294-309; 2003.

[43] Xu, Z. M.; Tong, C. Y.; Eisenach, J. C. Acetylcholine stimulates the release of nitric oxide from rat spinal cord. *Anesthesiology* **85:**107-111; 1996.

[44] Rees, D. D.; Palmer, R. M. J.; Schulz, R.; Hodson, H. F.; Moncada, S. Characterization of 3 Inhibitors of Endothelial Nitric-Oxide Synthase Invitro and Invivo. *Brit J Pharmacol* **101:**746-752; 1990.

[45] Cannon, R. O. Role of nitric oxide in cardiovascular disease: focus on the endothelium (vol 44, pg 1809, 1998). *Clin Chem* **44:**2070-2070; 1998.

[46] Izzard, A. S.; Bund, S. J.; Heagerty, A. M. Myogenic tone in mesenteric arteries from spontaneously hypertensive rats. *Am J Physiol-Heart C* **270:**H1-H6; 1996.

[47] Falloon, B. J.; Bund, S. J.; Tulip, J. R.; Heagerty, A. M. In-Vitro Perfusion Studies of Resistance Artery Function in Genetic-Hypertension. *Hypertension* **22:**486-495; 1993.

[48] Watanabe, J.; Karibe, A.; Horiguchi, S.; Keitoku, M.; Satoh, S.; Takishima, T.; Shirato, K. Modification of Myogenic Intrinsic Tone and [Ca2+]I of Rat Isolated Arterioles by Ryanodine and Cyclopiazonic Acid. *Circ Res* **73:**465-472; 1993.

[49] Hori, N.; Wiest, R.; Groszmann, R. J. Enhanced release of nitric oxide in response to changes in flow and shear stress in the superior mesenteric arteries of portal hypertensive rats. *Hepatology* **28:**1467-1473; 1998.

[50] Arenas, I. A.; Xu, Y.; Davidge, S. T. Age-associated impairment in vasorelaxation to fluid shear stress in the female vasculature is improved by TNF-alpha antagonism. *Am J Physiol-Heart C* **290:**H1259-H1263; 2006.

[51] Roughton, F. J. W. Diffusion and chemical reaction velocity as joint factors in determining the rate of uptake of oxygen and carbon monoxide by red blood corpuscles. *Proc. Royal Soc. London - Series B, Biol. Sci.* **111:**1-36; 1932.

[52] Subczynski, W. K.; Lomnicka, M.; Hyde, J. S. Permeability of nitric oxide through lipid bilayer membranes. *Free Radic. Res.* **24:**343-349; 1996.

[53] Tsoukias, N. M.; Popel, A. S. Erythrocyte consumption of nitric oxide in presence and absence of plasma-based hemoglobin. *Am. J. Physiol.-Heart Circul. Physiol.* **282:**H2265-H2277; 2002.

[54] Huang, K. T.; Huang, Z.; Kim-Shapiro, D. B. Nitric Oxide Red Blood Cell Membrane Permeability at high and low Oxygen Tension. *Nitric Oxide* **16:**209-216; 2007.

[55] Baek, J. H.; D'Agnillo, F.; Vallelian, F.; Pereira, C. P.; Williams, M. C.; Jia, Y.; Schaer, D. J.; Buehler, P. W. The red blood cell storage lesion is defined in vivo by hemoglobin driven pathophysiology and can be attenuated with haptogobin therapy in guinea pigs. *J. Clin. Invest.* **122:**1444-1458; 2012.

[56] Willekens, F. L. A.; Werre, J. M.; Kruijt, J. K.; Roerdinkholder-Stoelwinder, B.; Groenen-Dopp, Y. A. M.; van den Bos, A. G.; Bosman, G.; van Berkel, T. J. C. Liver Kupffer cells rapidly remove red blood cell-derived vesicles from the circulation by scavenger receptors. *Blood* **105:**2141-2145; 2005.

# CHAPTER V

# MECHANISM OF FASTER NO SCAVENGING BY OLDER STORED RED BLOOD CELLS

C. Liu, X. Liu, J. Janes, R. Stapley, R. P. Patel, M. T. Gladwin, D. B. Kim-Shapiro

The following manuscript has been submitted for publication in the Journal of Biological Chemistry, and is reprinted with permission. Stylistic variations are due to the requirements of the journal. C. Liu designed and carried out experiments with the help of X. Liu and performed simulations with the help of J. Janes. C. Liu wrote the manuscript. D. B. Kim-Shapiro acted in an advisory and editorial capacity throughout the entire course of work.

**Mechanism of Faster NO Scavenging by Older Stored Red Blood Cells**

**Chen Liu[1], Xiaohua Liu[1], John Janes[1], Ryan Stapley[2], Rakesh P. Patel[2], Mark T. Gladwin[3,4], and Daniel B. Kim-Shapiro[1]**

From the [1]Department of Physics, Wake Forest University, Winston-Salem, NC 27109, the [2]Department of Pathology and Center for Free Radical Biology, University of Alabama at Birmingham, Birmingham, AL 35294, the [3]Vascular Medicine Institute, University of Pittsburgh, Pittsburgh, PA 15213, the [4]Department of Medicine, Division of Pulmonary, Allergy and Critical Care Medicine, University of Pittsburgh School of Medicine, Pittsburgh, PA 15213

Address correspondence to Daniel B. Kim-Shapiro, Department of Physics, Winston-Salem, NC 27109, Tel. 336-758-4993; Fax: 336-758-4973, Email: shpairo@wfu.edu

## ABSTRACT

The blood storage lesion involves morphological and biochemical changes of red blood cells that occur during storage. These changes include conversion of the biconcave disc morphology to a spherical one, decreased mean cell hemoglobin concentration (MCHC), varied volume, reduced integrity of the erythrocyte membrane with formation of microparticles, and increased cell-free hemoglobin. We studied the extent to which older stored red blood cells scavenge nitric oxide (NO) faster than fresher stored red blood cells. We found that older stored red blood cell scavenge NO about 1.7 to 1.8 times faster than fresher ones using electron paramagnetic resonance spectroscopy and stopped-flow absorption spectroscopy. Based on these quantitative data, we simulated NO scavenging by fresher or older stored red blood cells with a biconcave or spherical geometry respectively in order to explore the mechanism of NO scavenging related to biochemical and morphological changes of stored red blood cells. We found that red blood cells with a spherical geometry scavenges NO about 2 times slower than the ones

with a biconcave geometry, opposite to the experimental finding that older stored cells scavenge NO faster than fresh ones. Red blood cell MCHC, volume, and membrane permeability to NO must compensate for the effect of cell morphology in order to explain our experimental findings. Computer simulations show that a lower intracellular hemoglobin concentration or a smaller erythrocytic volume increases NO scavenging by red blood cells and membrane permeability to NO needs to increase 5 to 70 fold in order to explain our experimental results.

**INTRODUCTION**

Blood transfusion is one of the most common medical therapies, with about 14 million units of red blood cells (RBCs) having been transfused in the United States in 2011 [1]. The average age of red blood cells at transfusion is approximately 18 days. According to the blood banking standard, RBCs preserved in ADOSL can be stored up to 42 days. However, a growing body of literature has demonstrated an association between an increased incidence of adverse clinical outcomes of blood transfusion and the storage of RBCs [2-7]. The adverse effect of blood transfusion is also suggested to be related to the number of units transfused [8, 9].

A number of chemical and morphological changes in RBCs occur during blood storage including a reduction in levels of 2, 3-diphosphoglycerate, ATP, and pH values, as well as an increase of potassium and lactate [10]. These changes result in a reduced deformability, increased osmotic fragility, spheroechinocyte formation, reduced integrity of the erythrocyte membrane with formation of microparticles (MPs), and increased cell-free hemoglobin (Hb) in plasma [11-17]. The geometry of the red blood cell tends to become more spherical during storage thereby having a smaller surface area to volume

ratio, the mean cell hemoglobin concentration in RBCs decreases, and the structure of RBC membrane changes significantly during storage [18, 19]. In addition, RBC volume varies during blood storage but the type of change depends on which additive preservation solutions is used [20, 21]. Changes in RBCs during storage are referred as the blood storage lesion. Precise mechanisms that explain how the blood storage lesion is associated with adverse effects of blood transfusion remain unclear.

Nitric oxide (NO) functions as the endothelial derived relaxing factor, decreases platelet activation and vascular cell adhesion, influences oxidative and nitrosative stress, functions in host defense, and influences a large number of cellular functions through protein modification [22-26]. We hypothesize that the blood storage lesion is associated with a loss of NO signaling. It has been well established that oxygenated cell-free Hb reacts with NO at a high rate of 6 to 8 $\times 10^7$ $M^{-1}s^{-1}$ to form nitrate and methemoglobin [27-29]. MPs are small phospholipid vesicles that contain hemoglobin and they react with NO only about 3 times slower than cell-free Hb, but still 1000 times faster than RBCs [30-32]. Several mechanisms are responsible for the reduced rate of NO scavenging by hemoglobin encapsulated in RBCs. NO diffusion to the RBC is limited by an unstirred layer around the RBC which is due to the fast scavenging of NO close to RBC [33-36]. A RBC cell-free zone is created when RBCs are pushed to the center of vessel during flow and it separates RBCs from endothelial cells where NO is produced [37, 38]. Another mechanism that accounts for slower NO scavenging by RBCs is that the RBC membrane has a finite permeability to NO, like a physical barrier which slows down the diffusion [35, 39]. These diffusion barriers are regulated by RBC size, shape, and surface area; biophysical properties that are changed during RBC storage [19]. Since hemoglobin and

red cell microparticles scavenge NO close to 1000 times faster than red cell encapsulated hemoglobin, red cell breakdown in storage or post transfusion substantially reduces NO bioavailabiliy [31, 32]. In addition, recent studies show that the effects of storage will lead to an increased intrinsic NO scavenging by older stored RBCs, as measured by nitric oxide competition experiments and inhibition of aortic vasodilation [40, 41]. However, the extent of the increase in NO scavenging by older red blood cells compared to fresh ones was not fully explored and the mechanism for this phenomenon was not satisfactorily provided.

In this study, we further examine the rate of NO scavenging by both fresh and old stored RBCs using time-resolved stopped-flow absorption spectroscopy and electron paramagnetic resonance spectroscopy. Computational simulations are also conducted to explore the effects of morphological changes, RBC volume, MCHC, and permeability to NO on the rate of NO scavenging using 3D single RBC models. We use results of these simulations to account for the observed increase in NO scavenging by RBCs as a function of storage age.

**EXPERIMENTAL PROCEDURES**

Old and fresh, leukodepleted packed red blood cells were collected from packed red blood cell segments stored in the University of Alabama at Birmingham blood bank in AS-1 storage solution. The average storage length of old and fresh red blood cells in this study were 8.5 ± 1.4 days and 37.5 ± 2.9 days. Red blood cells were washed in phosphate buffered saline (PBS) at least three times or until the supernatants were clear. The hemoglobin concentration of the red blood cell solution (in heme) was determined by absorption spectroscopy using a Cary 100 spectrometer equipped with an integrating

sphere detector. Spectra of cell-free hemoglobin were taken on a Cary 50 Bio spectrometer (Varian Inc.). Cell-free hemoglobin was prepared as described previously [42]. All experiments were performed in PBS buffer and all chemicals were purchased from Sigma unless otherwise stated.

**Competition Experiments**

Competition Experiments were performed similarly to those described previously [35, 43]. Briefly, oxygenated cell-free Hb and Hb encapsulated in RBCs compete to react with NO to form methemoglobin (MetHb). The relative rates of NO uptake by RBCs compared to cell-free Hb can be determined by examining the concentrations of MetHb produced from each fraction using electron paramagnetic resonance (EPR) spectroscopy. In the experiments, cell-free Hb (100 μM in heme) was mixed with either old or fresh stored red blood cell solutions (50% Hct). The mixtures were stirred with a magnetic bar at a slow speed to keep the sample homogeneous throughout the experiment. The NO donor DEANONOate was prepared in a deoxygenated 0.01 M NAOH solution and added to the mixture to a final concentration of 20 μM. The first EPR tube was filled with the mixture at 45 minutes and the rest of the mixture was centrifuged at 3000g for 2 minutes. The supernatant was put in another EPR tube and the third EPR tube was filled with the RBC pellet. Control experiments were performed as described previously to account for any autoxidation or MetHb reductase activity [43]. All the EPR tubes prepared in the experiment were frozen simultaneously at 1 hour. The amounts of MetHb were measured by electron paramagnetic resonance using a Bruker EMX 10/12 spectrometer as described previously [43]. Hemolysis during the experiment was checked by examining

the hemoglobin concentrations in the supernatant prior to the addition of NO donor and after the centrifugation.

The ratio of the bimolecular rate constant of NO reacting with cell-free Hb ($k_f$) to the bimolecular rate constant of NO uptake by RBC-encapsulated Hb ($k_r$) was determined by the relative amount of MetHb formed in each fraction as shown in the equation:

$$\frac{[\mathbf{MetHb}]_\mathbf{f}}{[\mathbf{MetHb}]_\mathbf{r}} = \frac{\mathbf{K_f}[\mathbf{Hb}]_\mathbf{f}}{\mathbf{K_r}[\mathbf{Hb}]_\mathbf{r}} \qquad \textbf{Equation 1}$$

where the subscripts "f" and "r" stand for cell-free Hb and RBCs encapsulated Hb respectively. The concentrations indicated by brackets are the moles of the species over the total volume. Natural log terms on both sides of the equation were also calculated as previously described [44] in order to account for the fact that the total amount of oxygenated hemoglobin in the free and RBC fractions may decrease with time from its initial amount. The ratio $k_f/k_r$ calculated using equation 1 had less than 2% difference from the result calculated with natural log terms. Three methods were used to calculate $k_f/k_r$ using two MetHb concentrations of those in the mixture, supernatant, and RBCs pellet in order to avoid errors as described previously [43].

**Stopped-Flow Analysis**

Stopped-flow time-resolved absorption experiments of the reaction between NO and RBCs were conducted using a Molecular Kinetics three-syringe mixer (Indianapolis, IN) coupled to an Olis RSM spectrometer (Bogart, GA) as described previously [44]. The NO donor PROLINONOate (10 mM, Cayman Chemicals) was prepared in 0.01 M NAOH and loaded in the first syringe. Either old or fresh stored red blood cells (100μM in heme) were filled in the second syringe and the third syringe was loaded with deoxygenated PBS. Mixing was accomplished as follows: the NO donor was diluted to

500 μM by PBS and aged for 20 second in the first mixer so that the NO would be released. NO-containing buffer was then rapidly pushed into the second mixer and mixed with either old or fresh stored red blood cells. Experiments were conducted under aerobic conditions so that NO reacted with oxygenated Hb to make MetHb. As NO can also further react with MetHb to produce MetHb-NO, we only performed experiments with NO present at two-fold molar excess to oxygenated Hb. Time-resolved absorption spectra were collected and analyzed by Specfit software (Boston, MA) through singular value decomposition and global analysis as described previously [45].

**Computational simulations**

Three dimensional models were constructed to simulate competition and stopped-flow experiments performed in this study using COMSOL Multiphysics (Comsol Inc., Burlington, MA, version 4.3). We have assumed that RBCs are distributed homogenously within the reaction region. A single red blood cell was simulated as a 3D biconcave geometry contained in the reaction region of a cylindrical boundary for the reactions between fresh stored red blood cells and NO (Figure 21A). A spherical geometry within another sphere was adopted to simulate the reactions between old stored red blood cells and NO (Figure 21B). The comparison between NO scavenging by old and fresh stored red blood cells was conducted using those full 3D models.

In addition, to examine the effect of RBC volume, MCHC, and membrane permeability on NO scavenging by old red blood cells, we performed simulations where each of these parameters was varied while maintaining the other parameters constant. In order to save time and sufficiently resolve both the reaction region and RBCs with enough finite elements we exploited the spherical symmetry of the old red blood cell

model. The reaction was simulated solely over a 20×20 degree square cone cut out of the two sphere system, as previously described (Figure 21C)[44]. This reduced the number of degrees of freedom and allowed a sufficient number of finite elements. All simulations were performed using a user defined finer mesh with twice the refinement in the intracellular domain unless otherwise stated (Figure 21D).

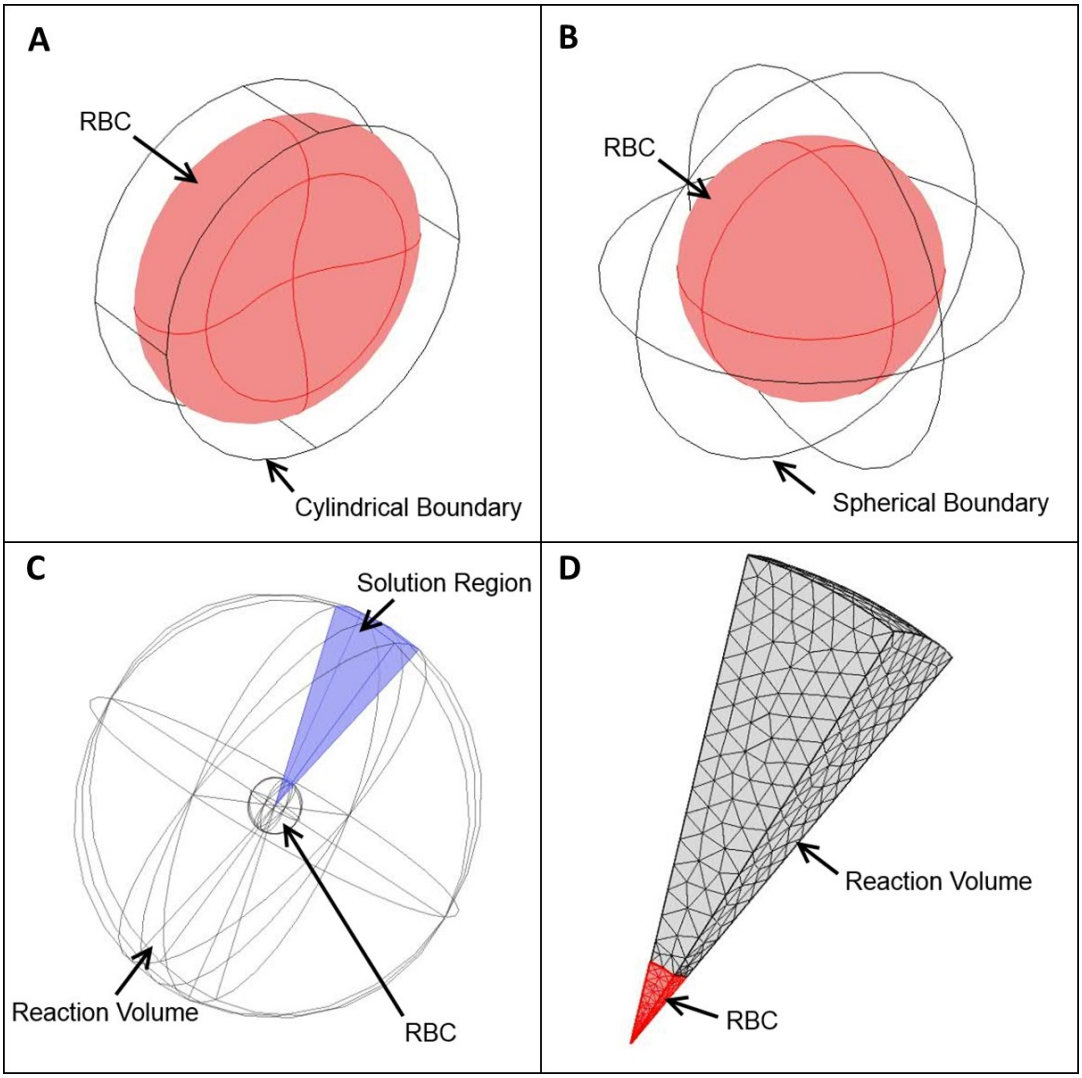


**Figure 21. Three-dimensional models.** (A) A full 3D model with a biconcave geometry contained in a cylindrical boundary for the reactions between fresh stored red blood cells and NO. (B) A full 3D model with a spherical geometry within another sphere for the reactions between old stored red blood cells and NO. (C) The 20×20 degree square cone

as the solution region. (D) A finite element mesh of the cone solution region with a user defined finer mesh and twice the refinement in the intracellular domain (red).

**Simulated Competition Experiments**

Competition experiments were simulated similarly to that described previously [46]. Briefly, NO is released by an NO donor and reacts with cell-free hemoglobin in the external space. In the extracellular space, the overall reaction rate for NO is given by

$$\boldsymbol{R = 2 \times k_{donor}[NO\ donor] - k_{Hb}[NO][Hb]} \qquad \textbf{Equation 2}$$

where R is the reaction rate, $k_{\text{donor}}$ is the rate constant that NO is released by the donor, and $k_{\text{Hb}}$ is the bimolecular rate constant of NO scavenging by oxygenated Hb. Concentrations are indicated by brackets.

In the intracellular compartment, NO diffused from extracellular space is scavenged by oxygenated Hb encapsulated by the RBC:

$$\boldsymbol{R = k_{Hb}[NO][Hb]} \qquad \textbf{Equation 2}$$

The boundary condition at the RBC membrane is defined as:

$$\boldsymbol{-n \cdot (-D\nabla C) = P_m(C_o - C_i)} \qquad \textbf{Equation 3}$$

where **n** is the unit normal vector, D is NO diffusion rate, C is its concentration, $P_m$ is NO permeability of RBC membrane, $C_0$ is NO concentration at the outer surface of the RBC, and $C_i$ is the concentration in the RBC.

The models for competition experiments simulated the first 5 milliseconds of the real experimental reaction. Parameters used in simulations are listed in Table VI. At 5 milliseconds, the average concentrations of MetHb for both cell and plasma fractions were plugged into equation 1 to calculate the relative rate $k_f/k_r$.

**TABLE VI. Competition simulation parameters**

| Parameter | Value | Units |
|---|---|---|
| RBC volume | 90 | $\mu m^3$ |
| Hct | 50 | % |
| Initial [RBC Hb] | 20 | mM |
| Initial [NO donor] | 20 | μM |
| Initial [cell-free Hb] | 100 | μM |
| $k_{Hb}$ | $8.9\times10^7$ | $M^{-1}s^{-1}$ |
| $k_{donor}$ | 1 | $s^{-1}$ |
| Extracellular NO diffusion coefficient | 3300 | $\mu m^2 s^{-1}$ |
| Intracellular NO diffusion coefficient | 880 | $\mu m^2 s^{-1}$ |
| Extracellular Hb diffusion coefficient | 1 | $\mu m^2 s^{-1}$ |
| Intracellular Hb diffusion coefficient | 0.27 | $\mu m^2 s^{-1}$ |
| RBC membrane permeability to NO | 5000 | $\mu m s^{-1}$ |

**Simulated Stopped-flow Experiments**

Stopped-flow experiments were simulated similarly to the simulations for competition experiments as well as to those described previously [44]. The bimolecular reaction rate constant *k* was calculated at 5 milliseconds after mixing using the formula,

$$\ln\left(\frac{[\boldsymbol{Hb}](\boldsymbol{t})}{[\boldsymbol{Hb}](\mathbf{0})}\right) = -\boldsymbol{k}[\boldsymbol{NO}](\mathbf{0}) \times \boldsymbol{t} \qquad \textbf{Equation 5}$$

where [Hb](t) and [Hb](0) are averaged hemoglobin concentrations at time t and in the beginning of the reaction. A constant concentration of NO was assumed in order to use pseudo first-order kinetics. Parameters used in simulations are summarized in Table VII.

**TABLE VII. Stopped-flow simulation parameters**

| Parameter | Value | Units |
|---|---|---|
| RBC volume | 90 | $\mu m^3$ |
| Hct | 0.5 | % |
| Initial [RBC Hb] | 20 | mM |
| Initial [NO] | 100 | μM |
| $k_{Hb}$ | $8.9\times10^7$ | $M^{-1}s^{-1}$ |
| Extracellular NO diffusion coefficient | 3300 | $\mu m^2 s^{-1}$ |
| Intracellular NO diffusion coefficient | 880 | $\mu m^2 s^{-1}$ |
| Intracellular Hb diffusion coefficient | 0.27 | $\mu m^2 s^{-1}$ |
| RBC membrane permeability to NO | 5000 | $\mu m s^{-1}$ |

**Examined Effects of RBC MCHC, Volume, and Permeability**

In order to further explore the effects of RBC volume, MCHC, and permeability on NO scavenging by older stored RBCs, a 20×20 degree square cone model was used and parameters were varied as described in Table VIII. Other studies have shown that RBC MCHC and volume change during blood storage and the type and extent of the changes depends on the additive preservation solution that is used to store the RBCs [18, 20, 21]. Therefore, in our simulations, RBC MCHC was varied from 14 to 22 mM and

the volume of RBC was decreased from 90 to 60 $\mu m^3$. These values overlap normal clinical reference ranges for RBC MCHC (19-22 mM) and volume (80-99 $\mu m^3$). In addition, it has been shown that significant changes in the RBC membrane occur during blood storage[18]. Thus, the simulations were conducted examining effects on changes in NO membrane permeability starting with a base RBC membrane permeability (Pm = 5000 $\mu ms^{-1}$) and varying it by up to 100 fold ( Pm×1-100) as shown in Table VIII.

**TABLE VIII. Parameters varied in simulations**

| Parameter | Value | Units |
|---|---|---|
| RBC MCHC | 14, 16, 18, 20, 22 | mM |
| RBC volume | 90, 80, 70, 60 | $\mu m^3$ |
| Tested range of permeability | Pm × (1-100) | |

**Statistical Analysis**

Analysis was performed with Microsoft Office Excel 2010 (Redland, OR). A student's t-test with two tails and equal variance was used to test for statistical significance. Results were considered significant when $P < 0.05$. All values are presented as mean ± SD.

**RESULTS**

**Competition Experiments Confirm Old Stored Red Blood Cells Scavenge NO Faster**

We conducted competition experiments to confirm the faster NO scavenging by old stored red cells using electron paramagnetic resonance spectroscopy. Figure 22A shows representative EPR spectra taken of the mixture (MXT), the supernatant (SPT), and RBC pellet (RBC) after 1 hour of incubating old or fresh stored red blood cells with

DEANONOate. The EPR spectra are subtracted by the baseline spectra from control experiments and corrected to the total volume of the mixture so that the sum of MetHb in the RBC pellet and in the supernatant is equal to the total MetHb in the mixture. MetHb concentrations in the mixture are same for experiments using old (17.5±2.1 μM) and fresh (17.4±2.2 μM) RBCs. The averaged MetHb concentration of the supernatant is larger when fresh RBCs were used (9.6±1.4 μM) than the concentration of the supernatant when old RBCs were used (7.6±1.7 μM). In contrast, the average MetHb concentration of the fresh RBC pellet (7.6±2.0 μM) is smaller than that of the old RBC pellet (10.7±2.9 μM). Given that released cell-free Hb will scavenge NO at the same rate (whether it come from fresh or old RBCs), these data show that older RBCs scavenge NO faster than freshly stored ones.

Figure 22B shows that the average ratios of $k_f/k_r$ for old and fresh red blood cells from multiple experiments are 76 ± 13 and 131 ± 35 respectively, similar in general magnitude to our previous measurements [36]. Thus, we were able to calculate the ratio of the bimolecular rate constant of NO uptake by old stored red blood cells ($k_{old}$) to that of NO uptake by fresh stored red blood cells ($k_{fresh}$) as about 1.7, which suggests that older stored red blood cell scavenge NO about 1.7 times faster than fresher ones.

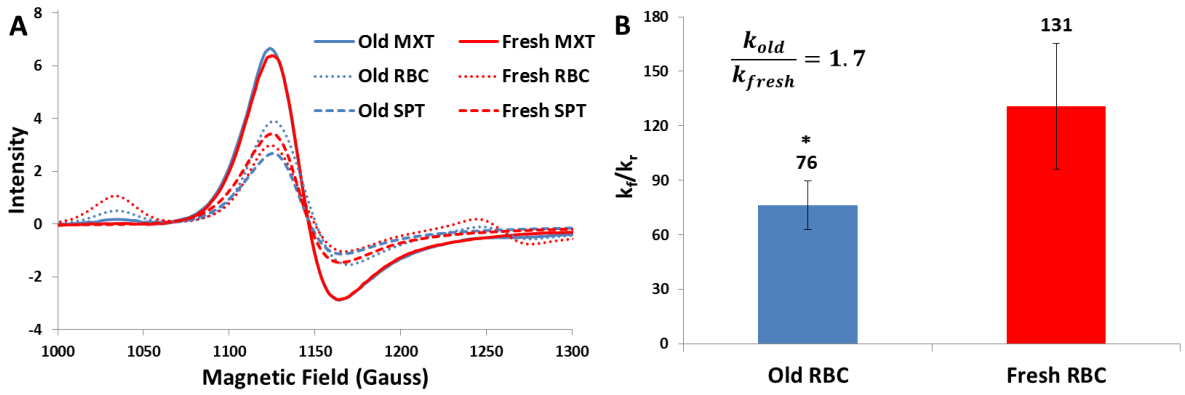


**Figure 22. Competition measurements determining relative rates of NO reacting with old (blue) vs fresh red cells (red).** (A) EPR spectra taken of the mixture (MXT, solid), the supernatant (SPT, dashed), and RBC pellet (RBC, dotted) for old and fresh stored red blood cells. (B) The ratios of the bimolecular rate constant of NO reacting with cell-free Hb to the bimolecular rate constant of NO uptake by old and fresh stored RBC-encapsulated Hb are 76 ± 13 and 131 ± 35 respectively(n=6). The ratio of the bimolecular rate constant of NO uptake by old stored red blood cells ($k_{old}$) to that of NO uptake by fresh stored red blood cells ($k_{fresh}$) is about 1.7. ∗, P<0.005.

### Old Stored Red Blood Cells Scavenge NO Faster in Stopped-Flow Experiments

To further compare the reaction rate of NO scavenging by old and fresh stored red blood cells, we performed stopped-flow experiments with NO and either old or fresh stored red blood cells. The experiments were conducted with a NO:Hb ratio of 2 under aerobic conditions. Figure 23A shows representative kinetics of the absorption at 574 nm for both old (40 days) and fresh (7days) stored red blood cells. It is apparent that old stored red blood cells scavenge NO faster than fresh ones. Figure 23B shows that the bimolecular rate constants of NO reacting with old and fresh stored red blood cells calculated from stopped-flow experiments are $(6.8 \pm 0.6)\times10^4$ $M^{-1}s^{-1}$ and $(3.8 \pm 0.1)\times10^4$ $M^{-1}s^{-1}$ (n=4), which is consistent with our previous measurements [36] Therefore, old stored red blood cells scavenge NO about 1.8 times faster than fresh ones in Stopped-flow experiments.

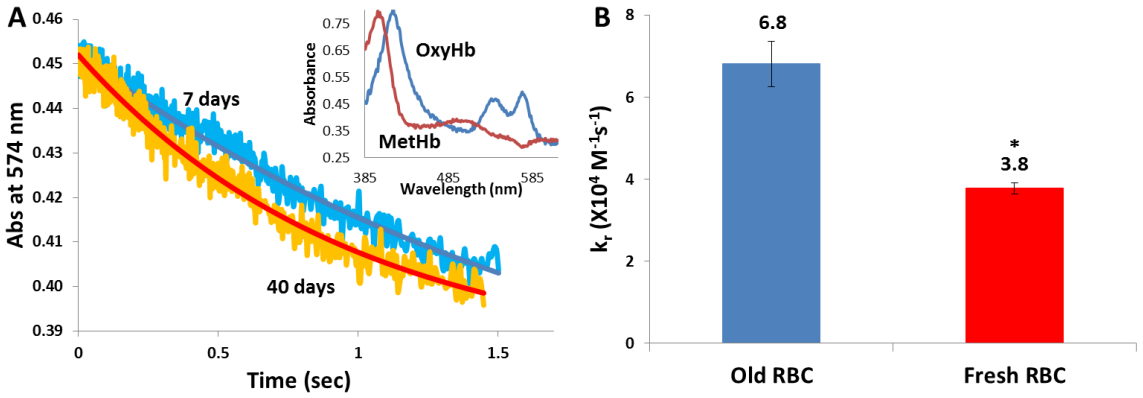


**Figure 23. Stopped-flow absorption measurements of NO reactions with old and fresh red cells.** (A) Kinetics of absorption at 574 nm for both old and fresh red blood cells scavenging NO. Both the raw data (noisy) and the fits from singular value decomposition and global analysis are shown. The initial specie OxyHb and final specie MetHb are shown in the inset. (B) Bimolecular rate constants of NO binding to old and fresh stored red blood cells are 6.8 ± 0.6×104 $M^{-1}s^{-1}$ and 3.8 ±0.1×104 $M^{-1}s^{-1}$ (n=4). *, P < 0.005.

**Biconcave Geometry is Favored in NO Scavenging**

Competition and stopped-flow experiments were simulated when the RBC was represented by a biconcave geometry or a spherical geometry to explore the effect of the surface to volume ratio on NO scavenging. With the same volume, a biconcave geometry (predominating in fresh red cells) has a larger surface area than a spherical geometry (predominating in old red cells). As expected, results show that the RBC with a biconcave geometry scavenges more NO than the RBC with a spherical geometry for both competition (Figure 24A) and stopped-flow experiments (Figure 24B). In the simulations of competition experiments, the ratios kf/kr for old and fresh RBCs are 181 and 83 respectively. Thus, the simulations show that the biconcave geometry scavenges NO about 2.2 times faster than the spherical geometry. From simulations of stopped-flow experiments, we found that the biconcave geometry scavenges NO 1.4 times faster than

the spherical geometry. These simulations show that the morphological changes that occur during RBC storage result in slower NO scavenging, contrary to what is observed experimentally. Thus other factors such as RBC MCHC, volume, or NO permeability must play substantial roles in governing NO scavenging by stored RBCs.

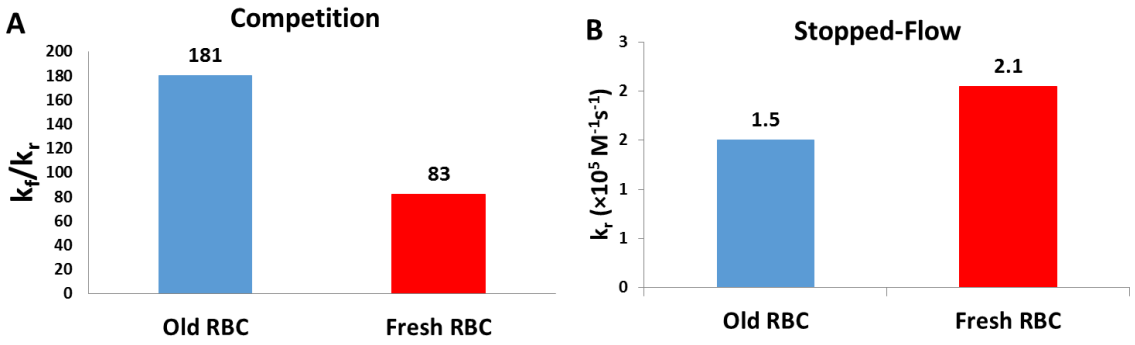


**Figure 24. NO scavenging by old and fresh stored red blood cells due to geometries examined using full 3D models.** (A) The ratios of the bimolecular rate constant $k_f/k_r$ calculated by simulating competition experiments. The ratios $k_f/k_r$ are 181 and 83 for old (spherical) and fresh (biconcave) stored RBCs respectively. (B) Bimolecular rate constant $k_r$ calculated by simulating stopped-flow experiments. The values of $k_r$ are 1.5 and 2.1×105 $M^{-1}s^{-1}$ for old and fresh stored RBCs respectively.

**Effects of RBC MCHC and Volume on NO scavenging**

Other factors that account for an increased NO scavenging by older stored RBCs were examined by varying RBC intracellular Hb concentration and the volume of RBC using a 20×20 degree square cone model as shown in Table VIII. For simulations of competition experiments, the ratio $k_f/k_r$ is increased from 96 to 146 when RBC MCHC is increased from 14 to 22 mM (Figure 25A). The ratio $k_f/k_r$ is increased from 120 to 133 when RBC volume changes from 60 to 90 $\mu m^3$ (Figure 25B). In simulations of stopped-flow experiments, the bimolecular rate constant of NO scavenging by the RBC is decreased from 1.8 to 1.0 $\times 10^5$ $M^{-1}s^{-1}$ and from 1.4 to 1.2×$10^5$ $M^{-1}s^{-1}$ when MCHC is

increased from 14 to 22 mM (Figure 25C) and RBC volume is increased from 60 to 90 $\mu m^3$ respectively (Figure 25D). Simulations of both competition experiments and stopped-flow experiments show that the RBC scavenges NO faster with a lower MCHC or a smaller volume, which is consistent with what we have found previously [30, 47].

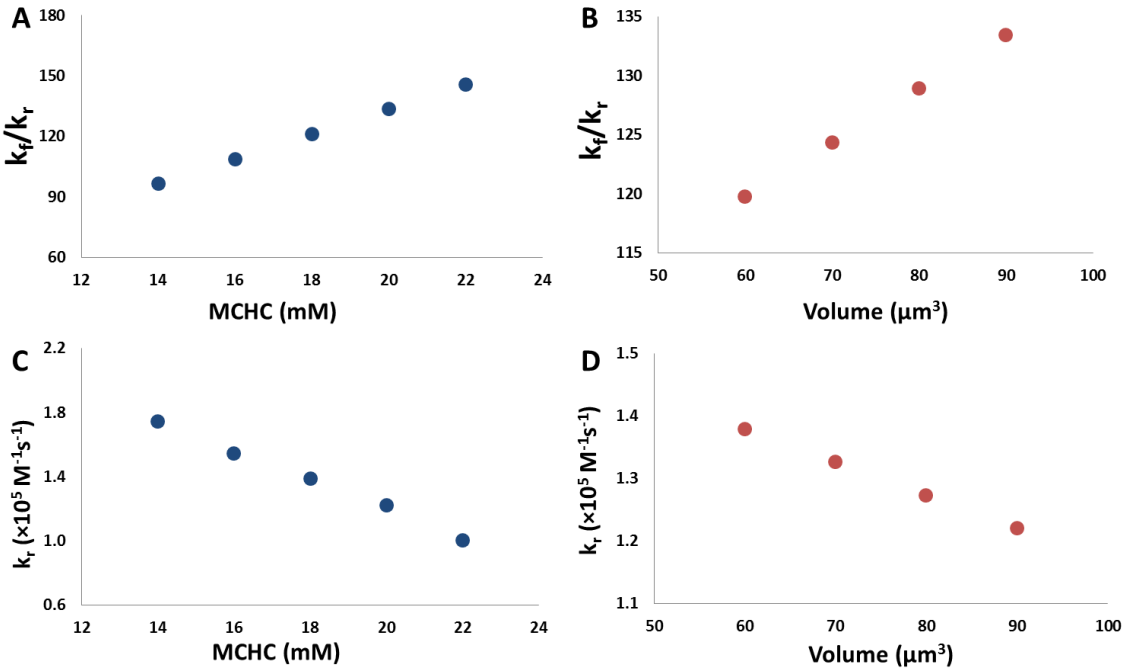


**Figure 25. The effects of RBC MCHC and volume on NO scavenging by RBCs studied using the 20×20 degree square cone model.** The ratio of bimolecular rate constants $k_f/k_r$ is calculated by simulating competition experiments and plotted as a function of MCHC (A) or volume (B) of the RBC. Bimolecular rate constant *kr* is calculated by simulating stopped-flow experiments and plotted as a function of MCHC (C) or volume (D) of the RBC.

## Membrane Permeability Plays a Role in an Increased NO Scavenging by Older Stored RBCs

The effect of RBC membrane permeability on NO scavenging rates was investigated by simulating competition and stopped-flow experiments using the 20×20

degree square cone model. In the simulation, permeability was varied from Pm (5000 $\mu ms^{-1}$) to 100 times this base value of Pm ($5\times10^5$ $\mu ms^{-1}$). Simulations of fresh RBCs used a volume of 90 $\mu m^3$ and MCHC of 20 mM while 60 $\mu m^3$and 14 mM were used for old stored RBCs. Since a decreased volume or MCHC leads to increased NO scavenging, a volume of 60 $\mu m^3$ and a MCHC of 14 mM should give us the minimum value of permeability that explains the experimenally observed increased NO scavenging by older stored RBCs. In addition, we used 90 $\mu m^3$ and 20 mM to obtain an estimate of the maximum value of permeability needed to explain our experimental results. Although some reports show that RBC volume increased during storage in certain additive solutions [20, 21], we used a substantially lower value in simulations of older RBCs in order to maxmize effects of volume changes and thereby obtain the minimum necessary changes in permeability.

For competition experiments, experimental data show that old stored RBCs scavenge NO 1.7 times faster than fresh stored RBCs and simulations show that the old stored RBCs with a spherical geometry scavenge NO about 2.2 times slower than the fresh stored RBCs with a biconcave geometry. To explain the experimental data and compensate for the effect of geomerty, increased permeability would have to result in a 3.8 fold increase NO scavenging for old red cells compared to fresh ones. This magnitude increase corresponds to a $k_f/k_r$ ratio of 35, which is 3.8 times smaller than the ratio $k_f/k_r$ of 133 we obtained using the 20×20 degree square cone model with a volume of 90 $\mu m^3$ and a MCHC of 20 mM. The results show that the permeability needs to increase 5 to 30 fold in order to explain the increased NO scavenging by older stored RBCs we observed from competition experiments (Figure 26A).

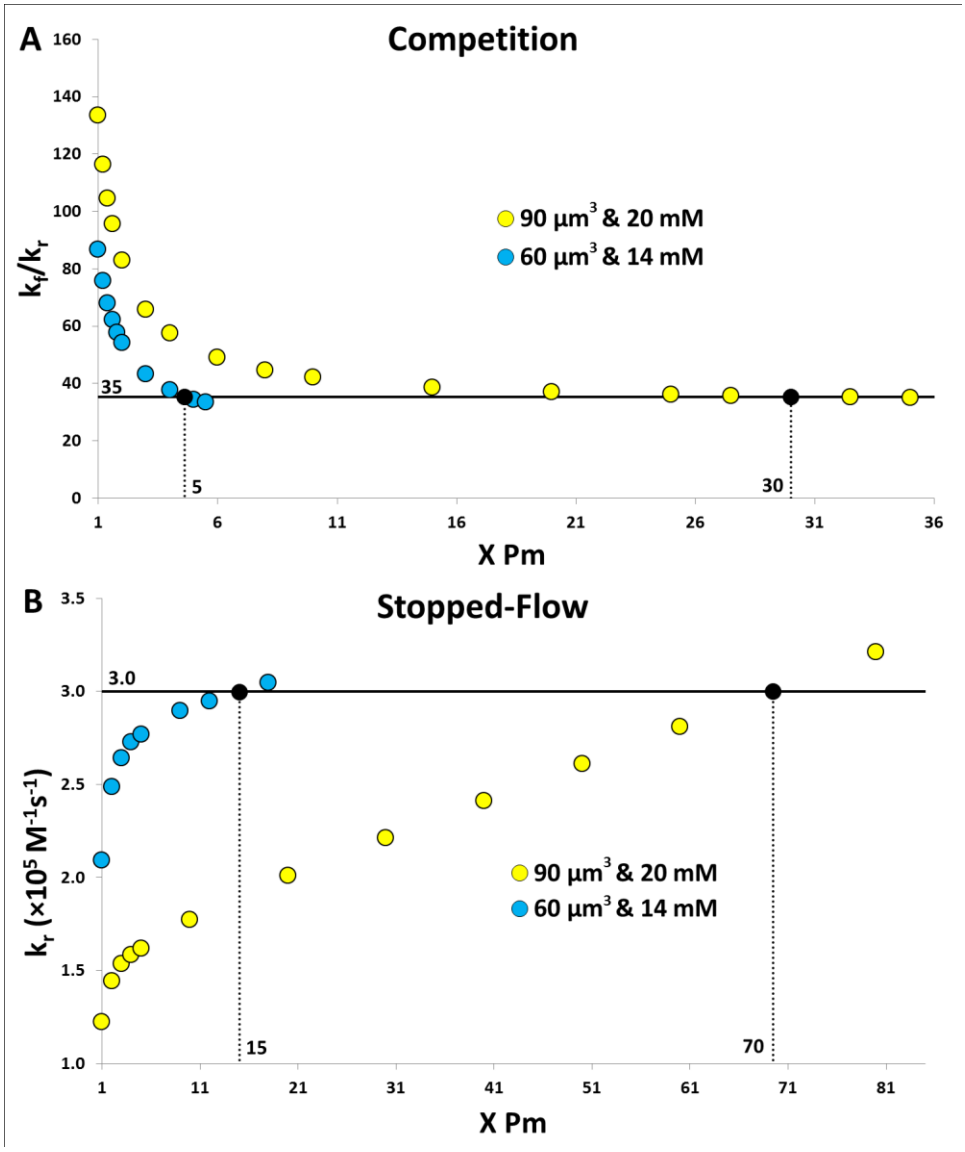


**Figure 26. The effects of RBC membrane permeability to NO studied using the 20×20 degree square cone model with two extreme scenarios ( volume: 90 µm$^3$, MCHC: 20mM; volume: 60 µm$^3$, MCHC: 14 mM).** The horizontal axis is the membrane permeability which is plotted in terms of a factor multiplied by the base value Pm = 5000 µms$^{-1}$ (A) the ratio $k_f/k_r$ is plotted as a function of RBC permeability varied in simulations of competition experiments. The goal ratio $k_f/k_r$ of 35 appears as a horizontal black line. The simulated ratios that are the same as the goal ratio are shown as black circles and the corresponding membrane permeabilities are indicated on the x axis above. (B) The bimolecular rate constant $k_r$ was calculated from simulations of stopped-flow experiments with varied permeabilities. The goal $k_r$ of 3.0×105 M$^{-1}$s$^{-1}$ appears as a horizontal black line. The simulated values of $k_r$ that are the same as the goal are shown as black circles and the corresponding membrane permeabilities are indicated on the x axis above.

We observed that old stored RBCs scavenge NO 1.8 times faster than fresh stored RBCs in stopped-flow experiments and the spherical geometry scavenges NO 1.4 times slower than the biconcave geometry in simulations of stopped-flow experiments. In order to explain the experimental data and compenstate for the effect of geometry, the effect of permeability would have to result in a 2.5 fold increase in the bimolecular rate constant. This increase corresponds to a bimolecular rate constant of $3.0\times10^5$ $M^{-1}s^{-1}$ which is 2.5 times larger than the bimolecular rate constant of $1.2\times10^5$ $M^{-1}s^{-1}$ we obtained from simulations using the 20×20 degree square cone model with a volume of 90 $\mu m^3$ and a MCHC of 20 mM. The results show that an increase of 15 to 70 fold in the peremeability is needed to explain the increased NO scavenging by older stored RBCs we observed from stopped-flow experiments (Figure 26B).

**DISCUSSION**

In this study, we performed experiments using EPR and stopped-flow instruments to further examine the increased NO scavenging by older stored RBCs. We found that older stored RBCs react with NO 1.7-1.8 times faster than fresh stored RBCs. This is consistent with recent published data showing that there is a two-fold difference between the rates of old and fresh stored RBCs scavenging NO [41].

During storage, the geometry of the red blood cell tends to become more spherical, the mean cell hemoglobin concentration in RBCs decreases, RBC volume varies, and the structure of RBC membrane changes significantly[18, 19]. We explored the effects of these changes on NO scavenging to see if they could account for increased NO scavenging by older stored RBCs.

A spherical geometry has less surface area than a biconcave geometry and a larger surface area is expected to increase the rate of NO scavenging. As expected, the simulations using full 3D models demonstrate that the old stored RBC with a spherical geometry scavenges NO about 1.7 to 2.2 times slower than the fresh stored RBC with a biconcave geometry. Thus, other factors must exist to compensate for the effects of geometry and increase NO scavenging by older RBCs as observed experimentally.

We further examined the effects of RBC MCHC and volume, on NO scavenging by RBCs using the 20×20 degree square cone model. In the simulations that varied RBC MCHC, we found that a decreased MCHC leads to an increased NO scavenging by RBCs with a MCHC of 14 mM resulting in a 1.4 times faster rate compared to a MCHC of 20 mM. Although the MCHC of stored RBC does not decrease to as low as 14 mM, we simulated this extreme value to explore the limits of MCHC effects. Similarly, we found that a smaller RBC volume leads to faster NO scavenging by RBCs. RBCs with a volume of 60 $um^3$ react with NO about 1.1 times faster than RBCs with a volume of 90 $\mu m^3$.

The last factor we studied was RBC membrane permeability to NO. In these simulations, we used the 20×20 degree square cone model to examine two extreme scenarios with a range of permeability: (1) a RBC with 90 $um^3$ volume and 20 mM MCHC and (2) a RBC with 60 $um^3$ volume and 14 mM MCHC. The first scenario represents normal fresh stored RBCs and the second scenario represents the worst case of a stored RBC. According to our simulations, the permeability needs to increase about 5 to 70 fold in order to explain the increased NO scavenging by older stored RBCs. Our previous computational simulations of competition experiments at different oxygen saturations using similar parameters show that the RBC membrane permeability to NO

needs to increase 20 to 40 fold in order to achieve an increase of 3 to 4 fold in the ratio $k_f/k_r$ [48]. Thus, our current result focused on blood storage effects is consistent with our previous one comparing oxygenated and deoxygenated cells.

Nitric oxide acts as an important signaling molecule in vivo that regulates blood flow, decreases adhesion molecules expression and platelets activation. Stored RBCs break down during blood storage which results in release of cell-free hemoglobin from RBCs, microparticle formation, and intrinsic erythrocyte changes. The extent and mechanisms of cell-free hemoglobin and microparticles scavenging NO have been well established [30, 31]. Both cell-free hemoglobin and microparticles react with NO very fast, about 1000 times faster than RBCs and enter the cell-free zone where RBCs are absent due to flow pressure gradient [32]. Although the rate of NO scavenging by RBCs is less than cell-free hemoglobin and microparticles, the concentration of erythrocytic Hb is much greater than cell-free Hb (~12 mM RBC Hb vs. ~80 μM cell-free Hb under some conditions). Stored RBCs contribute to NO scavenging when chemical and morphological changes in RBCs occur during blood storage, especially when RBC membrane permeability to NO increases 5 to 70 fold as we suggest in this work. We hypothesize that the combination of red cell breakdown associated hemolysis and microparticle formation together with increased intrinsic RBC NO scavenging can lead to an "NO shock" upon transfusion of substantial amounts of older stored blood. This "NO shock" can lead to reduced oxygen delivery in the microcirculation, increased platelet activation and inflammation, and other deleterious effects that contribute to pathological consequences of the storage lesion.

**ACHNOWLEDGEMENTS:**

This work was supported by NIH Grants HL098032 (D.K.-S.), HL095468 (RP) and the Graduate Fellowship from the Center for Molecular Communication and Signaling at Wake Forest University. R.S. is supported by Cardiovascular T32 Pre-doctoral Training Grant.

REFERENCES


1. *The 2011 National Blood Collection and Utilization Survey Report*, 2013, United States Department of Health and Human Services.
2. Koch, C.G., et al., *Duration of red-cell storage and complications after cardiac surgery.* New England Journal of Medicine, 2008. **358**(12): p. 1229-1239.
3. de Watering, L.V., et al., *Effects of storage time of red blood cell transfusions on the prognosis of coronary artery bypass graft patients.* Transfusion, 2006. **46**(10): p. 1712-1718.
4. Vandromme, M.J., et al., *Transfusion and pneumonia in the trauma intensive care unit: an examination of the temporal relationship.* J Trauma, 2009. **67**(1): p. 97-101.
5. Weinberg, J.A., et al., *Transfusions in the less severely injured: does age of transfused blood affect outcomes?* J Trauma, 2008. **65**(4): p. 794-8.
6. Leal-Noval, S.R., et al., *Transfusion of blood components and postoperative infection in patients undergoing cardiac surgery.* Chest, 2001. **119**(5): p. 1461-8.
7. Zallen, G., et al., *Age of transfused blood is an independent risk factor for postinjury multiple organ failure.* Am J Surg, 1999. **178**(6): p. 570-2.
8. Edgren, G., et al., *Duration of red blood cell storage and survival of transfused patients (CME).* Transfusion, 2010. **50**(6): p. 1185-95.
9. Triulzi, D.J. and M.H. Yazer, *Clinical studies of the effect of blood storage on patient outcomes.* Transfus Apher Sci, 2010. **43**(1): p. 95-106.
10. van de Watering, L., *Red cell storage and prognosis.* Vox Sang, 2011. **100**(1): p. 36-45.

11. Dumaswala, U.J., et al., *Improved red blood cell preservation correlates with decreased loss of bands 3, 4.1, acetylcholinestrase, and lipids in microvesicles.* Blood, 1996. **87**(4): p. 1612-1616.

12. Tinmouth, A. and I. Chin-Yee, *The clinical consequences of the red cell storage lesion.* Transfus Med Rev, 2001. **15**(2): p. 91-107.

13. Tinmouth, A., et al., *Clinical consequences of red cell storage in the critically ill.* Transfusion, 2006. **46**(11): p. 2014-2027.

14. Greenwalt, T.J., D.J. Bryan, and U.J. Dumaswala, *Erythrocyte-Membrane Vesiculation and Changes in Membrane-Composition During Storage in Citrate-Phosphate-Dextrose-Adenine-1.* Vox Sanguinis, 1984. **47**(4): p. 261-270.

15. Latham, J.T., J.R. Bove, and F.L. Weirich, *Chemical and Hematologic Changes in Stored Cpda-1 Blood.* Transfusion, 1982. **22**(2): p. 158-159.

16. Aubuchon, J.P., T.N. Estep, and R.J. Davey, *The Effect of the Plasticizer Di-2-Ethylhexyl Phthalate on the Survival of Stored Rbcs.* Blood, 1988. **71**(2): p. 448-452.

17. Salzer, U., et al., *Vesicles generated during storage of red cells are rich in the lipid raft marker stomatin.* Transfusion, 2008. **48**(3): p. 451-462.

18. Almizraq, R., et al., *Storage of red blood cells affects membrane composition, microvesiculation, and in vitro quality.* Transfusion, 2013. **53**(10): p. 2258-2267.

19. Liu, X., et al., *Diffusion-limited reaction of free nitric oxide with erythrocytes.* Journal of Biological Chemistry, 1998. **273**(30): p. 18709-13.

20. Arduini, A., et al., *Cellular properties of human erythrocytes preserved in saline-adenine-glucose-mannitol in the presence of L-carnitine.* American Journal of Hematology, 2007. **82**(1): p. 31-40.

21. Veale, M.F., G. Healey, and R.L. Sparrow, *Effect of additive solutions on red blood cell (RBC) membrane properties of stored RBCs prepared from whole blood held for 24 hours at room temperature.* Transfusion, 2011. **51**: p. 25s-33s.

22. Furchgott, R.F. and J.V. Zawadzki, *The Obligatory Role of Endothelial-Cells in the Relaxation of Arterial Smooth-Muscle by Acetylcholine.* Nature, 1980. **288**(5789): p. 373-376.

23. Ignarro, L.J., et al., *Endothelium-Derived Relaxing Factor from Pulmonary-Artery and Vein Possesses Pharmacological and Chemical-Properties Identical to Those of Nitric-Oxide Radical.* Circulation Research, 1987. **61**(6): p. 866-879.

24. Katsuki, S., et al., *Stimulation of Guanylate Cyclase by Sodium Nitroprusside, Nitroglycerin and Nitric-Oxide in Various Tissue Preparations and Comparison to Effects of Sodium Azide and Hydroxylamine.* Journal of Cyclic Nucleotide Research, 1977. **3**(1): p. 23-35.

25. Palmer, R.M.J., A.G. Ferrige, and S. Moncada, *Nitric-Oxide Release Accounts for the Biological-Activity of Endothelium-Derived Relaxing Factor.* Nature, 1987. **327**(6122): p. 524-526.

26. Ignarro, L.J., *Nitric Oxide Biology and Pathobiology*2000, San Diego: Academic press.

27. Doyle, M.P. and J.W. Hoekstra, *Oxidation of Nitrogen-Oxides by Bound Dioxygen in Hemoproteins.* Journal of Inorganic Biochemistry, 1981. **14**(4): p. 351-358.

28. Eich, R.F., et al., *Mechanism of NO-induced oxidation of myoglobin and hemoglobin.* Biochemistry, 1996. **35**(22): p. 6976-6983.

29. Herold, S., M. Exner, and T. Nauser, *Kinetic and mechanistic studies of the NO center dot-mediated oxidation of oxymyoglobin and oxyhemoglobin.* Biochemistry, 2001. **40**(11): p. 3385-3395.

30. Azarov, I., et al., *Mechanisms of Slower Nitric Oxide Uptake by Red Blood Cells and Other Hemoglobin-containing Vesicles.* Journal of Biological Chemistry, 2011. **286**(38): p. 33567-33579.

31. Donadee, C., et al., *Nitric Oxide Scavenging by Red Blood Cell Microparticles and Cell-Free Hemoglobin as a Mechanism for the Red Cell Storage Lesion.* Circulation, 2011. **124**(4): p. 465-U294.

32. Liu, C., et al., *Nitric oxide scavenging by red cell microparticles.* Free Radic Biol Med, 2013. **65C**: p. 1164-1173.

33. Coin, J.T. and J.S. Olson, *Rate of Oxygen-Uptake by Human Red Blood-Cells.* Journal of Biological Chemistry, 1979. **254**(4): p. 1178-1190.

34. Liu, X.P., et al., *Diffusion-limited reaction of free nitric oxide with erythrocytes.* Journal of Biological Chemistry, 1998. **273**(30): p. 18709-18713.

35. Vaughn, M.W., et al., *Erythrocytes possess an intrinsic barrier to nitric oxide consumption.* Journal of Biological Chemistry, 2000. **275**(4): p. 2342-2348.

36. Azarov, I., et al., *Nitric oxide scavenging by red blood cells as a function of hematocrit and oxygenation.* J. Biol. Chem., 2005. **280**(47): p. 39024-38032.

37. Butler, A.R., I.L. Megson, and P.G. Wright, *Diffusion of nitric oxide and scavenging by blood in the vasculature.* Biochimica Et Biophysica Acta-General Subjects, 1998. **1425**(1): p. 168-176.

38. Liao, J.C., et al., *Intravascular flow decreases erythrocyte consumption of nitric oxide.* Proceedings of the National Academy of Sciences of the United States of America, 1999. **96**(15): p. 8757-8761.

39. Vaughn, M.W., et al., *Erythrocyte consumption of nitric oxide: Competition experiment and model analysis.* Nitric Oxide-Biology and Chemistry, 2001. **5**(1): p. 18-31.

40. Stapley, R., et al., *Erythrocyte storage increases rates of NO and nitrite scavenging: implications for transfusion-related toxicity.* Biochem J, 2012. **446**(3): p. 499-508.

41. Owusu, B.Y., et al., *Effects of Erythrocyte Aging on Nitric Oxide and Nitrite Metabolism.* Antioxidants & Redox Signaling, 2013. **19**(11): p. 1198-1208.

42. Huang, Z., et al., *Time dependence of oxygen-induced changes in deformability of sickle red blood cells.* Biophysical Journal, 2003. **84**(2): p. 31a-31a.

43. Kim-Shapiro, D.B., *Hemoglobin-nitric oxide cooperativity: Is NO the third respiratory ligand?* Free Radical Biology and Medicine, 2004. **36**(4): p. 402-412.

44. Geisser, M.E., et al., *Nociception before and after exercise in rats bred for high and low aerobic capacity.* Neuroscience Letters, 2008. **443**(1): p. 37-40.

45. Koch, L.G. and S.L. Britton, *Development of Animal Models to Test the Fundamental Basis of Gene-Environment Interactions.* Obesity, 2008. **16**: p. S28-S32.

46. Huang, Z., et al., *Nitric oxide binding to hemoglobin in oxygenated blood.* Biophysical Journal, 2002. **82**(1): p. 444a-444a.

47. Sakai, H., et al., *Encapsulation of concentrated hemoglobin solution in phospholipid vesicles retards the reaction with NO, but not CO, by intracellular diffusion barrier.* Journal of Biological Chemistry, 2008. **283**(3): p. 1508-1517.

48. Huang, K.T., Z. Huang, and D.B. Kim-Shapiro, *Nitric Oxide Red Blood Cell Membrane Permeability at high and low Oxygen Tension.* Nitric Oxide, 2007. **16**: p. 209-216.

# CHAPTER VI

# CONCLUSION

During the time I worked in the lab of Dr. Daniel Kim-Shapiro, I have participated in the investigation of the mechanisms of NO scavenging by cell-free hemoglobin, microparticles, and stored red blood cells. During blood storage, microparticles are formed as small phospholipid vesicles containing hemoglobin when the integrity of the erythrocyte membrane is reduced and other chemical and morphological changes in RBC occur [1-7]. Although increases in microparticles have been appreciated for decades, the ability of these microparticles to react with NO had never been evaluated prior to this study. In Chapter 2 and Chapter 3, we show that microparticle-encapsulated hemoglobin reacts with NO only 3 times slower than cell-free hemoglobin, but still about 1000 times faster than hemoglobin encapsulated in red blood cells [8, 9]. Hence, it is likely that, in vivo, microparticles will scavenge NO almost as fast as cell-free hemoglobin. This could be particularly important when microparticles are continuously elaborated during post-transfusion as they are not known to be cleared by haptoglobin. Therefore it became necessary to further investigate the effect of microparticles on NO bioavailability.

In Chapter 4, we show that both cell-free Hb and Hb contained in red cell microparticles increase overtime during blood storage [10]. The percentage of Hb in microparticles remained approximately 20% during storage when the red blood cells were stored in ADSOL and increased relative to cell-free hemoglobin when ACD preservation solution was used. To confirm our findings that microparticles react with

NO almost as fast as cell-free Hb, we examined the ability of microparticles to scavenge NO using a nitric oxide analyzer and we found that the ability of microparticles to scavenge NO is about 70% of that of cell-free hemoglobin. In addition, we further explored the ability of microparticles to scavenge NO in situ using single vessel myography. Because microparticles are intermediate in size compared to molecular Hb and red cells, we were interested to know whether microparticles enter cell-free zone, like cell-free hemoglobin. Our experiments examining the effect of flow on inhibition of NO scavenging by red cells vs cell-free Hb vs microparticles show that when microparticles were infused in the vessel, the flow effect on vasodilation was similar to the effect when cell-free hemoglobin was infused in the vessel, but significantly smaller than the effect when red cells were infused in the vessel. The similarity of microparticles and hemoglobin and the dissimilarity of microparticles and red blood cells suggest that microparticles do enter the cell-free zone. Finally, we simulated NO scavenging by microparticles and red cells within a 2D vessel. The simulations show that with microparticles entering the cell-free zone, as little as 5 μM microparticle-encapsulated Hb reduces NO bioavailability significantly.

The relative contribution of red cell microparticles vs. cell-free Hb in lowering NO bioavailability could have important implications in designing therapeutic strategies. Clearly, any strategy designed to increase clearance of cell-free Hb such as increasing haptoglobin concentrations would have no effect on pathology associated with MPs as MPs are not cleared by haptoglobin. Red cell microparticles have been reported to be cleared from plasma within the thirty minutes but end up in the liver and other tissue. The plasma concentration of microparticles may be substantial after transfusion even after

thirty minutes due to red cell breakdown of older transfused blood when it is in circulation.

Recently, we have also studied the effects of intrinsic changes of red blood cells during storage on NO scavenging. During blood storage, the geometry of the red blood cell tends to become more spherical, the mean cell hemoglobin concentration in RBCs decreases, and the structure of RBC membrane changes significantly during storage [11, 12]. In addition, RBC volume varies during blood storage but the type of change depends on which additive preservation solutions is used [13, 14]. In Chapter 5, we show that older stored red blood cell scavenge NO about 1.7 to 1.8 times faster than fresher ones examined using electron paramagnetic resonance spectroscopy and stopped-flow absorption spectroscopy. In order to understand the mechanisms of the increased NO scavenging by red blood cells, we simulated NO scavenging by fresher or older stored red blood cells with a biconcave or spherical geometry respectively and found that a spherical geometry scavenges NO about 2 times slower than the ones with a biconcave geometry. This effect of RBC morphology is opposite to the experimental finding that older stored cells scavenge NO faster than fresh ones. We hypothesized that red blood cell MCHC, volume, and membrane permeability to NO must compensate for the effect of cell morphology in order to explain our experimental findings. Computer simulations show that a lower intracellular hemoglobin concentration or a smaller erythrocytic volume increases NO scavenging by red blood cells and membrane permeability to NO needs to increase 5 to 70 fold in order to explain our experimental results.

Although the rate of NO scavenging by RBCs is less than cell-free hemoglobin and microparticles, the concentration of erythrocytic Hb is much greater than cell-free Hb

(~12 mM RBC Hb vs. ~80 μM cell-free Hb under some conditions). Stored RBCs contribute to NO scavenging when chemical and morphological changes in RBCs occur during blood storage, especially when RBC membrane permeability to NO increases 5 to 70 fold as we suggest in this work. We hypothesize that the combination of red cell breakdown associated hemolysis and microparticle formation together with increased intrinsic RBC NO scavenging can lead to an "NO shock" upon transfusion of substantial amounts of older stored blood. This "NO shock" can lead to reduced oxygen delivery in the microcirculation, increased platelet activation and inflammation, and other deleterious effects that contribute to pathological consequences of the storage lesion.

In conclusion, through my study in the lab of Dr. Daniel Kim-Shapiro, we have learned that hemolysis, microparticles formation, and intrinsic changes in red blood cells occur during blood storage. Microparticles can affect NO bioavalibity as much as cell-free hemolgobin with respect to the rate of NO scavenging and the extent of NO scavenging by microparticles is increased due to the fact that microparticles enter the cell-free zone like cell-free hemolgobin. Not all intrinsic changes in red blood cells increase NO scavenging, such as morphological changes of red blood cells to be more spherical, but decreased RBC MCHC or volume increases NO scavenging. RBC membrane permeability to NO has to increase to compensate the effect of geometry and explain the increased NO scavenging by older stored RBCs.

We propose that transfusion of older stored results in an acute loss of NO bioavailability that could also be sustained due to subsequent intravascular hemolysis and red cell breakdown. The loss of NO bioavailability could contribute to increased

inflammation, thrombosis, and other negative consequences that underlie the blood storage lesion. The data presented in this dissertation support this hypothesis.

REFERENCES


1. Greenwalt, T.J., C.G. McGuinness, and U.J. Dumaswala, *Studies in Red-Blood-Cell Preservation .4. Plasma Vesicle Hemoglobin Exceeds Free Hemoglobin.* Vox Sanguinis, 1991. **61**(1): p. 14-17.
2. Izzo, P., et al., *Erythrocytes stored in CPD SAG-mannitol: evaluation of their deformability.* Clinical Hemorheology and Microcirculation, 1999. **21**(3-4): p. 335-339.
3. Aubuchon, J.P., T.N. Estep, and R.J. Davey, *The Effect of the Plasticizer Di-2-Ethylhexyl Phthalate on the Survival of Stored Rbcs.* Blood, 1988. **71**(2): p. 448-452.
4. Dumaswala, U.J., et al., *Improved red blood cell preservation correlates with decreased loss of bands 3, 4.1, acetylcholinestrase, and lipids in microvesicles.* Blood, 1996. **87**(4): p. 1612-1616.
5. Greenwalt, T.J., D.J. Bryan, and U.J. Dumaswala, *Erythrocyte-Membrane Vesiculation and Changes in Membrane-Composition During Storage in Citrate-Phosphate-Dextrose-Adenine-1.* Vox Sanguinis, 1984. **47**(4): p. 261-270.
6. Haradin, A.R., R.I. Weed, and C.F. Reed, *Changes in Physical Properties of Stored Erythrocytes.* Transfusion, 1969. **9**: p. 229-235.
7. Lutz, H.U., S.C. Liu, and J. Palek, *Release of Spectrin-Free Vesicles from Human Erythrocytes During Atp Depletion .1. Characterization of Spectrin-Free Vesicles.* Journal of Cell Biology, 1977. **73**(3): p. 548-560.
8. Azarov, I., et al., *Mechanisms of Slower Nitric Oxide Uptake by Red Blood Cells and Other Hemoglobin-containing Vesicles.* Journal of Biological Chemistry, 2011. **286**(38): p. 33567-33579.

9. Donadee, C., et al., *Nitric Oxide Scavenging by Red Blood Cell Microparticles and Cell-Free Hemoglobin as a Mechanism for the Red Cell Storage Lesion.* Circulation, 2011. **124**(4): p. 465-U294.

10. Liu, C., et al., *Nitric oxide scavenging by red cell microparticles.* Free Radic Biol Med, 2013. **65C**: p. 1164-1173.

11. Almizraq, R., et al., *Storage of red blood cells affects membrane composition, microvesiculation, and in vitro quality.* Transfusion, 2013. **53**(10): p. 2258-2267.

12. Liu, X., et al., *Diffusion-limited reaction of free nitric oxide with erythrocytes.* Journal of Biological Chemistry, 1998. **273**(30): p. 18709-13.

13. Arduini, A., et al., *Cellular properties of human erythrocytes preserved in saline-adenine-glucose-mannitol in the presence of L-carnitine.* American Journal of Hematology, 2007. **82**(1): p. 31-40.

14. Veale, M.F., G. Healey, and R.L. Sparrow, *Effect of additive solutions on red blood cell (RBC) membrane properties of stored RBCs prepared from whole blood held for 24 hours at room temperature.* Transfusion, 2011. **51**: p. 25s-33s.

# SCHOLASTIC VITA

## CHEN LIU

**BORN:** OCTOBER 25, 1984, SHANDONG, CHINA

**EDUCATION:**

2013 Doctor of Philosophy in Physics, Wake Forest University, North Carolina
Dissertation: "The Role of Nitric Oxide in the Blood Storage Lesion"
Advisor: Dr. Daniel B. Kim-Shapiro

2013 Master of Business Administration, Wake Forest University, North Carolina

2009 Master of Science in Physics, Bowling Green State University, Ohio
Thesis: "A Numerical and Analytical Study of Phonation Threshold Pressure and Experiments with A Physical Model of the Vocal Fold Mucosa"
Advisor: Dr. Lewis P. Fulcher

2007 Bachelor of Science in Physics, East China University of Science and Technology, Shanghai, China

**RESEARCH EXPERIENCE:**

2010-Present Graduate Research Assistant
Department of Physics, Wake Forest University, North Carolina
Advisor: Dr. Daniel B. Kim-Shapiro

2007-2009 Graduate Research Assistant
Department of Physics, Bowling Green State University, Ohio
Advisor: Dr. Lewis P. Fulcher

**TEACHING EXPERIENCE:**

2009-2010 Lab instructors for Physics 113
Department of Physics, Wake Forest University, North Carolina

2007-2009 Lab instructors for Physics 111 & 112
Department of Physics, Bowling Green State University, Ohio

**AWARDS, HONORS & LEADERSHIP:**

2013 Graduate Student Research Fellowship Award, Center for Molecular Communication and Signaling, Wake Forest University

2013 Travel Award, the Fifth International Meeting on the Role of Nitrite and Nitrate in Physiology, Pathophysiology, and Therapeutics

2012 Young Investigator Award, Society for Free Radical Biology and Medicine

2011 President of Chinese Students and Scholars Association, Wake Forest University

**PUBLICATIONS:**

1. **Liu C.**, Liu X., Janes J., Stapley R., Patel R. P., Gladwin M. T., Kim-Shapiro D. B., Mechanism of Faster NO Scavenging by Older Stored Red Blood Cells. Journal of Biological Chemistry, **submitted**; 2013
2. **Liu C.**, Zhao W.X., Christ G.J., Gladwin M. T., Kim-Shapiro D.B., Nitric Oxide Scavenging by Red Blood Cell Microparticles. Free Radical Biology and Medicine, 2013. 65C: p. 1164-1173.
3. Donadee C., Raat N. J.H., Kanias T., Tejero J., Lee J. S., Kelley E. E., Zhao X., **Liu C.**, Reynolds H., Azarov I., Frizzell S., Meyer E. M., Donnenberg A. D., Qu L., Triulzi D., Kim-Shapiro D. B., Gladwin M. T., Nitric Oxide Scavenging by Red Blood Cell Microparticles and Cell-Free Hemoglobin as a Mechanism for the Red Cell Storage Lesion. Circulation, 2011. 124(4): p. 465-476.
4. Azarov I., **Liu C.**, Reynolds H., Tsekouras Z., Lee J.S., Gladwin M. T., and Kim-Shapiro D. B., Mechanisms of Slower Nitric Oxide Uptake by Red Blood Cells and Other Hemoglobin-containing Vesicles. Journal of Biological Chemistry, 2011. 286(38): p. 33567-33579.

**CONFERENCE PRESENTATIONS:**

1. **Liu C.**, "The Role of Nitric Oxide in the Blood Storage Lesion", oral presentation at the Center for Molecular Communication and Signaling annual retreat, Winston-Salem, NC, 2013
2. **Liu C.**, Zhao W.X., Christ G.J., Gladwin M. T., Kim-Shapiro D.B., "Nitric Oxide Scavenging by Red Blood Cell Microparticles", poster presentation at the Fifth International Meeting on the Role of Nitrite and Nitrate in Physiology, Pathophysiology, and Therapeutics, Pittsburgh, PA, 2013.
3. **Liu C.**, Zhao W.X., Christ G.J., Gladwin M. T., Kim-Shapiro D.B., "Nitric Oxide Scavenging by Red Blood Cell Microparticles", poster presentation at the 19$^{th}$ annual meeting of the Society for Free Radical Biology and Medicine, San Diego, CA, 2012.
4. **Liu C.**, Zhao W.X., Christ G.J., Gladwin M. T., Kim-Shapiro D.B., "Nitric Oxide Scavenging by Red Blood Cell Microparticles", poster presentation the Carolina Biophysics Symposium, Raleigh, NC, 2012.
5. Azarov I., **Liu C.**, Reynolds H., Tsekouras Z., Lee J.S., Gladwin M. T., and Kim-Shapiro D. B., "Measurement and simulation of Nitric Oxide uptake by Hemoglobin-containing vesicles and Red Blood Cells", poster presentation at the 18$^{th}$ annual meeting of the Society for Free Radical Biology and Medicine, Atlanta, GA, 2011.
6. Azarov I., **Liu C.**, Reynolds H., Lee J.S., Donadee C.,Raat H., Gladwin M. T., and Kim-Shapiro D. B., "Kinetics of Nitric Oxide reactivity with Micro Vesicle-Encapsulated Hemoglobin", poster presentation at the 17$^{th}$ annual meeting of the Society for Free Radical Biology and Medicine, Orlando, FL, 2010.

**PROFESSIONAL MEMBERSHIPS**

Society for Free Radical Biology and Medicine